Publication No. 02-172-240

PILOT-SCALE TESTING AND DEMONSTRATION OF PICOBUBBLE-ENHANCED FLOTATION OF PHOSPHATE FOR INCREASED RECOVERY AND REDUCED REAGENT CONSUMPTION

FINAL REPORT

Prepared by

UNIVERSITY OF KENTUCKY
Department of Mining Engineering

in collaboration with

Mosaic Phosphates
and
Jacobs Engineering Group

under a grant sponsored by

April 2011

The Florida Industrial and Phosphate Research Institute (FIPR Institute) was created in 2010 by the Florida Legislature (Chapter 1004.346, Florida Statutes) as part of the University of South Florida Polytechnic and is empowered to expend funds appropriated to the University from the Phosphate Research Trust Fund. It is also empowered to seek outside funding in order to perform research and develop methods for better and more efficient processes and practices for commercial and industrial activities, including, but not limited to, mitigating the health and environmental effects of such activities as well as developing and evaluating alternatives and technologies. Within its phosphate research program, the Institute has targeted areas of research responsibility. These are: establish methods for better and more efficient practices for phosphate mining and processing; conduct or contract for studies on the environmental and health effects of phosphate mining and reclamation; conduct or contract for studies of reclamation alternatives and wetlands reclamation; conduct or contract for studies of phosphatic clay and phosphogypsum disposal and utilization as a part of phosphate mining and processing; and provide the public with access to the results of its activities and maintain a public library related to the institute's activities.

The FIPR Institute is located in Polk County, in the heart of the Central Florida phosphate district. The Institute seeks to serve as an information center on phosphate-related topics and welcomes information requests made in person, or by mail, email, fax, or telephone.

Florida Industrial and Phosphate Research Institute
1855 West Main Street
Bartow, Florida 33830
(863) 534-7160
Fax: (863) 534-7165
http://www.fipr.poly.usf.edu

PILOT-SCALE TESTING AND DEMONSTRATION OF PICOBUBBLE-ENHANCED FLOTATION OF PHOSPHATE FOR INCREASED RECOVERY AND REDUCED REAGENT CONSUMPTION

FINAL REPORT

Daniel Tao
Principal Investigator

with

Rick Honaker and Maoming Fan

UNIVERSITY OF KENTUCKY
Department of Mining Engineering
234 MMRB
Lexington, KY 40506 USA

in collaboration with
Mosaic Phosphates and Jacobs Engineering Group

Prepared for

UNIVERSITY OF SOUTH FLORIDA POLYTECHNIC
FLORIDA INDUSTRIAL AND PHOSPHATE RESEARCH INSTITUTE
1855 West Main Street
Bartow, FL 33830 USA

Project Manager: Patrick Zhang
FIPR Project Number: 05-02-172R

April 2011

DISCLAIMER

The contents of this report are reproduced herein as received from the contractor. The report may have been edited as to format in conformance with the FIPR *Style Manual*.

The opinions, findings and conclusions expressed herein are not necessarily those of the Florida Institute of Phosphate Research, nor does mention of company names or products constitute endorsement by the Florida Institute of Phosphate Research.

PERSPECTIVE

The efficient capture of hydrophobic particles by air bubbles is the key to effective flotation. It is generally recognized that small bubbles enhance flotation of small and medium-sized particles, while some large air bubbles are required to lift coarse particles. However, the attachment of coarse particles to large bubbles is weak, resulting in detachment and eventually the loss of coarse particles in flotation. Air bubbles of less than one micron in size, i.e., picobubbles, have been found to be effective in preventing detachment. These tiny bubbles also make particles floatable with significantly less surfactant coverage, thus reducing reagent use for flotation. Picobubble-enhanced flotation is still largely in the development stage, but is gaining broad interest among researchers, equipment manufacturers and flotation practitioners.

Prior lab testing results were very encouraging. Picobubbles improved phosphate recovery dramatically, particularly at lower collector dosages. For example, for an approximately 85% P_2O_5 recovery, collector use was 0.4 lb/ton with picobubbles versus 0.9 lb/ton without picobubbles. The same trend was observed for frother dosage. Experiments also demonstrated that picobubbles are more tolerable than larger bubbles to high-throughput flotation, enabling significant reduction in both energy consumption and capital costs.

It should be noted that FIPR organized an on-site evaluation of this laboratory development project. The project evaluation team, consisting of industry representatives from all Florida phosphate mining companies and FIPR staff, visited the research lab and observed picobubble-enhanced flotation. The effect of picobubbles was visually observed by the color change of flotation tailings under the same collector dosage. This team concluded that a pilot testing program was justified by the encouraging lab results, which the FIPR Board of Directors considered seriously in making the decision to fund the current project.

The pilot testing program demonstrated the great potential for efficiency improvement using picobubble-enhanced flotation technology, showing an increase in P_2O_5 recovery and flotation separation efficiency of up to 5 absolute percentage points. For large particles, the improvements were more dramatic.

Patrick Zhang
Research Director - Beneficiation & Mining

ABSTRACT

The United States is the largest phosphate rock producer in the world. The Florida phosphate industry generates up to 85% of the United States' phosphate rock. In a typical central Florida phosphate beneficiation plant the phosphate ore is washed and classified into three major size fractions. The coarse +1.18 mm (+16 mesh) portion is primarily phosphate pebbles and no further upgrading is needed. The fine -106 μm (-150 mesh) phosphate portion contains virtually all of the clay minerals and is discarded as slimes due to lack of cost-effective beneficiation processes. The intermediate -1.18 mm +106 μm (-16 +150 mesh) portion is a mixture of quartz and phosphate minerals. Beneficiation of this size fraction is often accomplished using the "Crago" two-stage froth flotation process. The flotation recovery of coarse flotation feed (-16 +35 mesh) is often below 60%.

In this investigation, significant recovery improvement of coarse phosphate flotation was achieved with laboratory- and pilot-scale flotation columns. The laboratory-scale flotation column tests showed that picobubbles increased P_2O_5 recovery by up to 23%~30% for a given acid-insoluble (A.I.) rejection, depending on the characteristics of the phosphate samples. Picobubbles reduced the collector dosage by ⅓ to ½. Picobubbles almost doubled the coarse phosphate flotation rate constant and increased the flotation selectivity index by up to 25%. The pilot-scale picobubble-enhanced flotation tests with the unsized plant feed indicated that the use of picobubbles increased P_2O_5 recovery and flotation separation efficiency by up to about 5 absolute percentage points. A size-by-size analysis of flotation products revealed that the presence of picobubbles at a high flow ratio improved the flotation efficiency by 4.4% and 8.7% for the phosphate particles of 0.6 mm and 0.8 mm, respectively. It was found from fundamental studies using cavitation-generated picobubbles (<1μm) in a specially designed monobubble flotation column that both the low attachment probability and high detachment probability were responsible for the low flotation recovery of coarse phosphate particles.

ACKNOWLEDGEMENTS

This research program was funded by the Florida Institute of Phosphate Research (FIPR) (grant number 05-02-172R). The project manager, Dr. Patrick Zhang, provided valuable advice and support, which is greatly appreciated. Special thanks are given to the Mosaic Company for supplying the phosphate specimens and testing site and ArrMaz Custom Chemicals Inc. for providing chemicals employed in this study.

TABLE OF CONTENTS

LIST OF FIGURES

Figure **Page**

LIST OF FIGURES (CONT.)

Figure **Page**

LIST OF FIGURES (CONT.)

Figure **Page**

LIST OF TABLES

Table **Page**

EXECUTIVE SUMMARY

EXPERIMENTAL SETUP AND SAMPLES

A pilot-scale flotation column that utilizes picobubbles was designed and manufactured based on the test results obtained in the laboratory picobubble-enhanced coarse phosphate flotation. In consultation with the FIPR project manager and industrial partners an appropriate field testing site was selected for coarse phosphate flotation at Mosaic Phosphates. Two 55-gallon drums of phosphate flotation feed sample was acquired from the selected testing site at the Four Corners plant of Mosaic Phosphates in Bowling Green for laboratory flotation tests and characterization.

PHOSPHATE SAMPLE AND PICOBUBBLE SIZE CHARACTERIZATION

The size distribution analysis results of a representative sample showed that most particles, 81.34%, were coarser than 0.3 mm; fewer than 2% particles were smaller than 0.15 mm and fewer than 1% particles were larger than 1.18 mm. The 0.425~1.18 mm portion accounted for 40.22%. Chemical composition analysis (P_2O_5) was performed with each of the size fractions.

The Mosaic Phosphates sample was analyzed with XRD. The major mineral composition of the phosphate samples was quartz (SiO_2) and apatite ($Ca_5F(PO_4)_3$). The contents of the other minerals such as dolomite ($CaMg(CO_3)_2$), wavellite ($(AlOH)_3(PO_4)_2 \bullet 5H_2O$), crandallite ($Ca_{0.7}Sr_{0.3}Al_3(PO_4)_2(OH)_5H_2O$), and K feldspar ($KAlSi_3O_8$) in the phosphate sample were very low. Analyzing the phosphate sample with an S4 Pioneer wavelength dispersive X-ray fluorescence spectrometer (WDXRF) showed that the P_2O_5 content in the Mosaic phosphate sample was 10.18%. The content of another major acid-soluble constituent, CaO, was 16.74%. The content of the major acid-insoluble constituent, SiO_2, was 67.04%.

The bubble size distribution of Venturi-tube-generated bubbles was analyzed with a Cillas 1064 Laser Particle Size Analyzer. The median size of the bubbles was about 830 nm. Two major peaks were observed at bubble sizes of 900 nm and 70 μm in the population frequency curve of the bubbles generated by the Venturi tube and static mixer.

LABORATORY FLOTATION TESTS

Laboratory flotation tests were performed with the coarse phosphate sample from Mosaic Phosphates. Picobubble-enhanced column flotation resulted in a flotation yield of 35%, flotation recovery of 98%, and separation efficiency of 94%. These results were obtained at a collector dosage of 0.9 kg/t in the presence of picobubbles, producing a concentrate of 28.79% P_2O_5. In contrast, in the absence of picobubbles at a higher

collector dosage of 2.1 kg/t the maximum flotation yield was 33.8%, flotation recovery was 94%, and the separation efficiency was 89.8%.

The presence of picobubbles increased the P_2O_5 recovery of phosphate particles more significantly for the +0.85-1.18 mm than the +0.85-1.18 mm and +0.60-0.85 mm particle size fractions. The presence of picobubbles increased the A.I. rejection. The effect of picobubbles on A.I. rejection decreased as particle size increased. The presence of picobubbles increased A.I. rejection less significantly for the +0.85-1.18 mm particle size range than the other particle fractions. At a given P_2O_5 recovery, the presence of picobubbles increased the P_2O_5 grade by about 0.7-1.0%.

PILOT-SCALE COLUMN FLOTATION TESTS

A pilot-scale flotation column 6" in diameter and 5' in height was designed and fabricated. A Venturi tube of 2" pipe diameter was used as the picobubble generator and a static mixer of 2" diameter as the conventional bubble generator. A 1.5/1 AH ultra heavy duty slurry pump was utilized to circulate the slurry.

A three-factor, three-level Box-Behnken experimental design was conducted for the flotation tests. Three process parameters investigated were frother dosage, collector dosage, and recycling slurry flow rate ratio (slurry flow rate through cavitation tube/slurry through static mixer). A long-duration test was carried out in the presence of picobubbles (flow rate ratio: 50%), and in the absence of picobubbles (flow rate ratio: 0%). The flotation feed, tailing and product of 35 tests with picobubbles, 20 tests without picobubbles and 9 tests of the corresponding flotation mechanical cell were collected and analyzed.

The pilot picobubble-enhanced flotation tests indicated that the use of picobubbles increased P_2O_5 recovery and flotation separation efficiency by up to about 5 absolute percentage points. A size-by-size analysis of flotation products revealed that the presence of picobubbles at a high flow ratio improved flotation efficiency by 4.4% and 8.7% for phosphate particles of 0.6 mm and 0.8 mm, respectively.

INTRODUCTION

Annual phosphate production in the U.S. in 2008 was about 30 million metric tonnes and the Florida and North Carolina phosphate industries account for more than 85% of U.S. production (Gurr 2009). The Florida phosphate matrix consists of one-third each of phosphate mineral, sand and clays. A typical Central Florida phosphate beneficiation plant classifies the phosphate feed into three major size fractions using hydrocyclones and vibrating screens. The coarse +1.18 mm (+16 mesh) portion is primarily phosphate pebbles and no further upgrading is needed. The fine -106 μm phosphate (-150 mesh) portion contains virtually all of the clay minerals and is discarded in the hydrocyclone overflow as the slimes. The lost phosphate in the phosphatic clays accounts for 20-33.3% of the matrix phosphate value (Zhang and Albarelli 1995). The intermediate portion -1.18 mm +106 μm (-16 +150 mesh) is a mixture of quartz and phosphate minerals. Beneficiation of this size fraction involves fatty acid-fuel oil flotation of the phosphate minerals followed by de-oiling with H_2SO_4 and quartz flotation using an amine collector. Froth flotation is used almost exclusively for the upgrading of phosphate. Mechanical flotation cells, flotation columns, and belt flotation are currently employed by the industry. The coarse phosphate particles (-1.18 mm +425 μm or -16 +35 mesh) are relatively difficult to recover by flotation and require high dosages of collector. The loss of phosphate can be very significant with the coarse phosphate particles. An enhanced flotation process for phosphate will boost recovery of both coarse and fine particles and reduce reagent cost, which is of great economic and environmental importance for the industry.

Froth flotation is the most widely used process for the beneficiation of minerals, including Florida phosphate. In this process hydrophobic particles are captured by air bubbles, ascend to the top of the pulp zone, and eventually report to the froth product whereas hydrophilic particles remain in the pulp and are discharged as tailings. However, the high separation efficiency of froth flotation is limited to a very narrow particle size range, which is usually 10-100 μm (Gaudin and others 1931; Morris 1952; Trahar and Warren 1976; King 1982; Feng and Aldrich 1999). The low flotation efficiency of fine particles is mainly due to the low probability of bubble-particle collision while the main reason for poor flotation recovery of coarse particles is the high probability of detachment of particles from bubble surfaces (Yoon and others 1989; Drzymala 1994; Oteyaka and Soto 1995; Ralston and Dukhin 1999; Yoon 2000, Tao 2008).

Efforts have been made to improve flotation recovery of the coarse phosphate particles. Davis and Hood (1993) found that an optimized conditioning process improved the recovery. Moudgil (1992) reported that the recovery of coarse particles could be enhanced by means of collector emulsification, the addition of fines, the use of more effective frother, etc. Maksimov and others (1993) reported that weak agitation combined with sufficiently high ascending pulp flow in a mechanical flotation cell substantially increased the flotation recovery of coarse mineral particles. For example, the flotation recovery of +0.2 mm apatite was increased by 12-14% and the flotation rate by three times while power consumption decreased by 50%. Oteyaka and Soto

(1995) developed a mathematical model for coarse particle flotation in columns with negative bias and their simulation results indicated that a higher flotation recovery of coarse particles could be achieved by the use of small bubbles and high air hold-up. The benefits of negative bias were also recognized by El-Shall and others (2001a, 2001b). Rodrigues and others (2001) observed that the flotation recovery of coarse particles was strongly affected by hydrodynamic conditions and maximum flotation recovery was achieved when the hydrodynamic parameters were in a certain range. They attributed the low flotation recovery of coarse particles under too quiescent conditions to particle settling and that under too turbulent conditions to disruption of particle/bubble aggregates. However, a practical and cost-effective flotation approach has not been developed to increase flotation recovery and reduce flotation reagent consumption at the same time.

It is known that picobubbles, or gas nuclei of less than 1 μm, naturally exist in liquids such as seawater, distilled water, and blood (Johnson and Cooke 1981; Yount 1989). Picobubbles attach more readily to particles than large bubbles due to their lower ascending velocity and rebound velocity from the surface as well as their higher surface free energy to be satisfied. More efficient attachment of particles and improved flotation rate have been observed when tiny bubbles co-exist with conventional-sized air bubbles (Dzienisiewicz and Pryor 1950; Shimoliizaka and Matsuoka 1982). Klassen and Mokrousov (1963) showed that combined flotation by gas nuclei from air supersaturation and by mechanically generated bubbles produced a higher flotation recovery than by either of them alone. Gas nuclei or picobubbles on particle surfaces activate flotation by promoting the attachment of larger bubbles (as shown in Figure 1) since the attachment between gas nuclei or picobubbles and large bubbles is more favored than bubble/solid attachment. In other words, picobubbles act as a secondary collector for particles, reducing flotation collector dosage, enhancing particle attachment probability and reducing the probability of detachment. This leads to substantially improved flotation recovery of poorly floating coarse phosphate particles and reduced reagent cost (Tao and others 2006a, 2006b; Fan and Tao 2008a, 2008b, 2008c), which is the largest single operating cost in commercial phosphate flotation plants. Application of this process to coal flotation resulted in an increase in flotation yield of up to 15 wt%, a frother dose reduction of 10%, and a collector dose reduction of 90% (Attalla and others 2000).

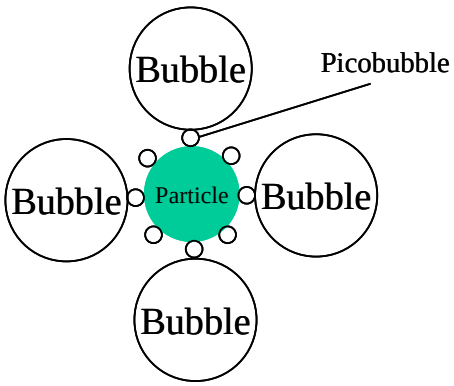

Figure 1. Enhanced Bubble Particle Attachment by Use of Picobubbles.

The overall objective of the project is to demonstrate on a pilot scale the technical viability of picobubble flotation technology for the beneficiation of coarse or unsized flotation feed. This was accomplished by conducting a pilot-scale investigation of a picobubble-enhanced flotation column with coarse and unsized phosphate flotation feed from Mosaic Phosphates. The flotation column was 6" in diameter and 5' in height and featured a picobubble generator based on the hydrodynamic cavitation principle and a conventional bubble generator. It was designed, fabricated, installed, tested, and evaluated for its technical and economic performance. The on-site flotation tests were conducted at sites provided by the collaborating company, Mosaic Phosphates. The results obtained from this project will be used to validate at a pilot scale of about 0.5 t/h the technical performance data obtained from the previous laboratory experiments and to conduct an engineering evaluation of process reliability and economic feasibility. It was expected that when completed successfully, the project would achieve increased phosphate recovery and reduced reagent consumption on a pilot scale to an extent similar to that observed in the laboratory-scale investigation.

METHODS AND TECHNIQUES

FLOTATION FEED SAMPLES

One coarse phosphate sample was collected from the conditioner feed streams in the Four Corners phosphate beneficiation plant of Mosaic Phosphates and placed in sealed containers. The phosphate samples were thoroughly mixed and split into small lots for storage in the lab. Representative samples were taken for size distribution analysis and chemical analysis.

CHEMICAL ANALYSIS

A Bruker D-8 Discover X-2 Advanced Diffraction Cabinet System (XRD) analysis was conducted to identify the principal elements in the coarse phosphate sample used in the flotation tests. The D-8 Discover X-2 uses a CuKa radiation source. A Scintag X-2 powder diffractometer, which has proved extremely useful for qualitative and quantitative powder sample analysis, was equipped with a Pelteir detector with a stationary sample stage. The chemical composition of the phosphate samples was analyzed with an S4 Pioneer wavelength dispersive X-ray fluorescence spectrometer (WDXRF). As described by the manufacturer, the S4 Pioneer with advanced 4 kW excitation technology provides the highest sensitivity. Improved analytical performance for light elements is guaranteed with the very thin beryllium tube window in combination with optimized excitation parameters. Up to 10 primary beam filters, 4 collimators, and 8 crystals can be utilized, which provides great analytical flexibility. The integrated standardless evaluation for all kind of samples like rocks, minerals, metals, hydrocarbons and industrial products allows the fast and easy determination of element concentrations from 100% down to the ppm-level without performing a calibration. [Bruker AXS n.d.]

P_2O_5 content analysis was performed according to the procedure described in *Methods Used and Adopted by the Association of Florida Phosphate Chemists* (AFPC 1991). About 1 gm of the dried and ground representative sample was digested in 50 ml of boiling aqua regia (a mixture of nitric and hydrochloric acids) on a hotplate until the reaction was complete. After cooling, this solution was filtered through a Whatman 42 filter paper into a 1000 ml volumetric flask. The filter paper and residue were then washed at least five times to remove all traces of dissolved salts and acid. The filtrate was diluted with distilled water and thoroughly mixed. The concentrations were analyzed using an Inductively Coupled Plasma (ICP) emission spectrometer.

Acid-soluble components and acid-insoluble components were also analyzed using the method described in *Methods Used and Adopted by the Association of Florida Phosphate Chemists.* Acid-insoluble material was measured as an aqua-regia-insoluble material. Insoluble analysis was performed using the gravimetric method. Using a clean, tarred crucible, the filter paper and residue obtained from the digestion step was ignited at 900°C. After the crucible cooled, the acid insoluble in the sample was calculated.

BUBBLE SIZE MEASUREMENT

A Cillas 1064 laser particle size analyzer was used to measure the Venturi tube-generated picobubbles and the conventional-sized bubbles generated by a static mixer.

FLOTATION REAGENTS

The collector employed in the present study was a mixture of a fatty acid and fuel oil at the ratio of 3:2 by weight. A glycol frother (F-507) was used. Both frother and collector were obtained from ArrMaz Custom Chemicals Inc. Soda ash was used as the pH modifier for the feed sample.

LABORATORY KINETIC FLOTATION OF PHOSPHATE SAMPLE

Kinetic flotation tests were conducted with the phosphate sample to investigate the rate of separation by determining P_2O_5 recovery versus time at certain time intervals. The data was used to guide the design and operation of the pilot-scale flotation column for picobubble-enhanced phosphate flotation. The laboratory flotation kinetics tests were performed with the coarse phosphate sample from Mosaic Phosphates.

LABORATORY FLOTATION WITH PHOSPHATE SAMPLES OF VARYING SIZES

The specially designed flotation column was used to investigate the effect of picobubbles on the flotation of phosphate samples of varying sizes. The column was made of Plexiglas of 2 inches in diameter and 2-6 feet in adjustable height. The cavitation tube and the static mixer, both of which are compact and have no moving parts, were used to generate picobubbles and conventional-sized bubbles, respectively. The flotation procedure is described as follows:

(1) Fatty acid (FA-18G) and fuel oil were mixed thoroughly at a 7:3 ratio by weight as the flotation collector. The collector was used at a dosage of 0.9 kg/t.
(2) A 2 kg phosphate sample was employed to make flotation feed slurry for each run. Hydroxide was used to adjust the pH between 9.1 and 9.5.
(3) The flotation feed was conditioned for three minutes at a predetermined solids concentration (75% solids for coarse phosphate) using a mechanical agitator.
(4) The conditioned phosphate sample was diluted to 25% solids content by weight and fed tangentially into the flotation column through a peristaltic pump, which allowed a consistent underflow stream. The phosphate slurry feed rate was 800 ml/minute.
(5) A glycol frother (F-507) was used for the coarse phosphate flotation tests.

(6) The total recycling flow rate for picobubble and conventional-sized bubble generation was maintained at 8.0 l/min, which split at a three-way connector into the cavitation tube and the static mixer. As a result, the flow-rate ratio (flow rate in cavitation tube/flow rate in the static mixer) could be adjusted.

Based on previous studies on the role of picobubbles in coarse phosphate particle flotation, a size-by-size analysis was performed to investigate the picobubbles' effect on column flotation of coarse phosphate of different sizes. The coarse phosphate particles (+0.425-1.18 mm) were classified into three particle size fractions: +0.85-1.18 mm, +0.60-0.85 mm, and +0.425-0.60 mm. The collector dosage and frother dosage were fixed at 0.9 kg/ton and 10 ppm, respectively. The results of the investigation of the effect of picobubbles on the flotation rate of each particle size fraction were used to guide the design and operation of the pilot-scale flotation column for picobubble-enhanced phosphate flotation.

PILOT-SCALE PICOBUBBLE-ENHANCED COLUMN FLOTATION

Based on the extensive study of picobubble-enhanced flotation with a laboratory-scale flotation column in the previous FIPR project, a pilot-scale flotation column of 6" in diameter and 5' in height was designed and fabricated. Figure 2 shows the installation of the pilot-scale column in the testing site. A Venturi tube of 2" pipe diameter was used as the picobubble generator and a static mixer of 2" diameter as the conventional bubble generator. The Kenics® KM Series static mixer with a patented helical mixing element was purchased from Chemineer, Inc., headquartered in Dayton, Ohio. Both bubble generators were installed outside of the flotation column for the convenience of maintenance, replacement, and configuration variation. A 1.5/1 AH ultra heavy duty slurry pump was utilized to circulate the slurry. The circulating slurry had dual functions, one for bubble generation and the other for scavenging.

(a)

(b)

Figure 2. Pilot-Scale Picobubble-Enhanced Flotation Column.

A three-factor three-level Box-Behnken experimental design was conducted for the flotation tests using Design-Expert 6.8 software acquired from Stat-Ease Inc., Minneapolis, MN. Three process parameters investigated were frother dosage, collector dosage, and recycling slurry flow rate ratio (slurry flow rate through cavitation tube/slurry flow rate through static mixer). The levels of process variables were coded as "-1", "0" and "+1", respectively, where "-1" represents the low level, "0" represents the middle level and "+1" represents the high level of the factors. The specific levels of individual variables are indicated in Table 1. The details of the designed experiments are shown in Table 2.

Table 1. Levels of Variables for a Three-Factor Three-Level Box-Behnken Design.

Variables	Code	Units	Level		
			Low	Middle	High
Frother dosage	A	ppm	0 (-1)	10 (0)	20 (+1)
Slurry flow rate ratio	B	%	20 (-1)	50 (0)	80 (+1)
Collector dosage	C	kg/ton	0.8 (-1)	1.6 (0)	2.4 (+1)

Table 2. Three-Factor Three-Level Experiments Based on Box-Behnken Design.

Std	Run	Frother Level	Flow Rate Ratio Level	Collector Dosage Level
6	1	1	-1	0
17	2	0	0	0
16	3	0	1	1
1	4	-1	0	1
10	5	-1	-1	0
4	6	0	-1	1
2	7	0	0	0
7	8	0	0	0
11	9	0	-1	-1
8	10	-1	1	0
12	11	0	0	0
9	12	1	0	1
5	13	-1	0	-1
15	14	0	1	-1
14	15	0	0	0
3	16	1	0	-1
13	17	1	1	0

PICOBUBBLE-ENHANCED INDUSTIAL-SCALE FLOTATION

The industrial-scale picobubble-enhanced phosphate particle flotation tests were carried out in the phosphate beneficiation plant. The picobubbles were generated by adding a 152.4 mm diameter cavitation tube with a neck of 76.2 mm diameter to a process water pipe, as shown in Figures 3 and 4. The picobubble slurry was distributed into one bank of flotation cells. The volume of each cell was 14.2 m^3 (500 cubic ft). There were five cells in each bank of the flotation machine with a capacity of 342 tph. A microscope at the field testing plant was used to observe flotation tailing and concentrate samples.

Figure 3. Top View of Industrial-Scale Performance Evaluation of Picobubble-Enhanced Phosphate Flotation Cell.

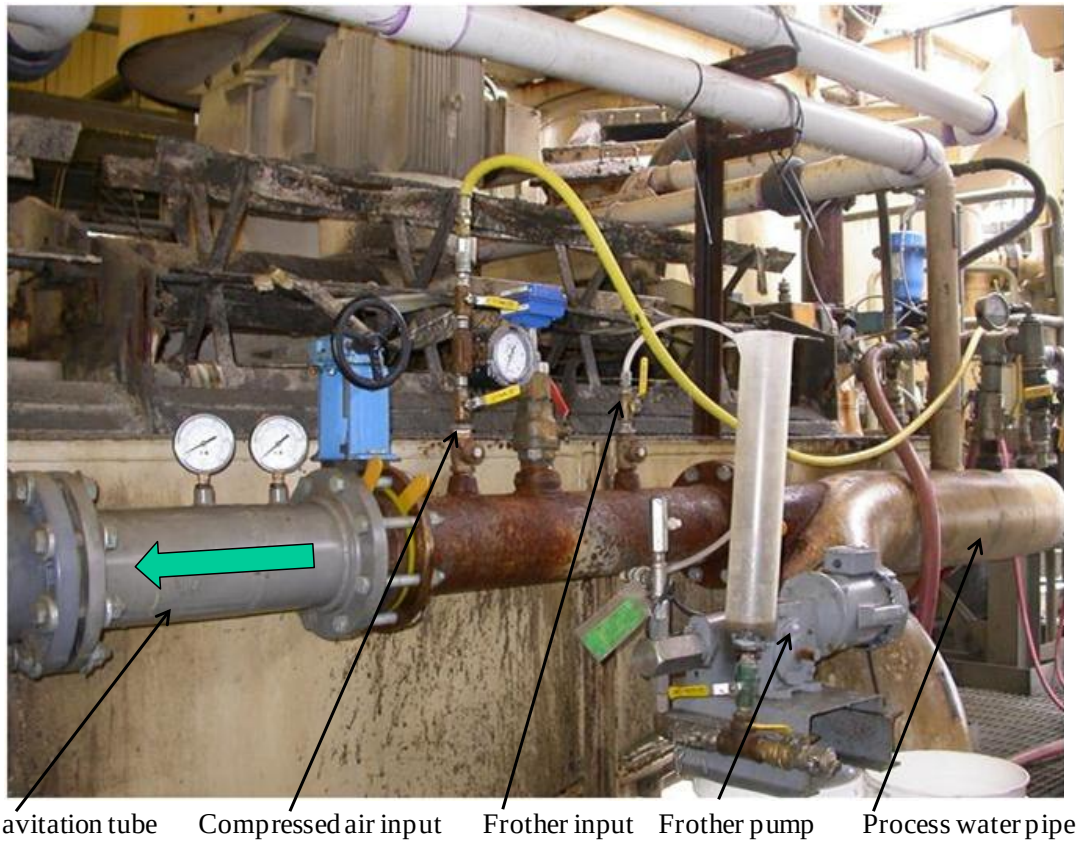

Figure 4. Cavitation Tube and Associated Parts for Commercial Testing.

A three-factor three-level Box-Behnken experimental design was conducted for the industrial flotation tests using the same software mentioned earlier. The three process parameters investigated were air flow rate, frother dosage flow rate, and processing water flow rate. The levels of process variables were coded as "-", "0" and "+", respectively, where "-" represents the low level, "0" represents the middle level and "+" represents the high level of the factors. The specific levels of individual variables are indicated in Table 3, and the details of the designed experiments are shown in Table 4.

Table 3. Levels of Variables for a Three-Factor Three-Level Box-Behnken Experimental Design of Flotation Tests with a Bank of Industrial-Scale Flotation Cells.

Variables	Code	Units	Level		
			Low	Middle	High
Air flow rate	A	liter/min	0	85	170
Frother flow rate	B	liter/min	0	0.025	0.05
Processing water flow rate	C	m^3/min	0	3.4	6.8

Table 4. Three-Factor Three-Level Experiments Based on Box-Behnken Design of Flotation Tests with a Bank of Industrial-Scale Flotation Cells.

Std	Run	Air Flow Rate (liter/min)	Frother Flow Rate (liter/min)	Process Water Flow Rate (m^3/min)
6	1	170	0.025	0
17	2	85	0.025	3.4
16	3	85	0.025	3.4
1	4	0	0.000	3.4
10	5	85	0.050	0
4	6	170	0.050	3.4
2	7	170	0.000	3.4
7	8	0	0.025	6.8
11	9	85	0.000	6.8
8	10	170	0.025	6.8
12	11	85	0.050	6.8
9	12	85	0.000	0
5	13	0	0.025	0
15	14	85	0.025	3.4
14	15	85	0.025	3.4
3	16	0	0.050	3.4
13	17	85	0.025	3.4

RESULTS AND DISCUSSION

FLOTATION FEED CHARACTERIZATION

The particle size, P_2O_5 and A.I. content analysis results of the coarse phosphate sample are shown in Figures 5-11. The phosphate sample, containing 15.6% moisture, was wet-screened into eight size fractions. The fractional curve and the curve of cumulative undersize percentage against particle size are shown in Figure 5. The curve of cumulative undersize against particle size shows that the median size of the phosphate sample was about 0.4 mm. Most particles, i.e., 81.34%, were coarser than 50 mesh or 0.3 mm. Fewer than 2% of the particles were smaller than 100 mesh or 0.15 mm, and fewer than 1% of the particles were larger than 16 mesh or 1.18 mm. Our research efforts were focused on the 0.425~1.18 mm portion, which accounted for 40.22%.

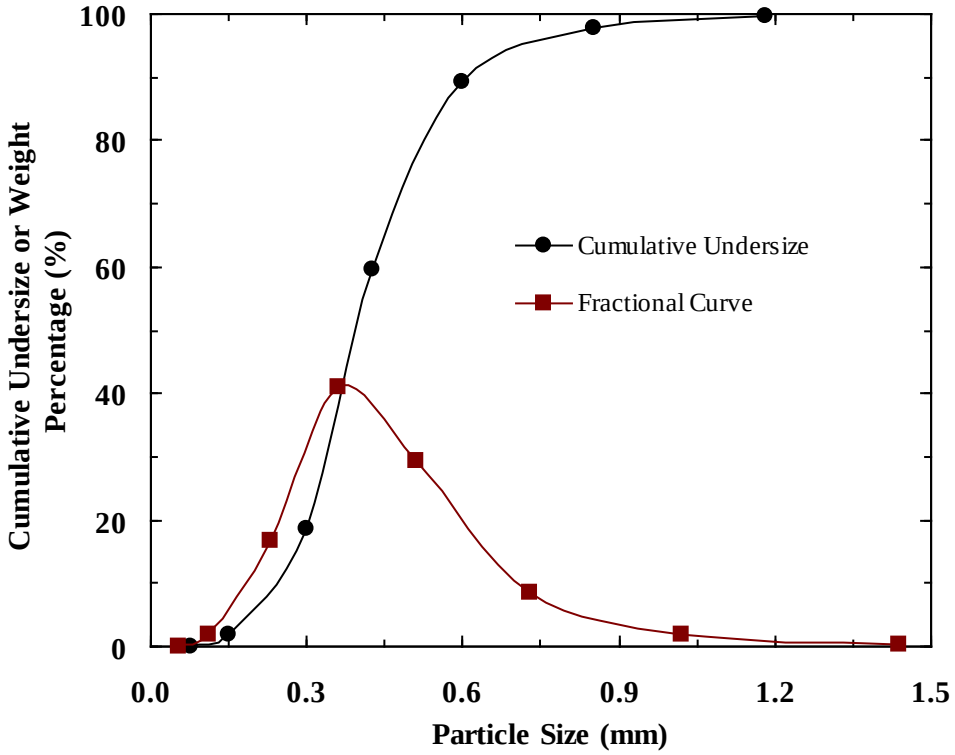

Figure 5. Phosphate Particle Size Distribution.

Figure 6 shows that for +0.30 mm size particles, the P_2O_5 content increased with increasing particle size while the A.I. content increased with decreasing particle size. However, the P_2O_5 content of the 0.30-0.15 mm size fraction was noticeably higher and the A.I. content was lower than the narrow size fractions of 0.425-0.30 mm and 0.15-0.075 mm, which was consistent with the sieve and P_2O_5 analysis results of a phosphate sample collected from the same phosphate beneficiation plant more than one year earlier. The P_2O_5 content in the +1.18 mm particle size fraction was about 25% and the acid

insols (A.I.) content was about 13.5%. The P_2O_5 content significantly decreased as the particle size decreased from 0.7 mm to 0.3 mm.

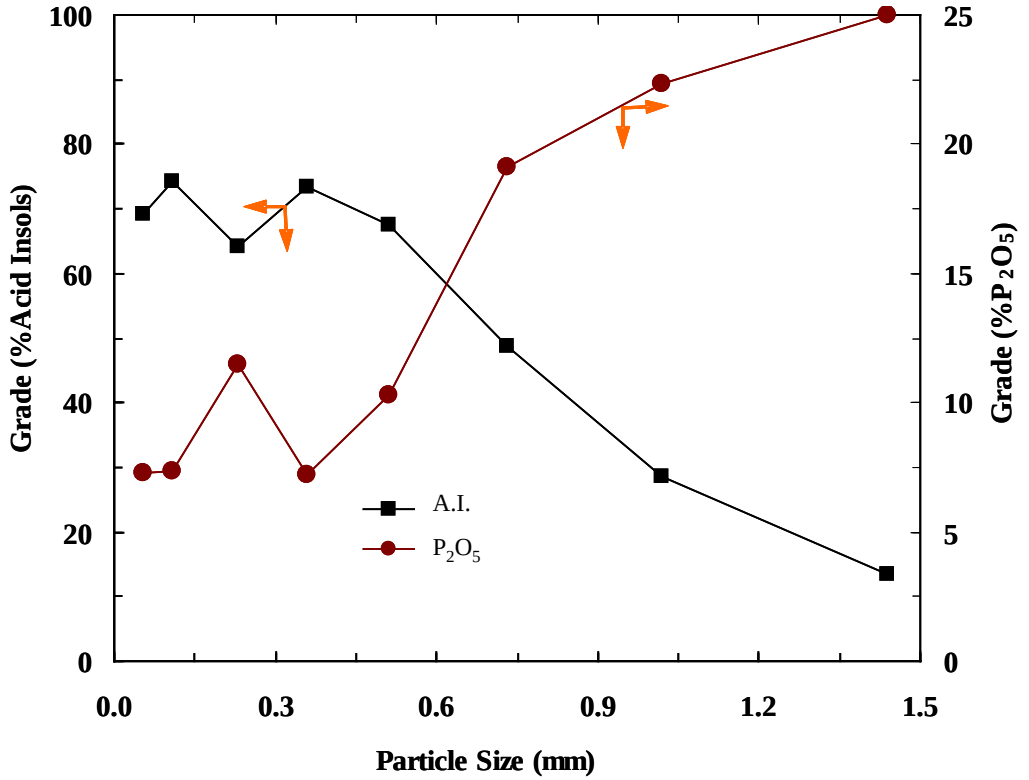

Figure 6. P_2O_5 and Acid Insols (A.I.) Contents as a Function of Particle Size.

Figure 7 shows the cumulative undersize A.I. content and cumulative oversize A.I. content as a function of particle size. Again, the 0.30-0.15 mm size fraction was the exception. The cumulative undersize A.I. content decreased slightly with increasing particle size for +0.425 mm particles and the cumulative oversize A.I. content decreased significantly with increasing particle size for +0.30 mm size fractions. The effect of the 0.3-0.15 mm particle size fraction on the cumulative undersize A.I. curve was more significant than on the cumulative A.I. oversize A.I. curve because the weight percentage of -0.15 mm was less than 2% while the weight percentage of the +0.3 mm size fraction was more than 80%. The A.I. content of the head sample was 67%. The cumulative oversize A.I. contents of the +0.3 mm fraction and +0.425 mm (35 mesh) fraction were 67.5% and 61.3%, respectively.

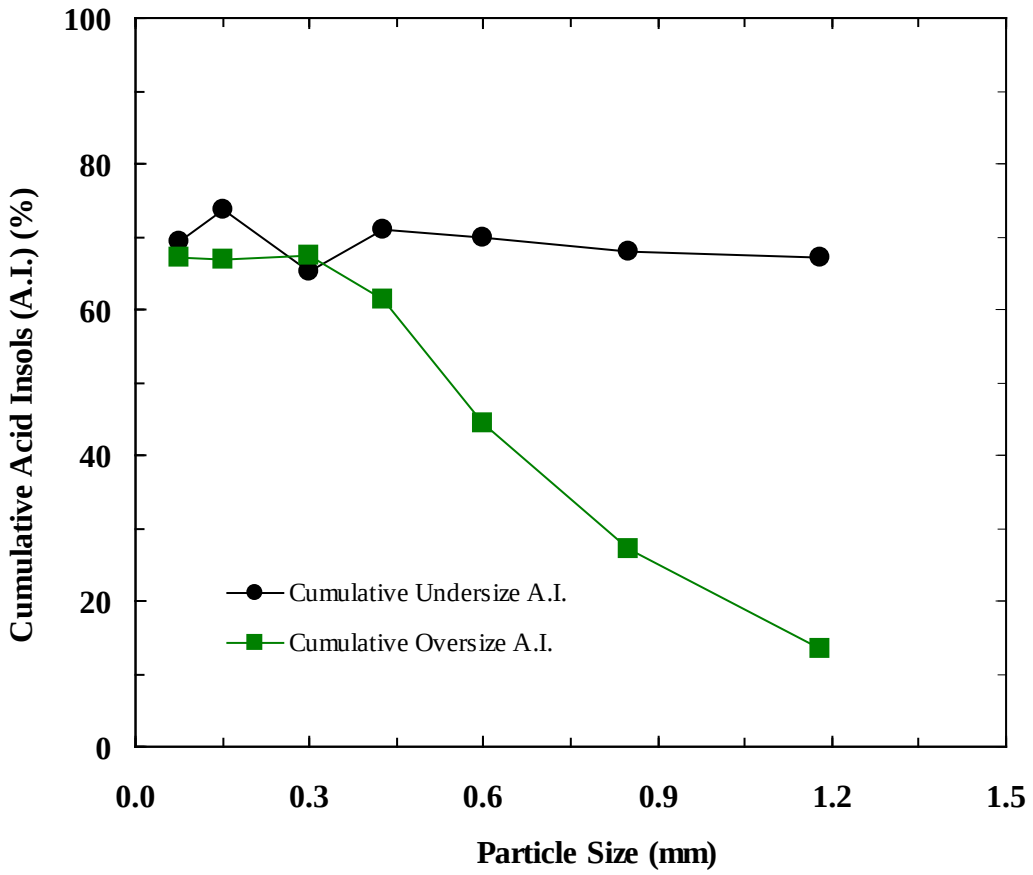

Figure 7. Cumulative Undersize and Oversize Acid Insols (A.I.) vs. Particle Size.

Figure 8 shows the cumulative undersize P_2O_5 content and cumulative oversize P_2O_5 content as a function of particle size. The cumulative undersize P_2O_5 content increased slightly with increasing particle size for the +0.425 mm size fraction while the cumulative oversize P_2O_5 content increased remarkably with increasing particle size for the +0.30 mm size fraction. The effect of the 0.3-0.15 mm particle size fraction on the cumulative undersize P_2O_5 curve was more significant than on the cumulative oversize P_2O_5 curve also because the weight percentage of the -0.15 mm fraction was much less than the weight percentage of the +0.3 mm size fraction. The P_2O_5 content of the head sample was 10.16%. The cumulative oversize P_2O_5 contents of the +0.3 mm fraction and +0.425 mm (35 mesh) fraction were 10% and 12.8%, respectively. The cumulative undersize P_2O_5 contents of -0.3 mm fraction and -0.425 mm (35 mesh) fraction were 8.4% and 11%, respectively.

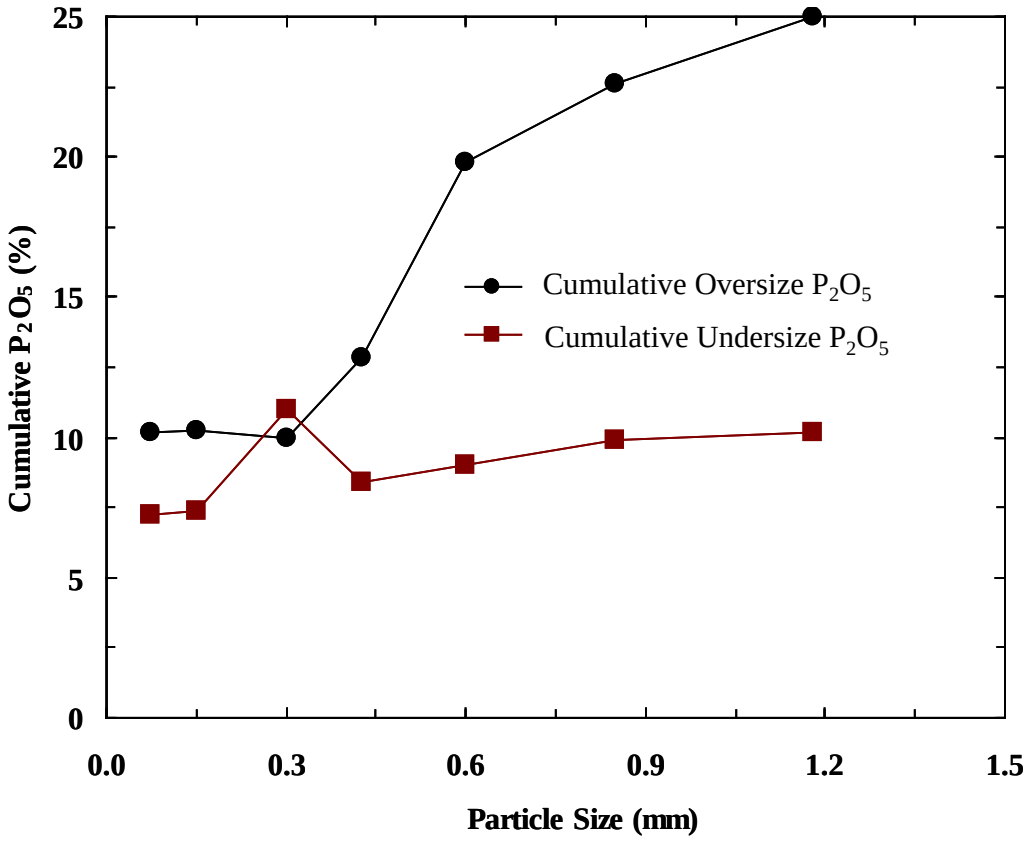

Figure 8. Cumulative Undersize and Oversize P_2O_5 vs. Particle Size.

The differences of weight percentage, A.I. content and P_2O_5 content in the different particle size fractions were reflected in the colors and appearances of each size fraction, as shown in Figures 9-11. Figure 11(a) shows a coarse brown apatite particle with some transparent fine quartz particle inclusions, while Figure 11(b) shows a coarse quartz particle with fine black apatite particle inclusions.

Figure 9. Particle Size Fractions of Mosaic Phosphates Sample.

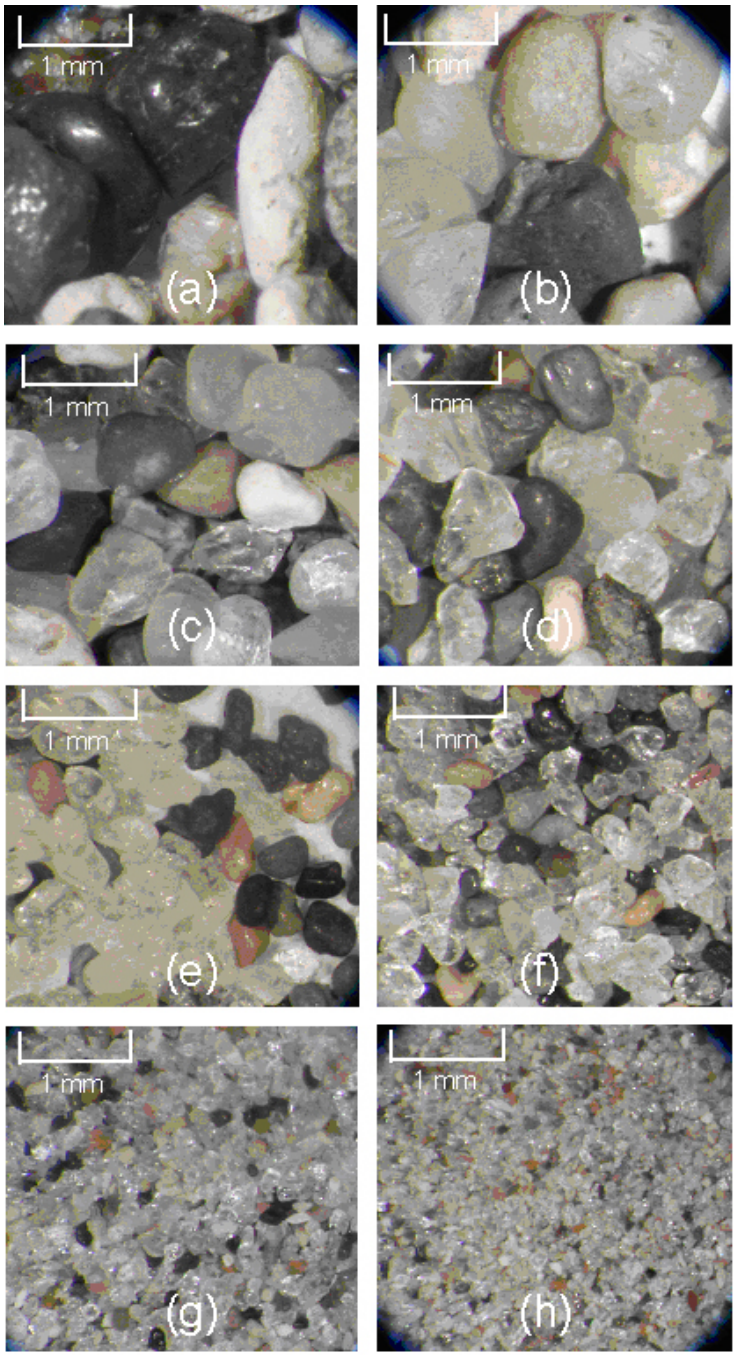

Figure 10. Particle Size Fractions of Mosaic Phosphates Sample: (a) +16 Mesh; (b) 16×20 Mesh; (c) 20×30 Mesh; (d) 30×40 Mesh; (e) 40×50 Mesh; (f) 50×100 Mesh; (g) 100×200 Mesh; (h) 200 Mesh.

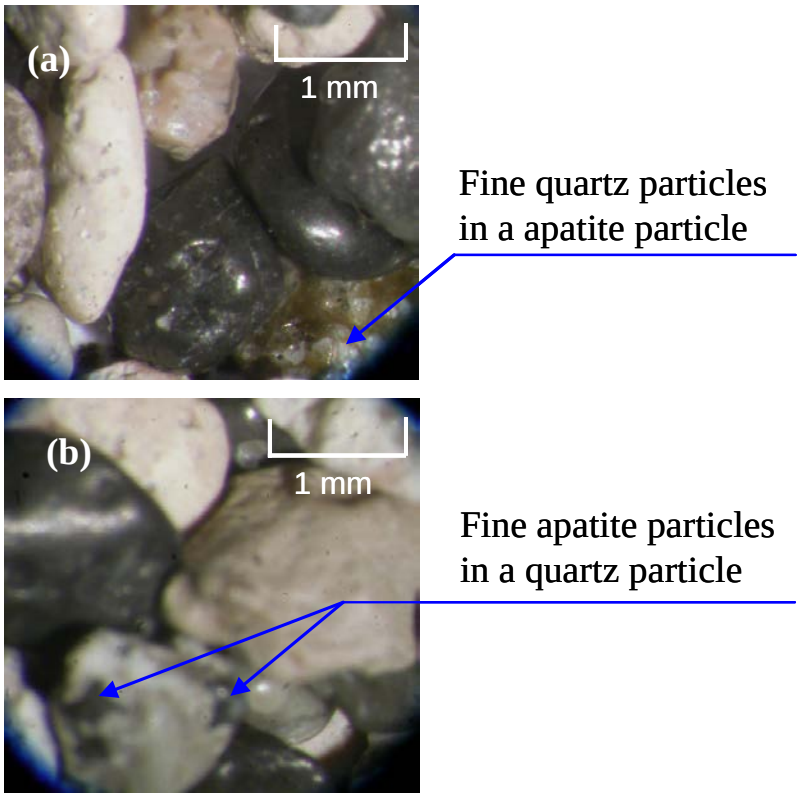

Figure 11. Coarse Fractions of Mosaic Phosphates Sample.

Figure 12 shows the XRD intensity (in cps, or counts per second) versus XRD 2θ of the Mosaic Phosphates sample. The amplitudes for specific XRD peaks indicate that the major mineral composition of the phosphate samples was quartz (SiO_2) and apatite ($Ca_5F(PO_4)_3$). The peak amplitudes for other minerals such as dolomite ($CaMg(CO_3)_2$), wavellite ($(AlOH)_3(PO_4)_2 \cdot 5H_2O$), crandallite ($Ca_{0.7}Sr_{0.3}Al_3(PO_4)_2(OH)_5H_2O$), and K feldspar ($KAlSi_3O_8$) etc. were very small, indicating that quantities of these minerals in the phosphate samples were very low.

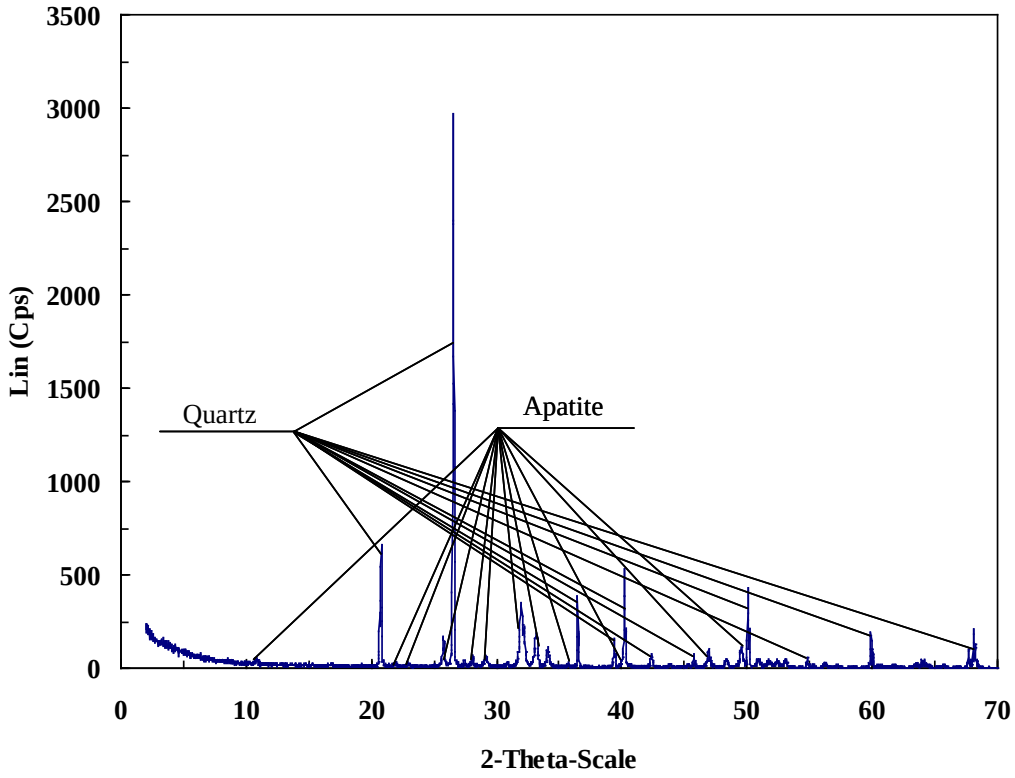

Figure 12. Mosaic Phosphates XRD Intensity (Counts per Second) Versus 2θ.

Table 5 summarizes the pertinent chemical composition of the phosphate sample that was analyzed with an S4 Pioneer wavelength dispersive X-ray fluorescence spectrometer (WDXRF). The P_2O_5 content in the Mosaic Phosphates sample was 10.18%. The content of another major acid-soluble constituent, CaO, was 16.74%. The content of the major acid-insoluble constituent, SiO_2, was 67.04%.

Table 5. XRF Chemical Analyses.

Composite	Content (%)
Al_2O_3	0.98
SiO_2	67.04
P_2O_5	10.18
K_2O	0.07
MnO	0.0118
CaO	16.74
BaO	0.003
TiO_2	0.02
Fe_2O_3	0.42
SrO_2	0.03
Na_2O	0.07
MgO	0.38
Other	4.07
Total	100

BUBBLE SIZE DISTRIBUTION

Figure 13 shows the size distribution of bubbles generated by both the Venturi tube and the static mixer at a frother dosage of 10 ppm. There are two major peaks observed on the population frequency curve. The finer size bubbles and coarser size bubbles were generated by the Venturi cavitation tube and the static mixer, respectively. The first peak is at the bubble size of 900 nm and the second is at 70 μm.

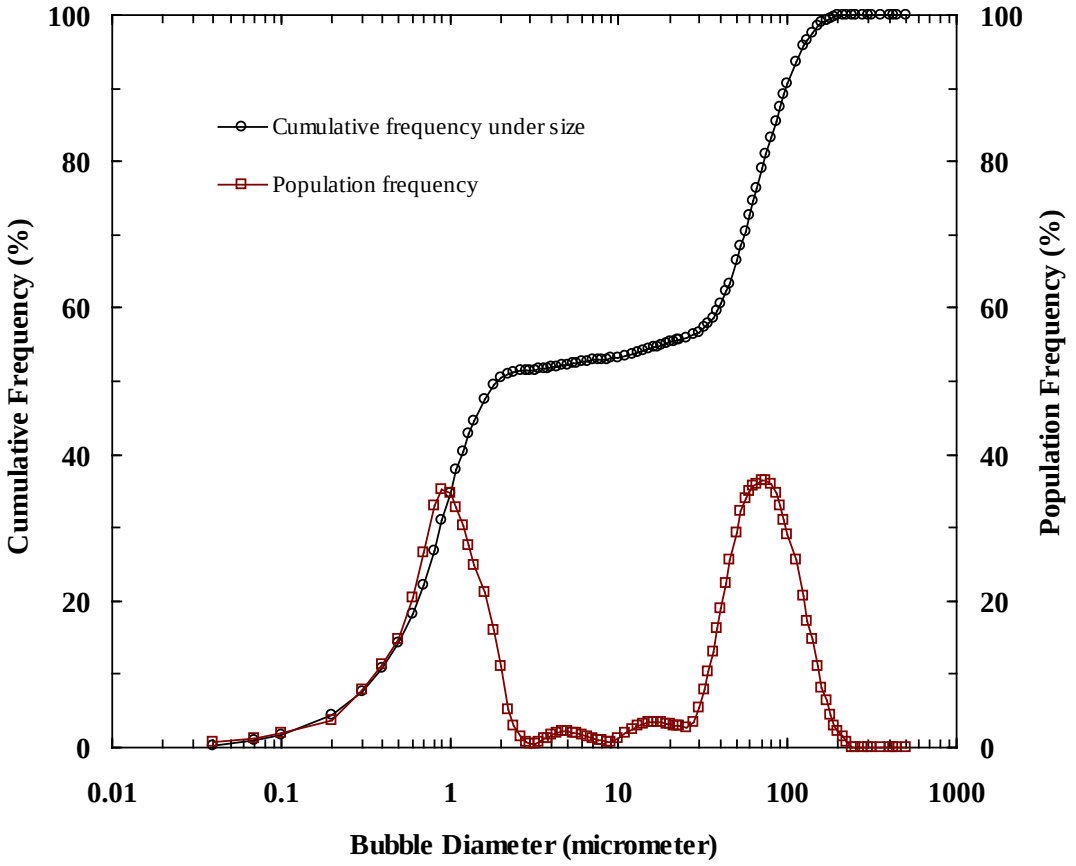

Figure 13. Size Distributions of Both Venturi Tube and Static Mixer-Generated Bubbles.

LABORATORY COLUMN FLOTATION

Figures 14-16 show the effect of picobubbles on flotation performance at varying collector dosages. The solid feed rate, superficial air velocity, and frother dosage were fixed constant at 240 g/min, 1.0 cm/s, and 10 ppm, respectively. Figure 14 shows the effects of picobubbles on flotation yield at varying collector dosages from 0.3 kg/ton to 2.1 kg/ton. The curves indicate that the flotation yield increased significantly as the collector dosage increased from a dosage of 0.3 kg/ton to 0.9 kg/ton, after which the flotation yield increased slightly. The flotation yield of 35% was achieved at lower collector dosage of 0.9 kg/t in the presence of picobubbles, producing a concentrate of 28.79% P_2O_5. In contrast, the maximum flotation yield was less than 34% at a collector

dosage of 2.1 kg/t in the absence of picobubbles. The improved flotation yield may be attributed to picobubbles that were selectively generated and attached onto the hydrophobic phosphate particles, acted as a secondary collector and reduced the effective density of the bubble-particle aggregate. In the figure, only the $\%P_2O_5$ curve and A.I. content curve in the presence of picobubbles were plotted because there were no significant differences between the product grade ($\%P_2O_5$ and %A.I.) in the presence and absence of picobubbles. The product grade $\%P_2O_5$ increased and %A.I. content in the concentrate decreased slightly as the collector dosage increased from 0.3 kg/ton to 0.9 kg/ton, because the coarse high-grade phosphate particles were more difficult to float than the fine phosphate particles, especially at a low collector dosage. When collector dosage increased, high-grade coarse phosphate particles were floated, the product grade increased and the A.I. content in the concentrate decreased.

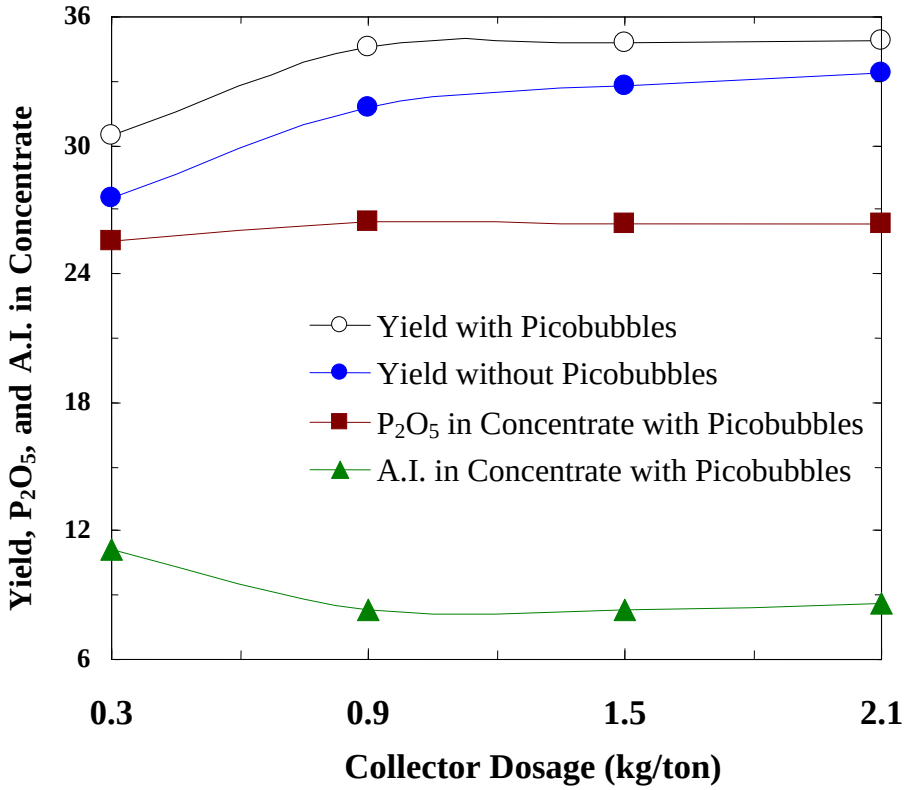

Figure 14. Effects of Picobubbles on Yield and Grade at Varying Collector Dosages.

Figure 15 shows the effects of picobubbles on flotation P_2O_5 recovery at varying collector dosages from 0.3 kg/ton to 2.1 kg/ton. The curves indicate that the P_2O_5 flotation recovery increased remarkably as the collector dosage increased from 0.3 kg/ton to 0.9 kg/ton. The P_2O_5 recovery increased slightly in the absence of picobubbles while remaining essentially constant in the presence of picobubbles as the collector dosage increased from 0.9 kg/ton to 2.1 kg/ton. The flotation recovery of more than 98% and a concentrate grade of 28.8% were achieved at a lower collector dosage of 0.9 kg/t in the presence of picobubbles. On the contrary, the maximum flotation recovery was less than 94%, which was achieved at a collector dosage of 2.1 kg/t in the absence of picobubbles.

It should be pointed out that there were no noticeable differences between the product grade (%P_2O_5 and %A.I.) in the presence of picobubbles and in the absence of picobubbles.

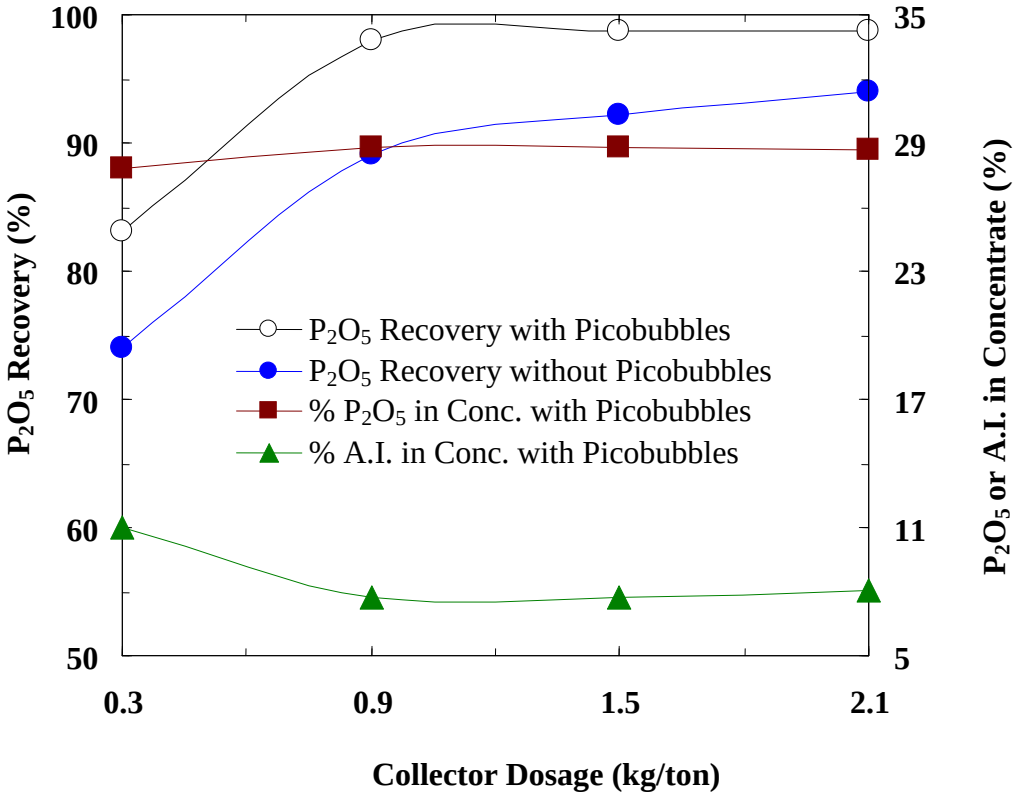

Figure 15. Effects of Picobubbles on P_2O_5 Recovery at Varying Collector Dosages.

Figure 16 shows the effect of picobubbles on flotation separation efficiency at varying collector dosages from 0.3 kg/ton to 2.1 kg/ton. Here, the separation efficiency is defined as the difference in P_2O_5 recovery and A.I. recovery, which is the sum of flotation P_2O_5 recovery and A.I. rejection minus 100%. The curves indicate that flotation separation efficiency increased noticeably as the collector dosage increased from 0.3 kg/ton to 0.9 kg/ton. The flotation separation efficiency increased slightly in the absence of picobubbles while remaining essentially constant in the presence of picobubbles as the collector dosage increased from 0.9 kg/ton to 2.1 kg/ton. The separation efficiency of more than 94% and an A.I. rejection of 96% were achieved at a lower collector dosage of 0.9 kg/t in the presence of picobubbles. However, in the absence of picobubbles, the maximum separation efficiency was 89.8%, which was achieved at a collector dosage of 2.1 kg/t.

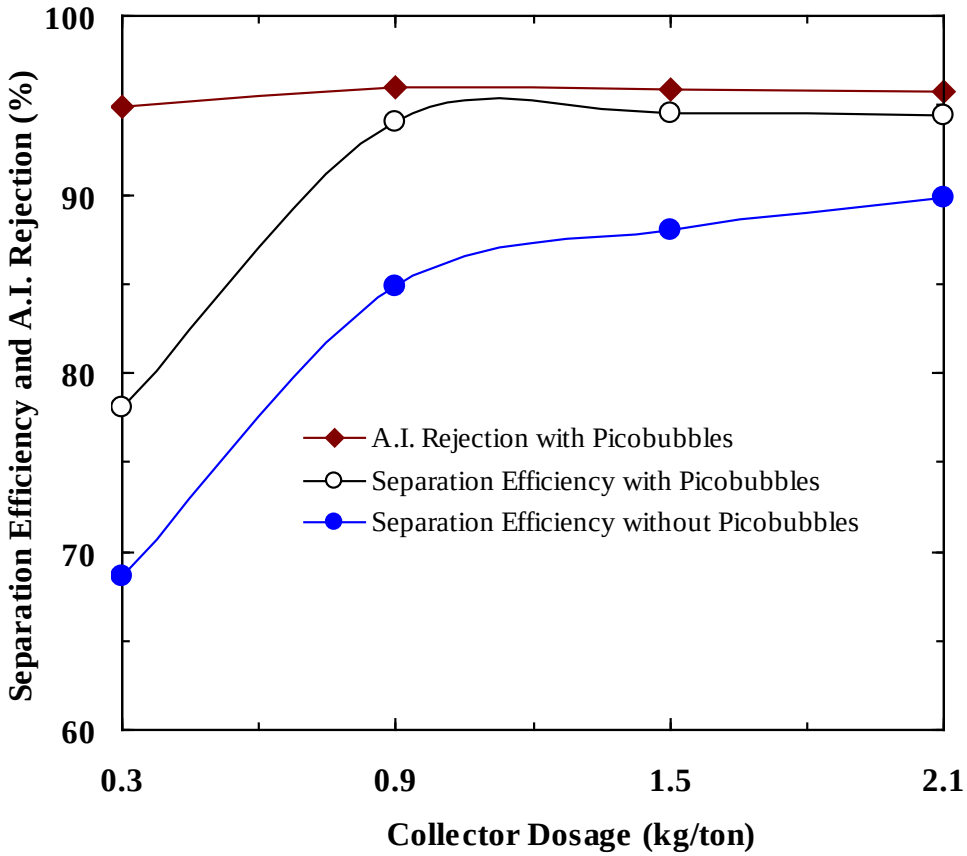

Figure 16. Effects of Picobubbles on Separation Efficiency at Varying Collector Dosages.

Figures 17-19 show the effect of picobubbles on flotation performance at varying frother dosages. The solid feed rate, superficial air velocity, and collector dosage were fixed constant at 240 g/min, 1.0 cm/s, and 0.9 kg/ton, respectively. Figure 17 shows the effects of picobubbles on flotation yield at varying frother dosages from 0 to 20 ppm. The yield versus frother dosage curve in the presence of picobubbles is above the curve in the absence of picobubbles, which means that the picobubbles increased the yield. The flotation yield increased significantly as the frother dosage increased from a dosage of 0 to 5 ppm. The flotation yield of 35% in the presence of picobubbles and the yield of 32.3% in the absence of picobubbles were achieved at a lower frother dosage of 5 ppm in the presence of picobubbles while the concentrate grade was constant at about 27.8% P_2O_5. The product grade $\%P_2O_5$ increased and %A.I. content in the concentrate decreased slightly as the frother dosage increased from 0 to 10 ppm, because the coarse high-grade phosphate particles were more difficult to float than the fine phosphate particles, especially at a low frother dosage. As the frother dosage increased, high-grade coarse phosphate particles were floated, the product grade increased and A.I. content in the concentrate decreased.

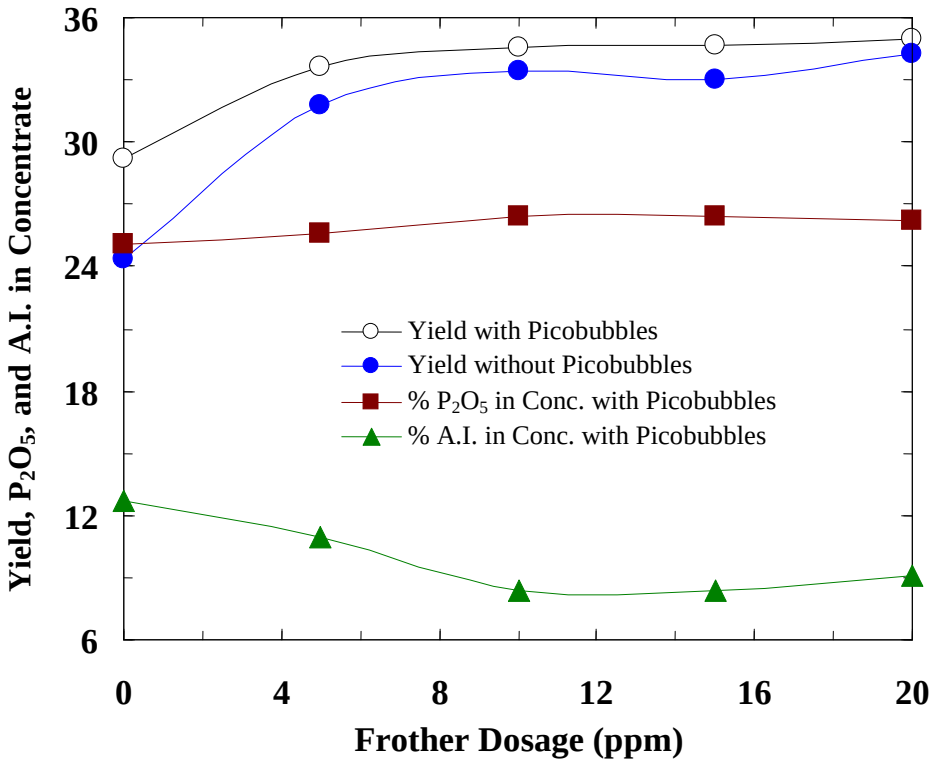

Figure 17. Effects of Picobubbles on Yield at Varying Frother Concentration.

Figure 18 shows the effects of picobubbles on flotation P_2O_5 recovery at varying frother dosages from 0 to 20 ppm. The curves indicate that picobubbles improved P_2O_5 recovery at a lower frother dosage more significantly than at higher frother dosages. The flotation P_2O_5 recovery increased remarkably as the frother dosage increased from 0 to 10 ppm. The flotation P_2O_5 recovery increased slightly in the absence of picobubbles while remaining essentially constant in the presence of picobubbles as the frother dosage increased from 10 ppm to 20 ppm. A flotation recovery of more than 98% and a concentrate grade of 28.8% were achieved at a frother dosage of 10 ppm in the presence of picobubbles. On the contrary, the maximum flotation recovery was 95.9%, which was achieved at a frother dosage of 20 ppm in the absence of picobubbles. There were no noticeable differences in the product grade (%P_2O_5 and %A.I.) in the presence and absence of picobubbles.

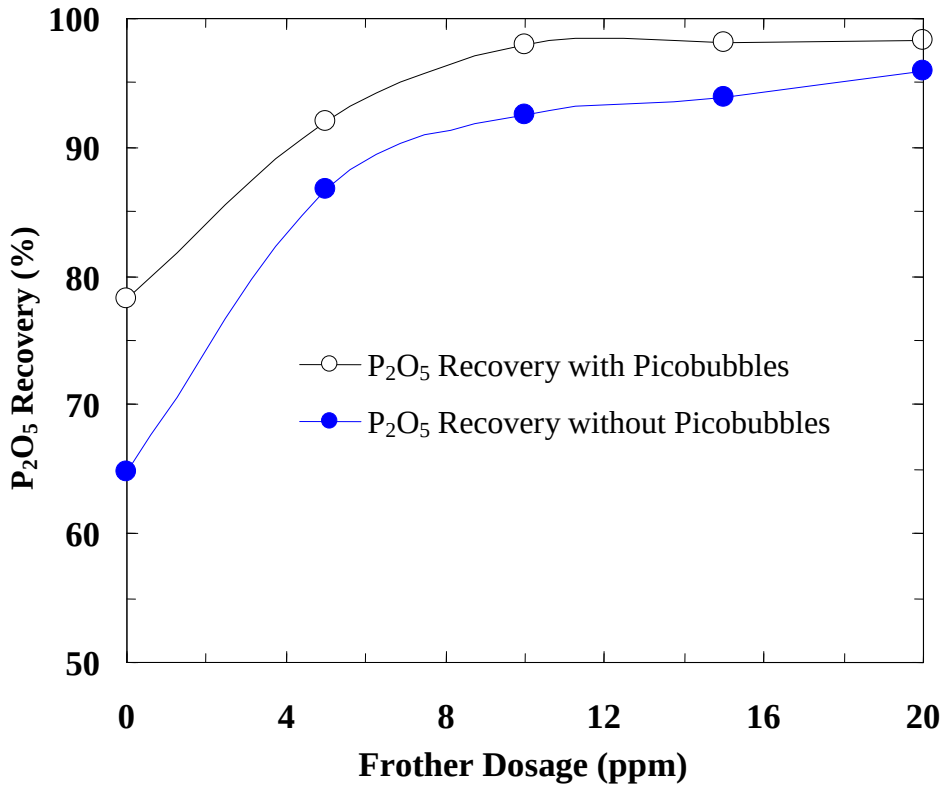

Figure 18. Effects of Picobubbles on P_2O_5 Recovery at Varying Frother Dosages.

Figure 19 shows the effects of picobubbles on flotation separation efficiency at varying frother dosages from 0 to 20 ppm. The separation efficiency curve in the presence of picobubbles lies above the curve in the absence of picobubbles, which indicates that the picobubbles improved the separation efficiency. Both of the separation efficiency curves show that flotation separation efficiency increased noticeably as the frother dosage increased from 0 ppm to 10 ppm. As the frother dosage increased from 10 ppm to 20 ppm, the flotation separation efficiency increased slightly in the absence of picobubbles while remaining essentially constant in the presence of picobubbles. A separation efficiency of 94% and an A.I. rejection of 96% were achieved at a frother dosage of 10 ppm in the presence of picobubbles. However, in the absence of picobubbles, the separation efficiency was 87.6% at a frother dosage of 10 ppm.

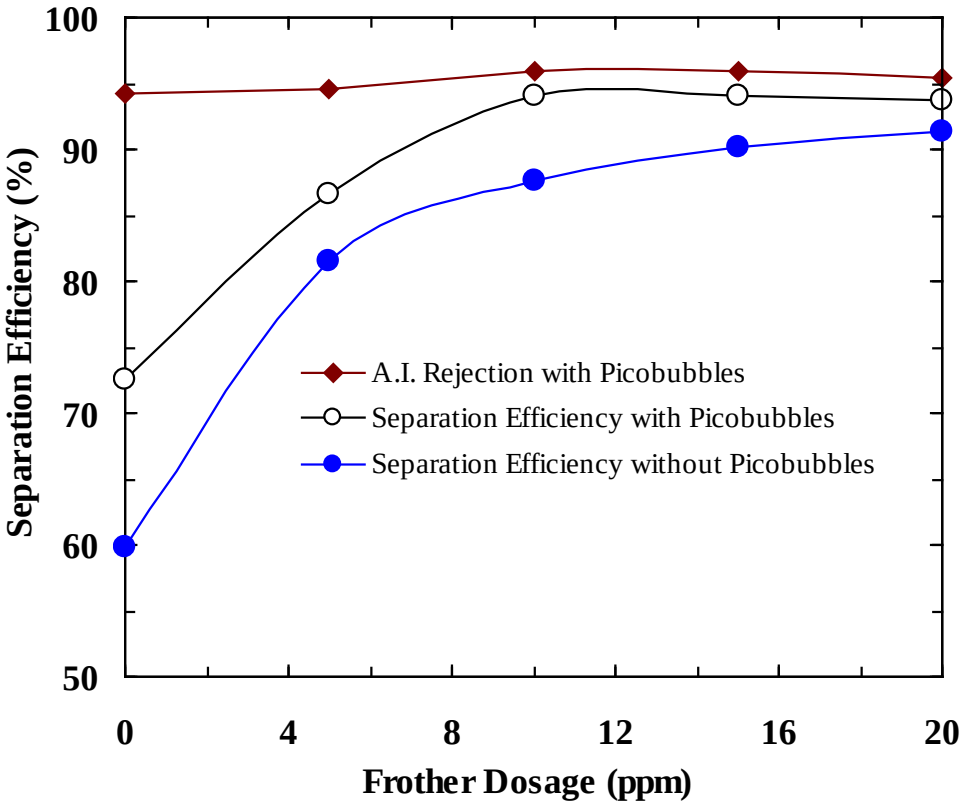

Figure 19. Effects of Picobubbles on Separation Efficiency at Varying Frother Dosages.

Based on the previous studies of the role of picobubbles in coarse phosphate particle flotation, a size-by-size analysis was performed to investigate their effect on coarse phosphate column flotation. The coarse phosphate particles (+0.425-1.18 mm) are classified into three particle size fractions: +0.85-1.18 mm, +0.60-0.85 mm, and +0.425-0.60 mm. The collector dosage and frother dosage were fixed at 0.9 kg/ton and 10 ppm, respectively. The investigation of the effect of picobubbles on the flotation rate of each particle size fraction was then performed.

Figure 20 shows the effect of picobubbles on the recovery-flotation time curves in which the P_2O_5 recovery for the +0.425-1.18 mm particle size fraction is plotted against the flotation time. The curves indicate that P_2O_5 recovery in the presence of picobubbles was significantly higher than in the absence of picobubbles, which means the presence of picobubbles can increase the flotation recovery of P_2O_5. When the cumulative flotation time was 1 minute, the P_2O_5 recovery in the presence of picobubbles was about 21% higher than in the absence of picobubbles. The difference in P_2O_5 recovery decreased as the cumulative flotation time was increased from 1 minute to 4 minutes. Figure 18 clearly demonstrates that the presence of picobubbles improved the flotation kinetics, owing to the higher-energy picobubbles adsorbed in the phosphate particles.

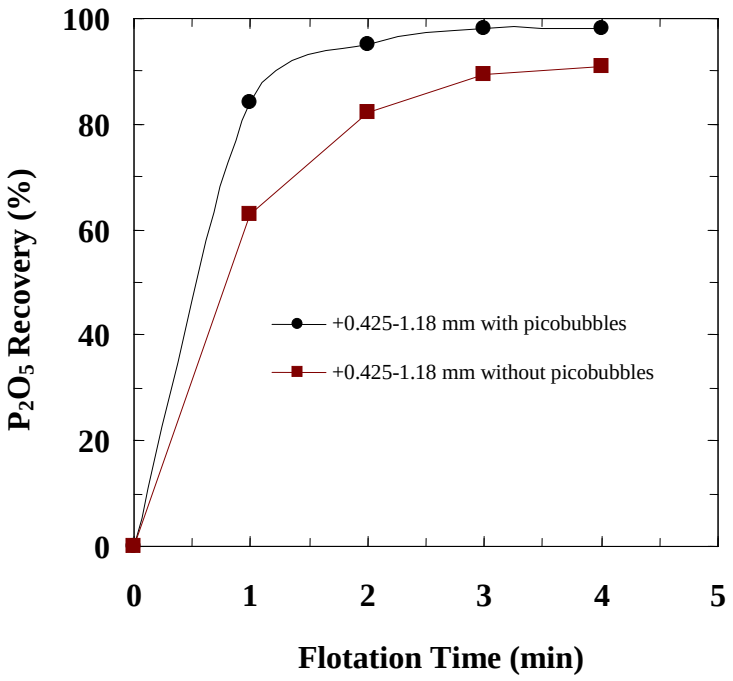

Figure 20. P_2O_5 Recovery as a Function of Flotation Time for +0.425-1.18 mm Phosphate.

Figures 21-23 show P_2O_5 recovery as a function of flotation time for +0.85-1.18 mm, +0.60-0.85 mm, and +0.425-0.60 mm phosphate particles, respectively. The P_2O_5 recovery in all size fractions in the presence of picobubbles was remarkably higher than in the absence of picobubbles. It can be clearly seen from comparing these three figures that the greatest effect of picobubbles on the improvement of P_2O_5 recovery occurred with the +0.85-1.18 mm particle size fraction. At 1 minute flotation time, the presence of picobubbles increased P_2O_5 recovery by about 27%, 25% and 19% for +0.85-1.18 mm, +0.60-0.85 mm, and +0.425-0.60 mm phosphate particles, respectively. The difference in P_2O_5 recovery for all particle size ranges decreased as the cumulative flotation time was increased from 1 minute to 4 minutes. The presence of picobubbles improved the flotation kinetics of each size fraction of phosphate particles studied.

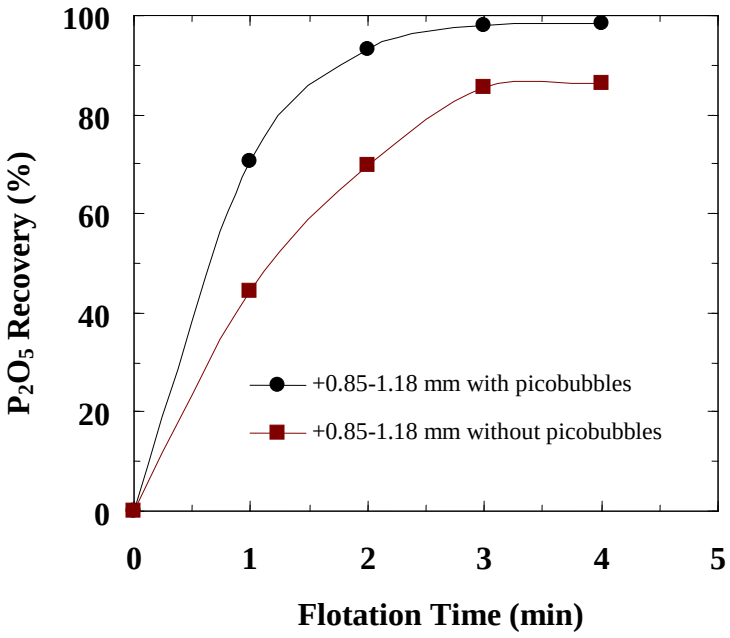

Figure 21. P_2O_5 Recovery as a Function of Flotation Time for +0.85-1.18 mm Phosphate.

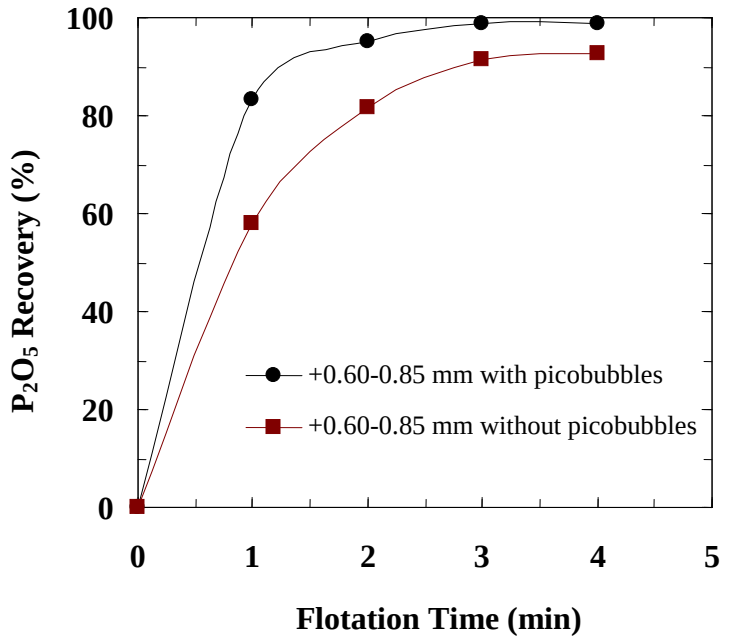

Figure 22. P_2O_5 Recovery as a Function of Flotation Time for +0.60-0.85 mm Phosphate.

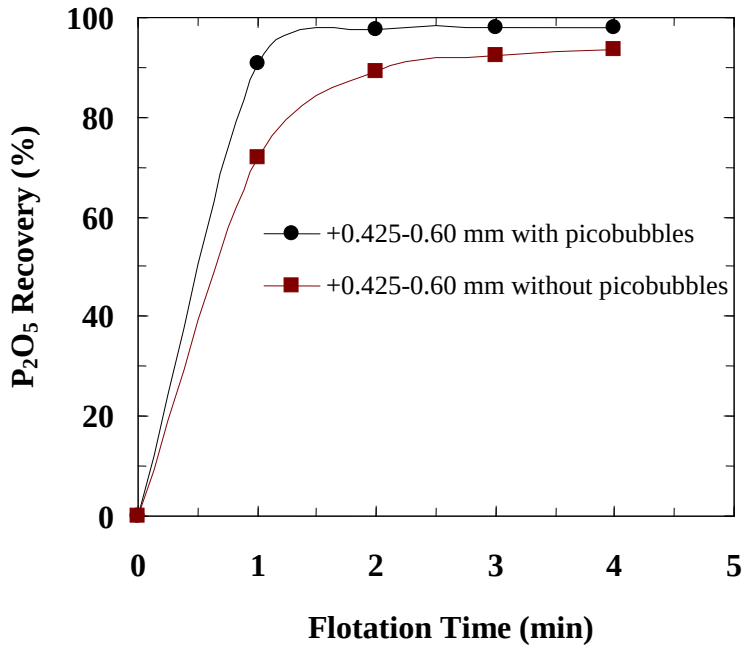

Figure 23. P_2O_5 Recovery as a Function of Flotation Time for +0.425-0.60 mm Phosphate.

Figures 24-27 show acid insols (A.I.) rejection as a function of flotation time for +0.425-1.18 mm, +0.85-1.18 mm, +0.60-0.85 mm, and +0.425-0.60 mm phosphate particles, respectively. The A.I. rejection of +0.425-1.18 mm, +0.60-0.85 mm, and +0.425-0.60 mm phosphate particle size fractions in the presence of picobubbles was higher than in the absence of picobubbles. In contrast with the picobubbles' effect on P_2O_5 recovery discussed previously, their presence increased the A.I. rejection less significantly for the +0.85-1.18 mm particle size range than the other particle fractions. The A.I. rejection of +0.85-1.18 mm phosphate particles in the presence of picobubbles was even slightly lower than in the absence of picobubbles because the flotation recovery with picobubbles was much higher than without picobubbles at two minutes of flotation time. After three minutes of flotation time, the A.I. rejection of +0.85-1.18 mm phosphate particles in the presence of picobubbles was higher than in the absence of picobubbles.

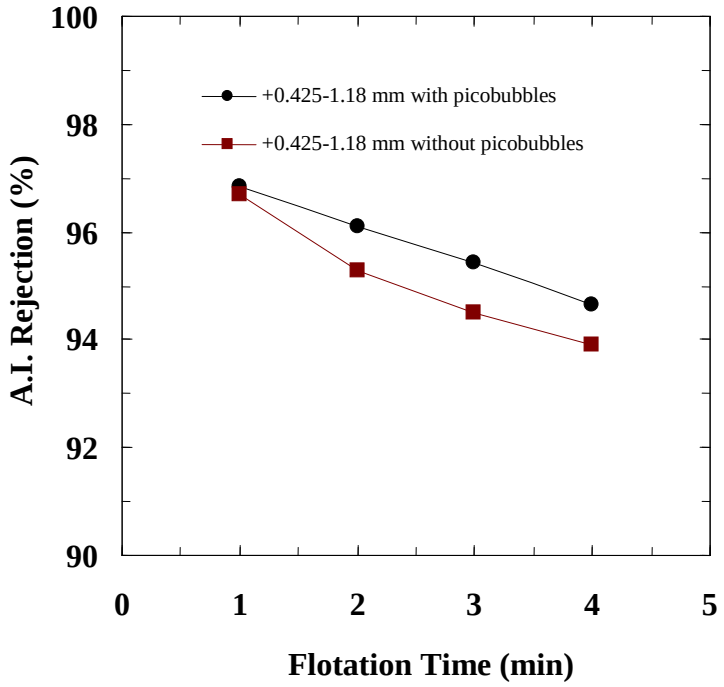

Figure 24. A.I. Rejection as a Function of Flotation Time for +0.425-1.18 mm Phosphate Particles.

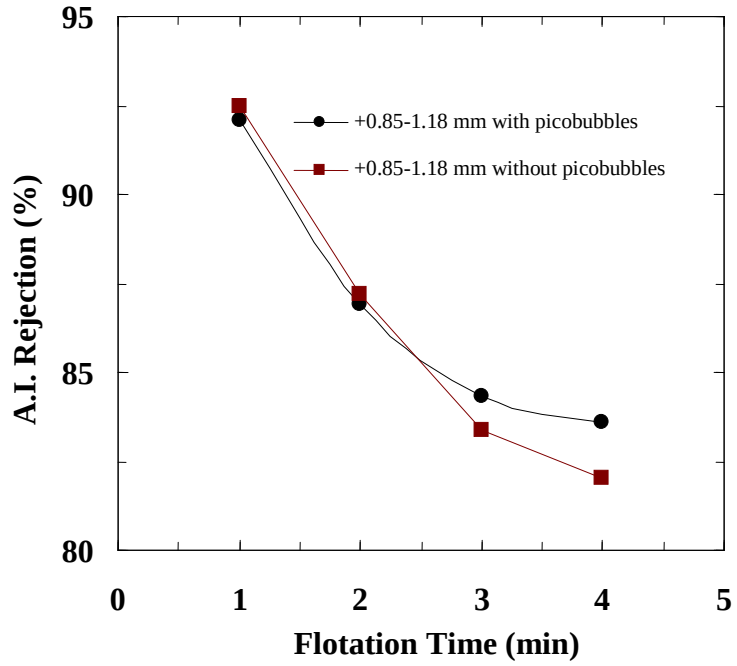

Figure 25. A.I. Rejection as a Function of Flotation Time for +0.85-1.18 mm Phosphate Particles.

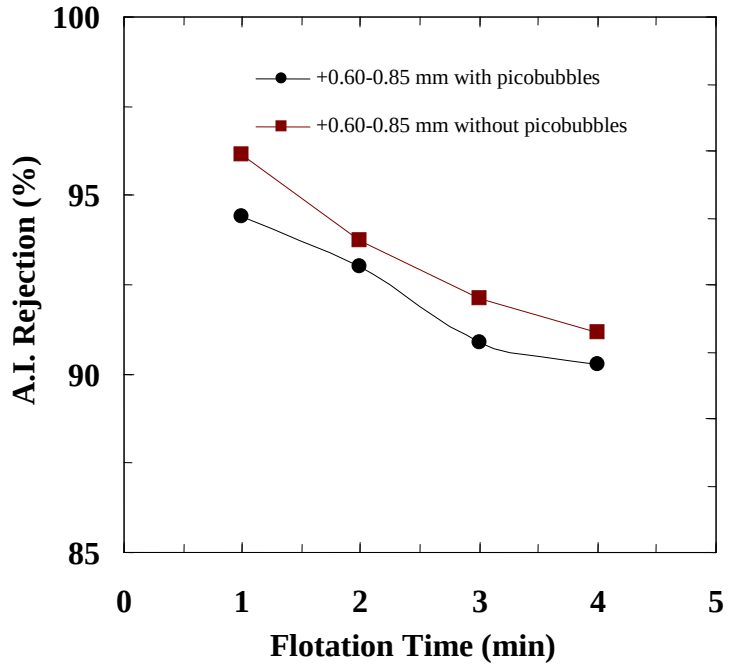

Figure 26. A.I. Rejection as a Function of Flotation Time for +0.60-0.85 mm Phosphate Particles.

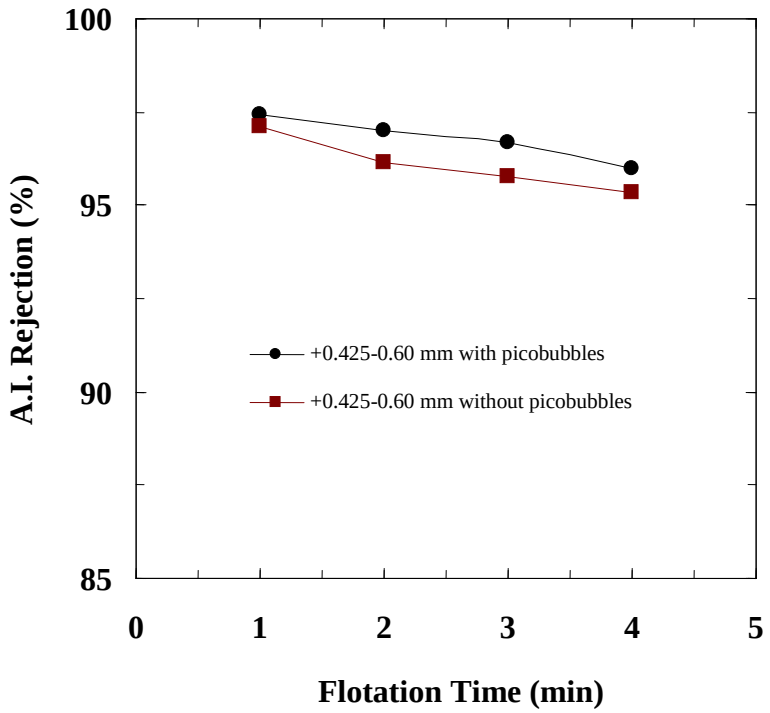

Figure 27. A.I. Rejection as a Function of Flotation Time for +0.425-0.60 mm Phosphate Particles.

Figures 28-31 show the effect of picobubbles on the flotation concentrate grade (P_2O_5) at varying P_2O_5 recovery for +0.425-1.18mm, +0.85-1.18 mm, +0.60-0.85 mm, and +0.425-0.60 mm phosphate particles, respectively. The P_2O_5 content in the flotation concentrate of all size fractions in the presence of picobubbles was higher than in the absence of picobubbles. At a 90% P_2O_5 recovery, the presence of picobubbles increased the P_2O_5 grade by about 0.7-1.0% for +0.425-1.18 mm, +0.60-0.85 mm, and +0.425-0.60 mm phosphate particles, which indicates that the presence of picobubbles improved the flotation selectivity for phosphate particles in each particle size.

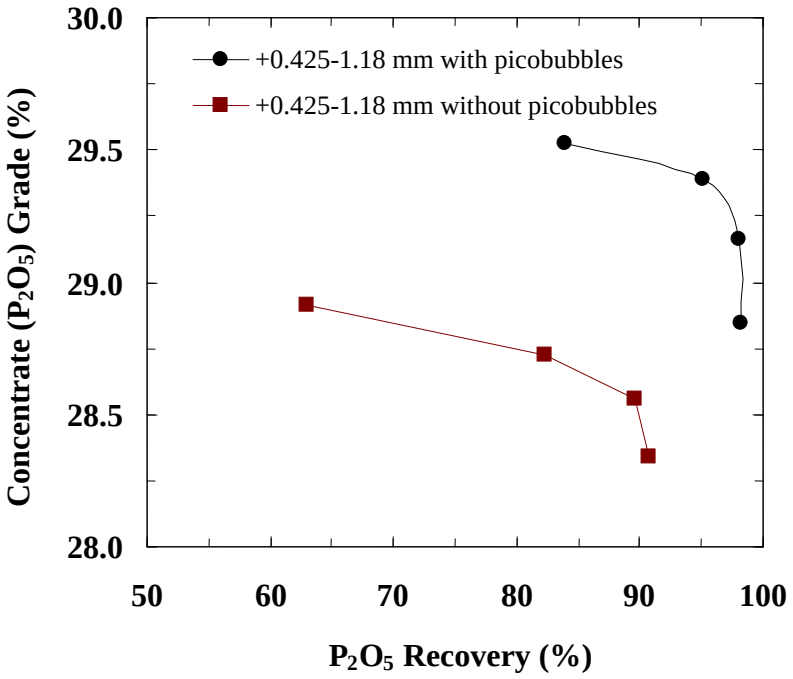

Figure 28. Concentrate Grade vs. Recovery for +0.425-1.18 mm Phosphate Particles.

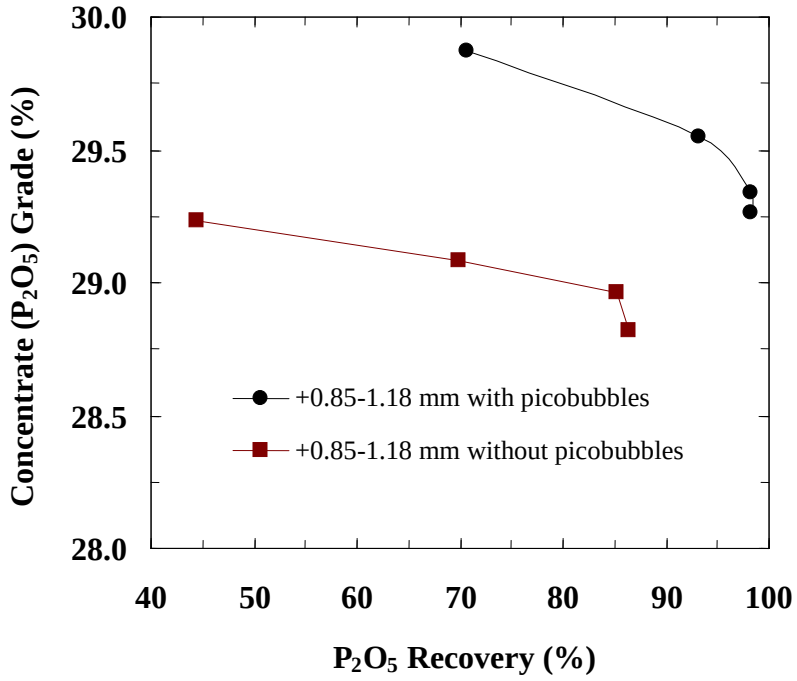

Figure 29. Concentrate Grade vs. Recovery for +0.85-1.18 mm Phosphate Particles.

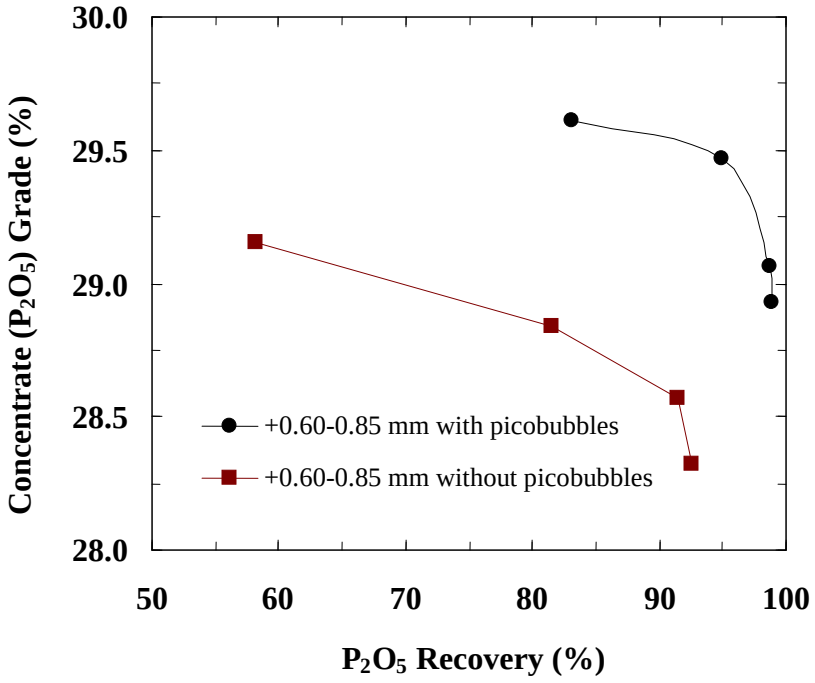

Figure 30. Concentrate Grade vs. Recovery for +0.60-85 mm Phosphate Particles.

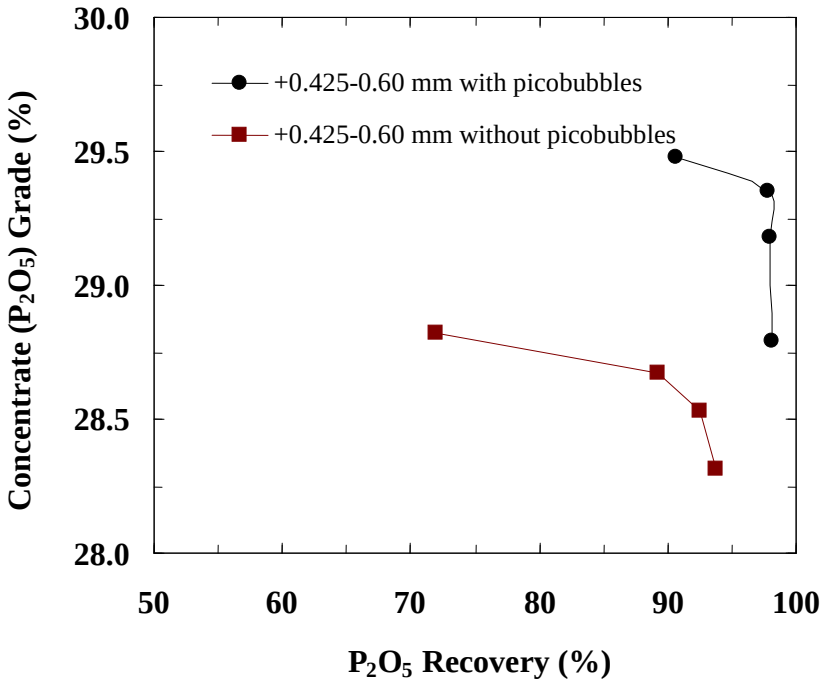

Figure 31. Concentrate Grade vs. Recovery for +0.60-85 mm Phosphate Particles.

PILOT-SCALE COLUMN FLOTATION TESTS

Response surface methodology was used to analyze the experiment data obtained with the pilot-scale flotation test results. Response surface, contours and cubic graphs were generated for P_2O_5 recovery, separation efficiency and concentrate grade as a function of frother concentration, slurry flow rate ratio between the cavitation tube and static mixer, and collector dosage. Figures 32-37 depict the effect of the studied parameters on P_2O_5 recovery, while Figures 38-43 reveal the effect of the studied parameters on separation efficiency.

The response surface and the contours of P_2O_5 recovery shown in Figure 32 depict the effect of frother dosage and flow rate ratio on P_2O_5 recovery when the collector dosage was at 1.6 kg/ton. The response surface and contours suggest that the P_2O_5 recovery increased with the flow rate ratio. The P_2O_5 recovery increased by about 5% as the flow rate ratio increased from 20 to 80%. There were no picobubbles generated when the process water flow rate was zero. Therefore, Figure 32 indicates the presence of picobubbles had significant effects on P_2O_5 recovery.

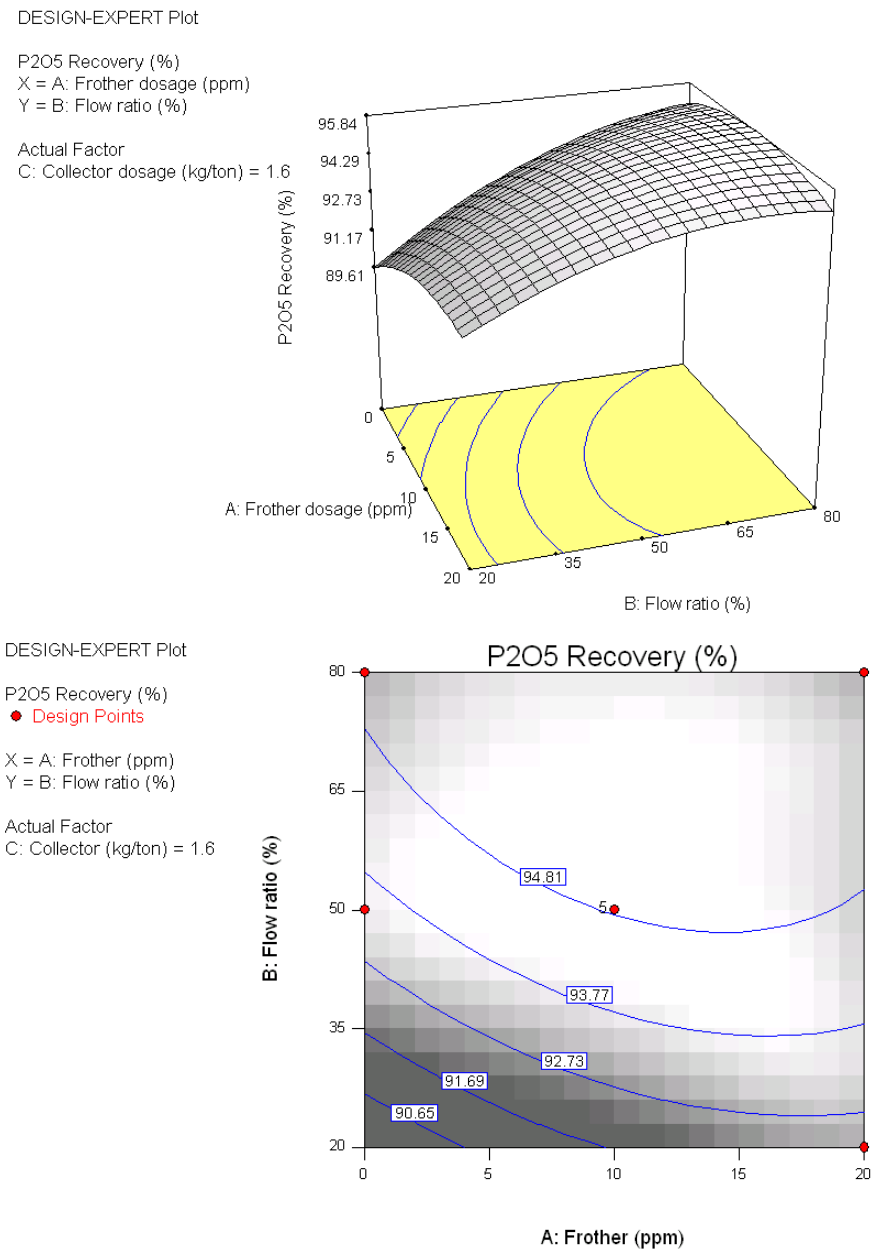

Figure 32. Effect of Frother Dosage and Flow Rate Ratio on P_2O_5 Recovery.

Figure 33 shows the effect of frother and collector dosage on P_2O_5 recovery at a flow rate ratio of 50%. The response surface and contours suggest that the area of highest P_2O_5 recovery was attained at the middle level of the flow rate ratio. It can be seen from Figure 33 that the collector dosage had a significant effect on P_2O_5 recovery. The P_2O_5 recovery increased by more than 5.5% as collector dosage increased from 0.8 kg/ton to 2.4 kg/ton.

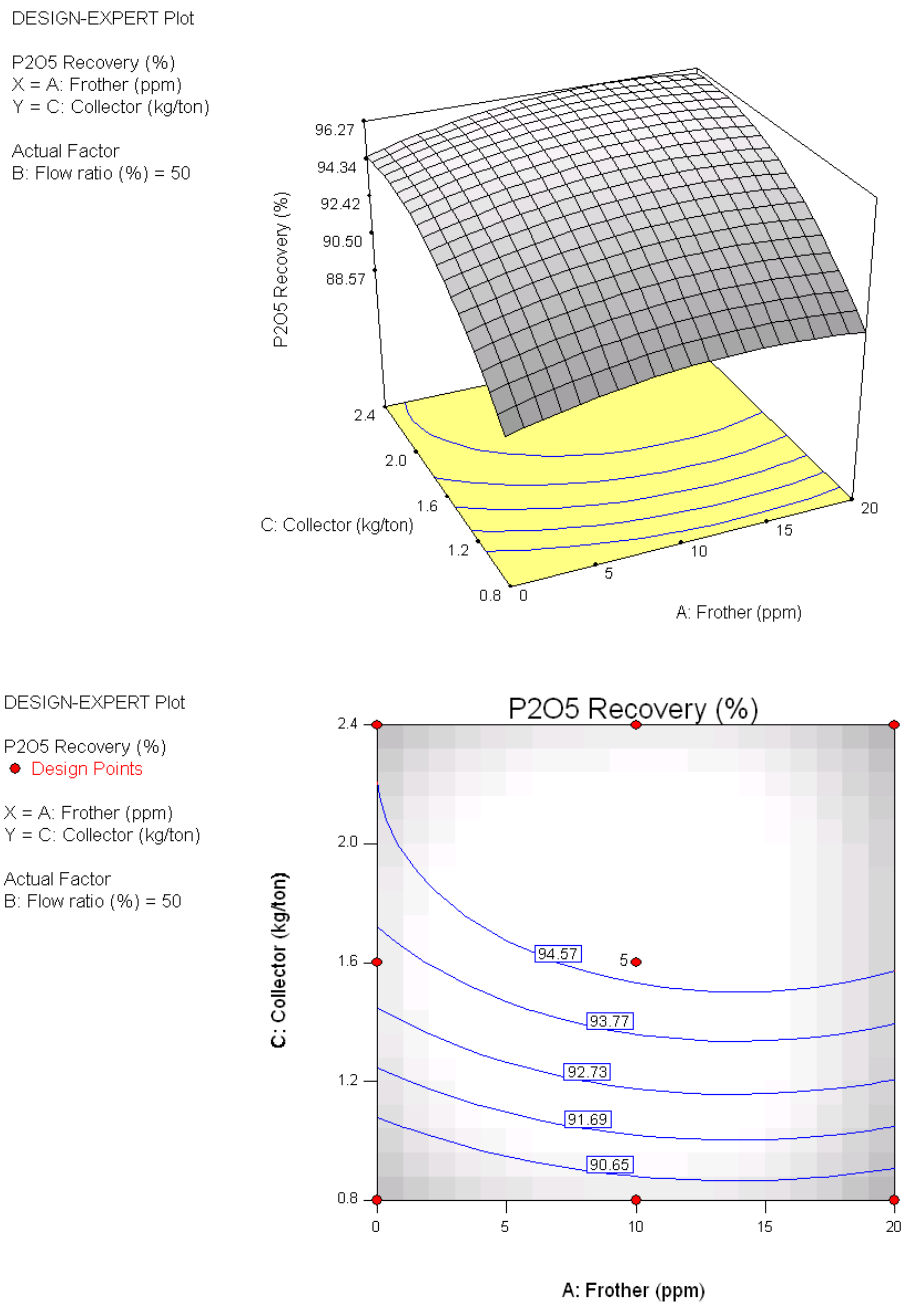

Figure 33. Effect of Collector Dosage and Frother Dosage on P_2O_5 Recovery.

Figure 34 depicts the effect of flow rate ratio and collector dosage on P_2O_5 recovery at a frother dosage of 10 ppm. The response surface and contours suggest that the area of highest P_2O_5 recovery was at the high level of the flow rate ratio and the high level of collector dosage. The P_2O_5 recovery increased by about 8% as the flow rate ratio and collector dosage increased from 20% and 0.8 kg/ton to 50% and 1.6 kg/ton, respectively. The presence of picobubbles generated by cavitation and the collector dosage had significant effects on P_2O_5 recovery.

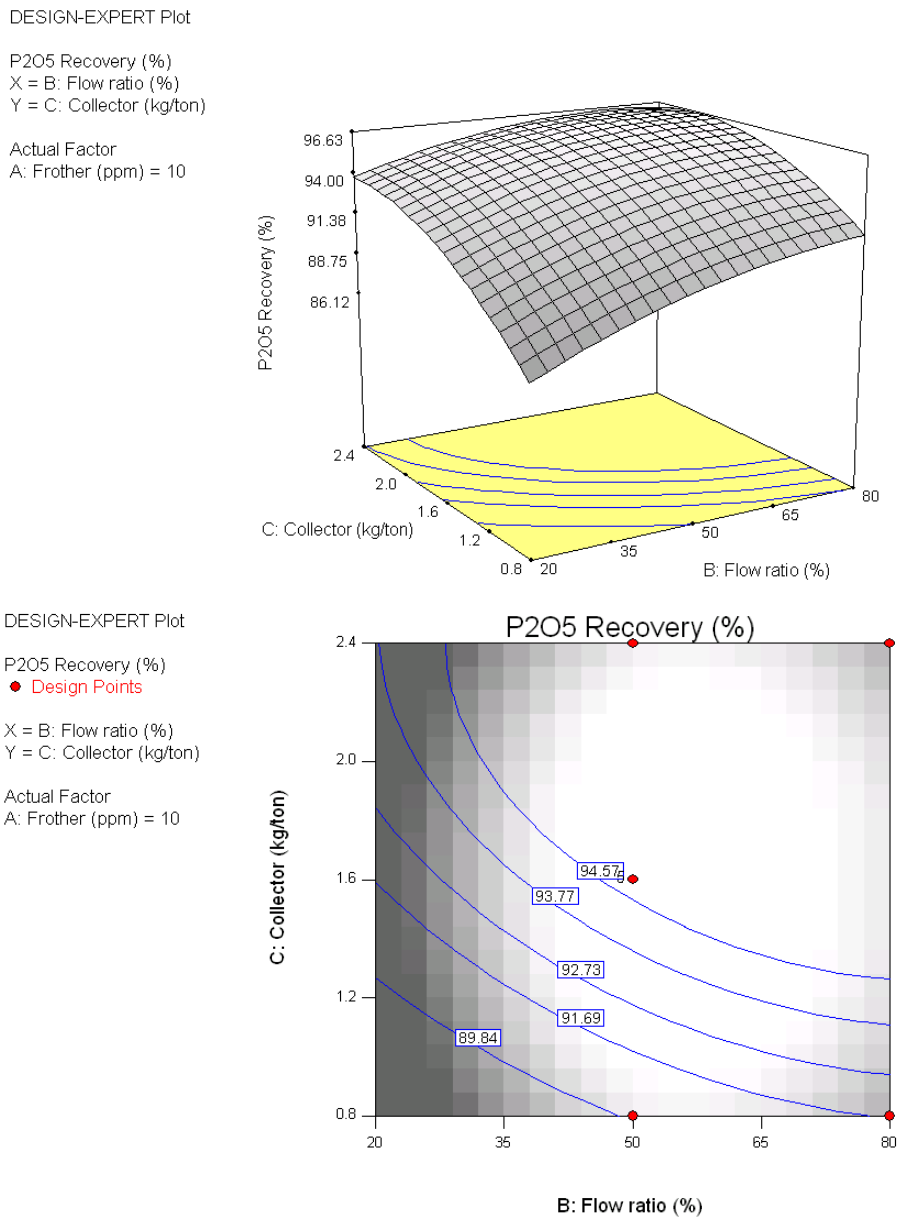

Figure 34. Effect of Flow Rate Ratio and Collector Dosage on P_2O_5 Recovery.

Figure 35 shows how the three factors of collector dosage, flow rate ratio and frother dosage affected the response, i.e., the P_2O_5 recovery. The P_2O_5 recovery was at maximum at the A+, B+, C+ settings (upper back right corner with a response of 95.56%). A normal probability plot of the residuals is shown in Figure 36. The data points are approximately linear, indicating no abnormalities.

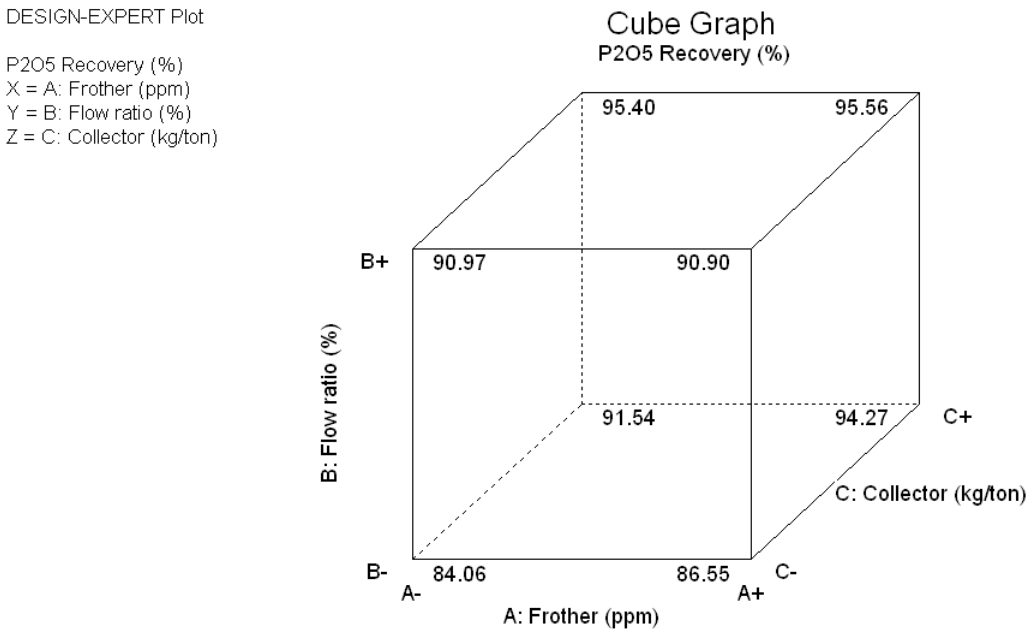

Figure 35. Effect of Frother Dosage, Flow Rate Ratio and Collector Dosage on P_2O_5 Recovery.

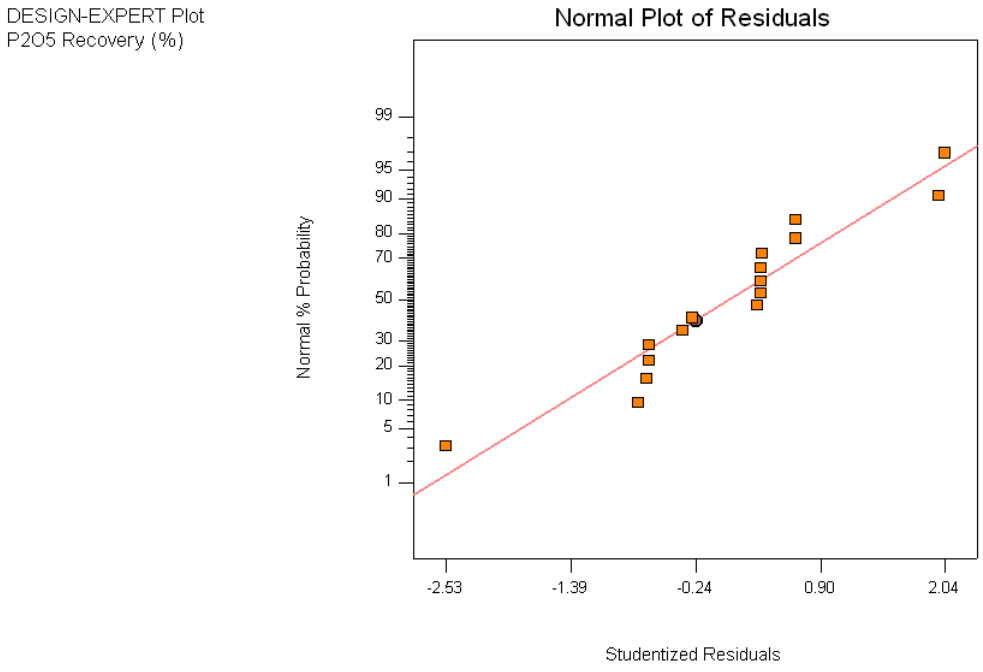

Figure 36. Normal Probability Plot of Residual for P_2O_5 Recovery.

The statistical analysis of the experimental data gave rise to Equation 1 for P_2O_5 recovery in terms of coded factors:

P_2O_5 Recovery (%) = A + 94.85 A + 0.66* A + 2.05* B + 3.04* C – 0.82* A^2 – 1.06* B^2 – 1.82* C^2 – 0.64* A * B + 0.059* A * C – 0.76* B * C (1)

which is equivalent to Equation 2:

P_2O_5 Recovery (%) = +70.17130

+0.32569	* Frother (ppm)
+0.25822	* Flow ratio (%)
+14.39428	* Collector (kg/ton)
-8.21096E-003	* Frother (ppm)^2
-1.17480E-003	* Flow ratio (%)^2
-2.83778	* Collector (kg/ton)^2
-2.13931E-003	* Frother (ppm) * Flow ratio (%)
+7.40582E-003	* Frother (ppm) * Collector (kg/ton)
-0.031841	* Flow ratio (%) * Collector (kg/ton) (2)

Table 6. Analysis of Variance Table of P_2O_5 Recovery (%).

Source	Sum of Squares	DF	Mean Square	F Value	Prob > F	
Model	89.77	9	9.97	9.27	0.0039	significant
A	*2.09*	*1*	*2.09*	*1.94*	*0.2062*	
B	*5.86*	*1*	*5.86*	*5.44*	*0.0524*	
C	*55.32*	*1*	*55.32*	*51.39*	*0.0002*	
A^2	*2.54*	*1*	*2.54*	*2.36*	*0.1683*	
B^2	*1.30*	*1*	*1.30*	*1.20*	*0.3087*	
C^2	*12.76*	*1*	*12.76*	*11.85*	*0.0108*	
AB	*0.58*	*1*	*0.58*	*0.54*	*0.4869*	
AC	*0.014*	*1*	*0.014*	*0.013*	*0.9123*	
BC	*0.88*	*1*	*0.88*	*0.81*	*0.3970*	
Residual	7.53	7	1.08			
Lack of Fit	*7.53*	*3*	*2.51*	*11407.33*	*< 0.0001*	*significant*
Pure Error	*8.806E-004*	*4*	*2.201E-004*			
Cor Total	97.31	16				

The model F-value of 9.27 implies the model is significant. There is only a 0.39% chance that a model f-value of this magnitude could occur due to noise. Values of Prob > F of less than 0.0500 indicate that model terms are significant. B, C, C^2 are significant model terms.

Figure 37 depicts the relationship between the actual and predicted P_2O_5 recovery values by the above P_2O_5 recovery model. It can be seen from the plot that the P_2O_5 recovery model may be used to predict the effect of collector dosage, flow rate ratio and frother dosage on P_2O_5 recovery.

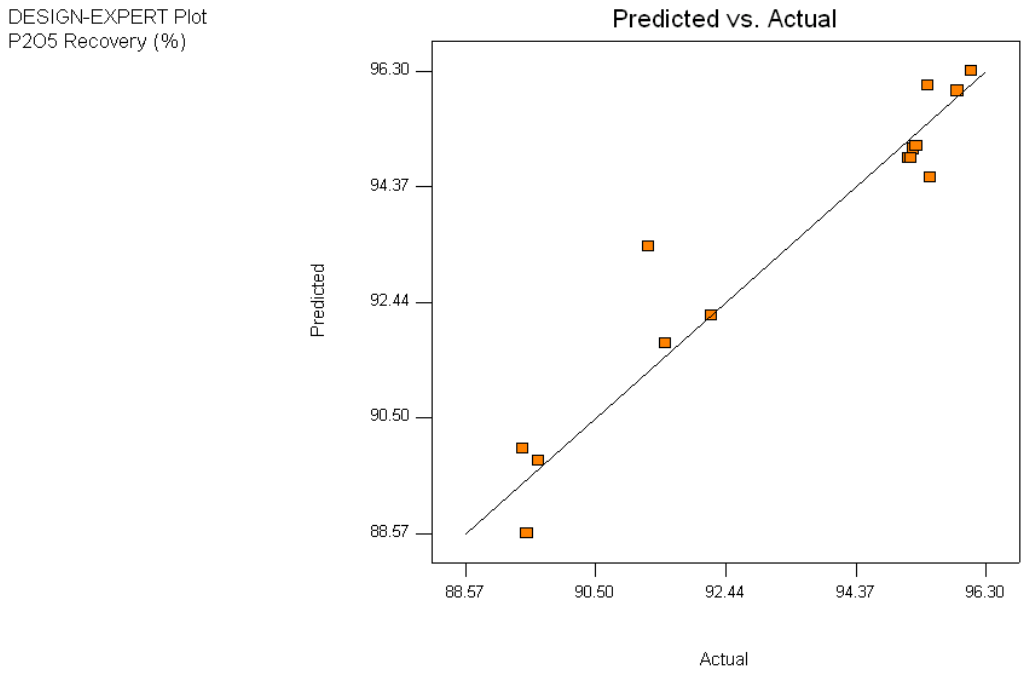

Figure 37. Relationship between Actual and Predicted P_2O_5 Recovery Values by P_2O_5 Recovery Model.

Figure 38 depicts the effect of frother dosage and flow rate ratio on separation efficiency (= P_2O_5 recovery + A.I. rejection – 100%) when collector dosage was 1.6 kg/ton. The response surface and contours suggest that the area of the highest separation efficiency was at the high level of flow rate ratio and the frother dosage of about 15 ppm. When the frother dosage was 10 ppm, the separation efficiency increased by about 4.5% as the flow rate ratio increased from 20% to 80%. This indicates the presence of picobubbles had significant effects on separation efficiency.

Figure 39 shows the effect of frother dosage and collector dosage on separation efficiency when the flow rate ratio was 50%. The response surface and contours suggest that the area of the highest separation efficiency was attained at the high level of flow rate ratio when the frother dosage was about 15 ppm. The separation efficiency increased by about 7% as collector dosage increased from 0.8 kg/ton to 2.4 kg/ton.

Figure 40 depicts the effect of flow rate ratio and collector dosage on separation efficiency when the frother dosage was 10 ppm. The response surface and contours suggest that the area of the highest separation efficiency was attained at the high level of flow rate ratio and high level of collector dosage. The separation efficiency increased by about 10% as flow rate ratio and collector dosage increased from 20% and 0.8 kg/ton to 80% and 2.4 kg/ton, respectively.

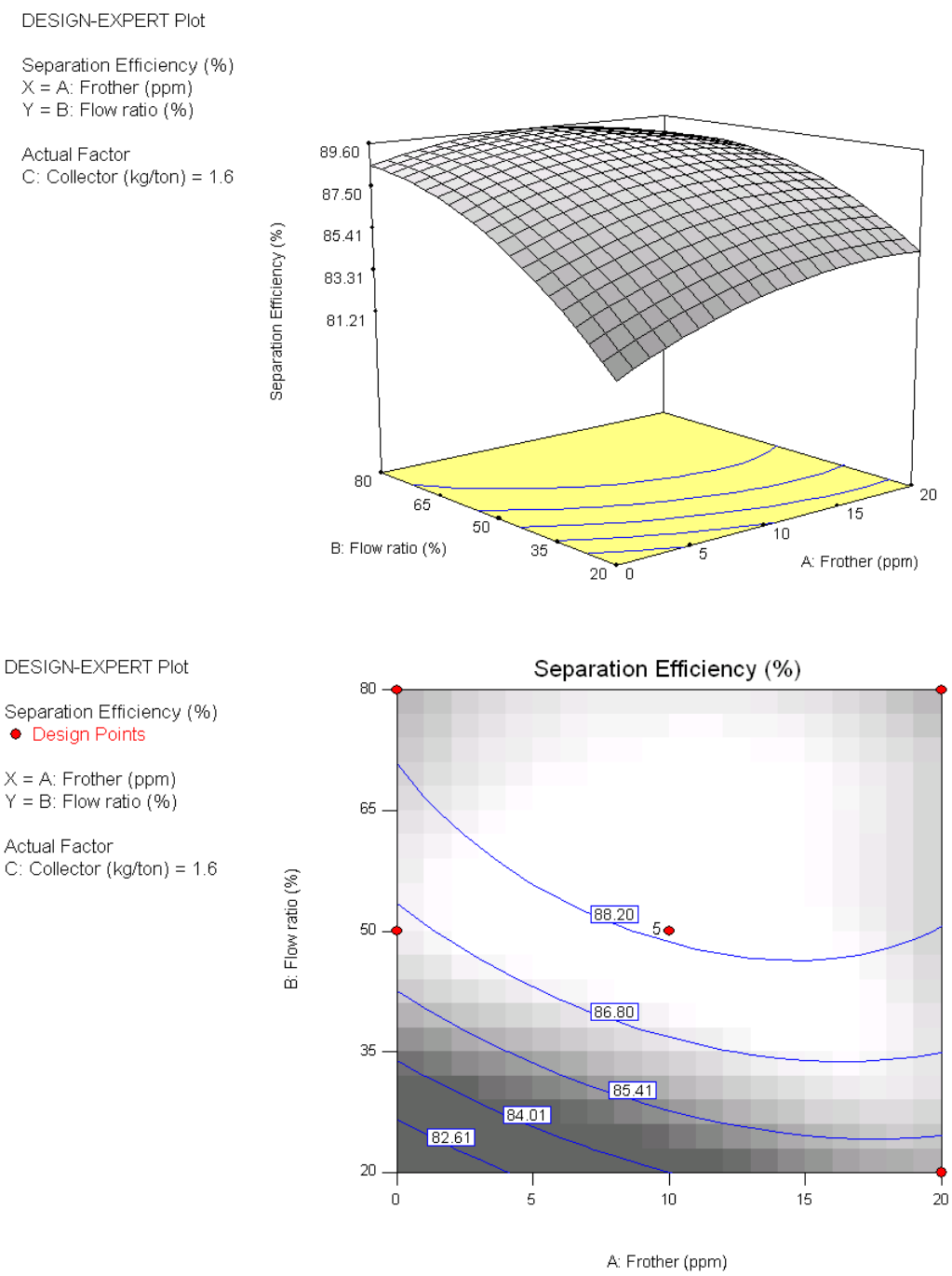

Figure 38. Effect of Flow Rate Ratio and Frother Flow Rate on Separation Efficiency.

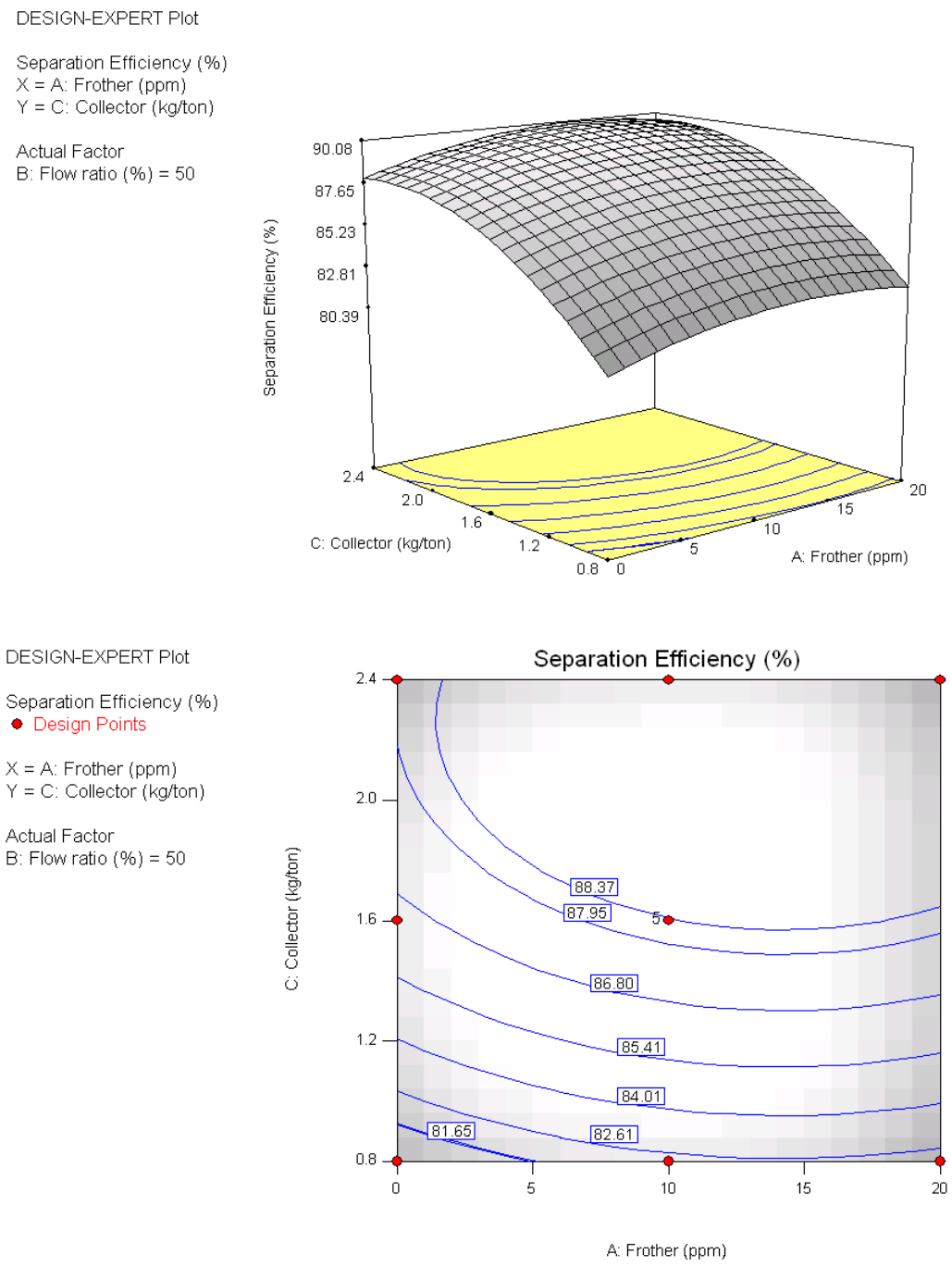

Figure 39. Effect of Frother Dosage and Collector Dosage on Separation Efficiency.

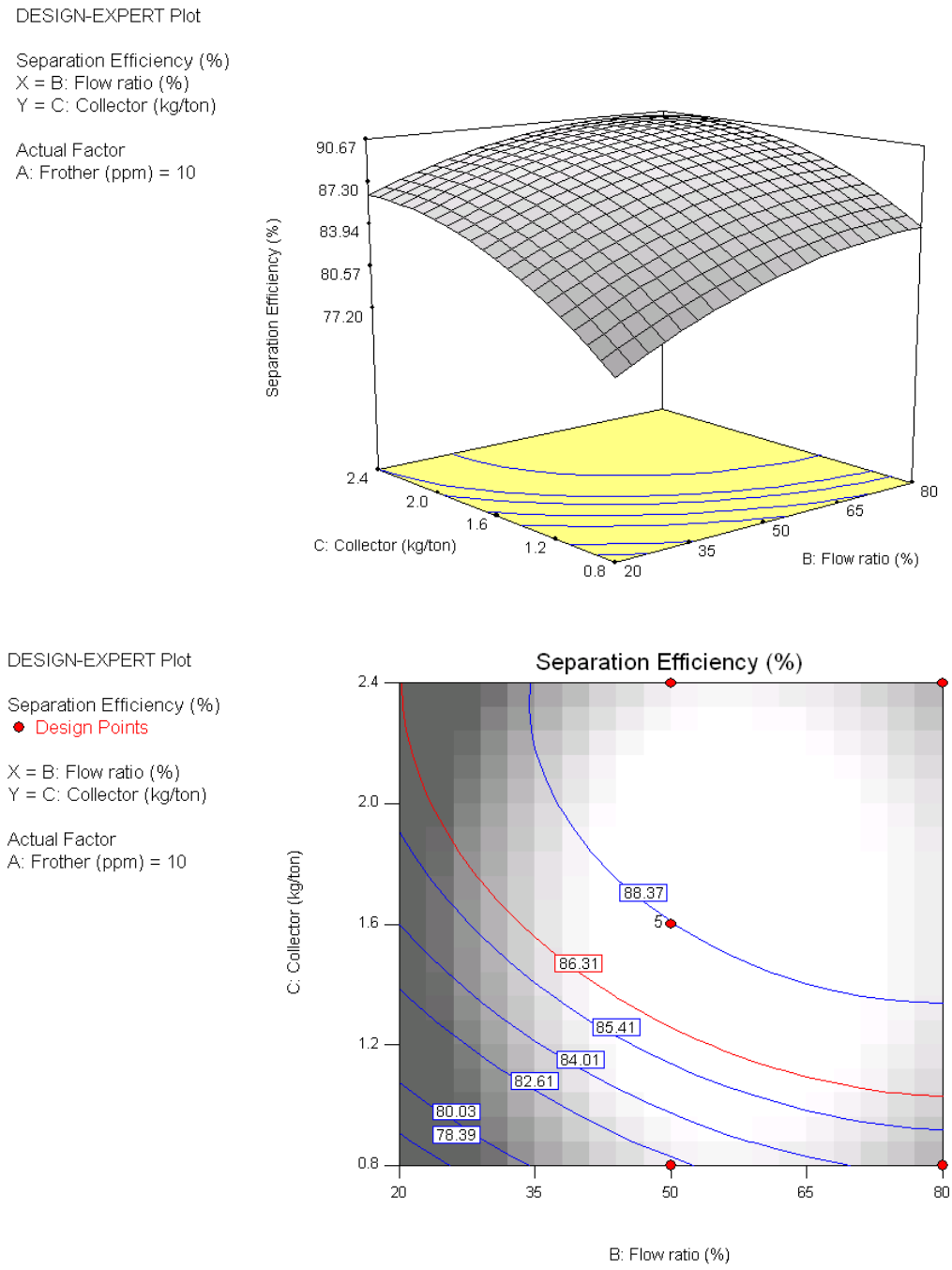

Figure 40. Effect of Flow Rate Ratio and Collector Dosage on Separation Efficiency.

Figure 41 depicts how three factors, collector dosage, flow rate ratio and frother dosage, affect the separation efficiency. As with the flotation recovery, the separation efficiency was at its maximum at the A+, B+, C+ settings (upper back right corner with response 89.26%). Figure 42 shows a normal probability plot of the residuals. The data points are approximately linear, indicating no abnormalities.

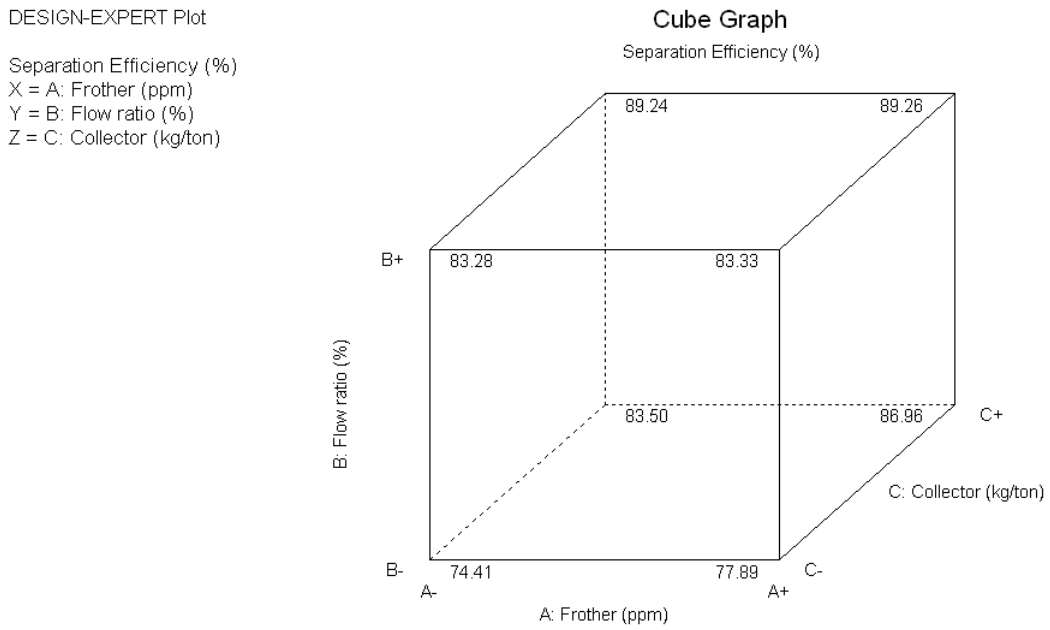

Figure 41. Effect of Frother Dosage, Flow Rate Ratio and Collector Dosage on Separation Efficiency.

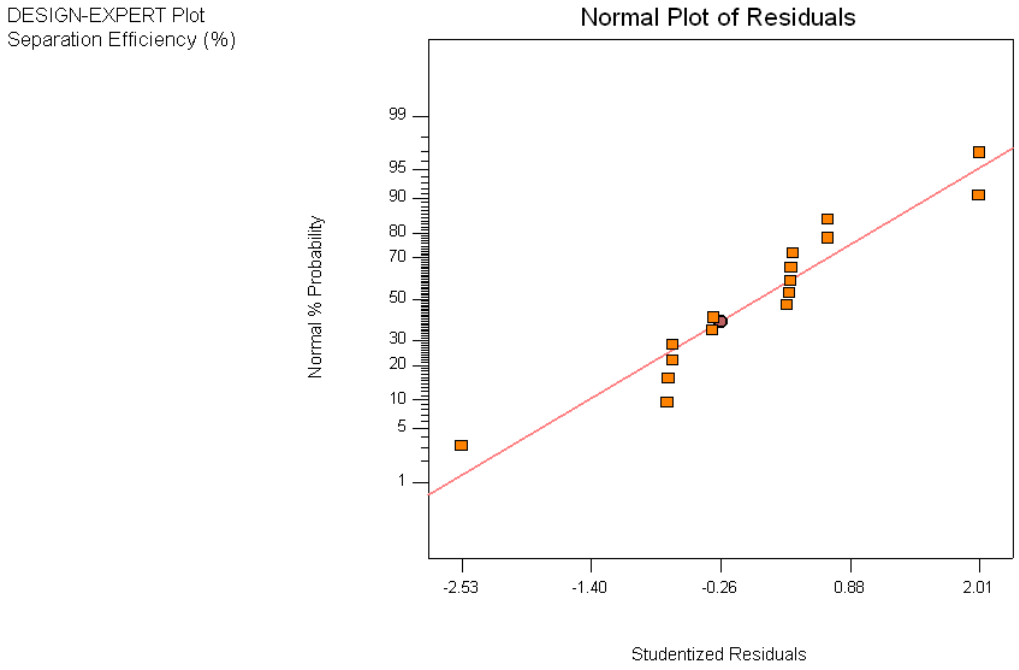

Figure 42. Normal Probability Plot of Residual for Separation Efficiency.

Equation 3 for separation efficiency in terms of coded factors was obtained from statistical analysis of the experimental data:

$$\begin{aligned}\text{Separation Efficiency (\%)} = {} & +88.33 \\ & + 0.88 * A \\ & +2.79 * B \\ & +3.75 * C \\ & -1.05 * A^2 \\ & -1.54 * B^2 \\ & -2.26 * C^2 \\ & -0.86 * A * B \\ & -5.746E\text{-}003 * A * C \\ & -0.78 * B * C \end{aligned} \quad (3)$$

Separation efficiency in terms of actual factors is described in Equation 4:

$$\begin{aligned}\text{Separation Efficiency (\%)} = {} & +56.86807 \\ & +0.44147 * \text{Frother (ppm)} \\ & +0.34570 * \text{Flow ratio (\%)} \\ & +17.61808 * \text{Collector (kg/ton)} \\ & -0.010477 * \text{Frother (ppm)}^2 \\ & -1.71634E\text{-}003 * \text{Flow ratio (\%)}^2 \\ & -3.52574 * \text{Collector (kg/ton)}^2 \\ & -2.86095E\text{-}003 * \text{Frother (ppm) * Flow ratio (\%)} \\ & -7.18286E\text{-}004 * \text{Frother (ppm) * Collector (kg/ton)} \\ & -0.032699 * \text{Flow ratio (\%) * Collector (kg/ton)} \end{aligned} \quad (4)$$

Table 7. Analysis of Variance Table of Separation Efficiency.

Source	Sum of Squares	DF	Mean Square	F Value	Prob > F	
Model	141.80	9	15.76	8.55	0.0049	significant
A	*3.65*	*1*	*3.65*	*1.98*	*0.2019*	
B	*10.86*	*1*	*10.86*	*5.90*	*0.0455*	
C	*84.59*	*1*	*84.59*	*45.91*	*0.0003*	
A^2	*4.14*	*1*	*4.14*	*2.25*	*0.1777*	
B^2	*2.77*	*1*	*2.77*	*1.50*	*0.2600*	
C^2	*19.69*	*1*	*19.69*	*10.69*	*0.0137*	
AB	*1.04*	*1*	*1.04*	*0.56*	*0.4777*	
AC	*1.321E-004*	*1*	*1.321E-004*	*7.169E-005*	*0.9935*	
BC	*0.92*	*1*	*0.92*	*0.50*	*0.5018*	
Residual	12.90	7	1.84			
Lack of Fit	*12.89*	*3*	*4.30*	*7507.81*	*< 0.0001*	*significant*
Pure Error	*2.290E-003*	*4*	*5.725E-004*			
Cor Total	154.69	16				

The model F-value of 8.55 implies the model is significant. There is only a 0.49% chance that this model F-value could occur due to noise. Since their values of Prob > F are less than 0.0500, B, C, C^2 are significant model terms. Values greater than 0.1000 indicate the model terms are not significant.

Figure 43 shows the relationship between actual and predicted separation efficiency values by the above separation efficiency model. The plot proves that the separation efficiency model may be used to predict separation efficiency according to collector dosage, flow rate ratio and frother dosage.

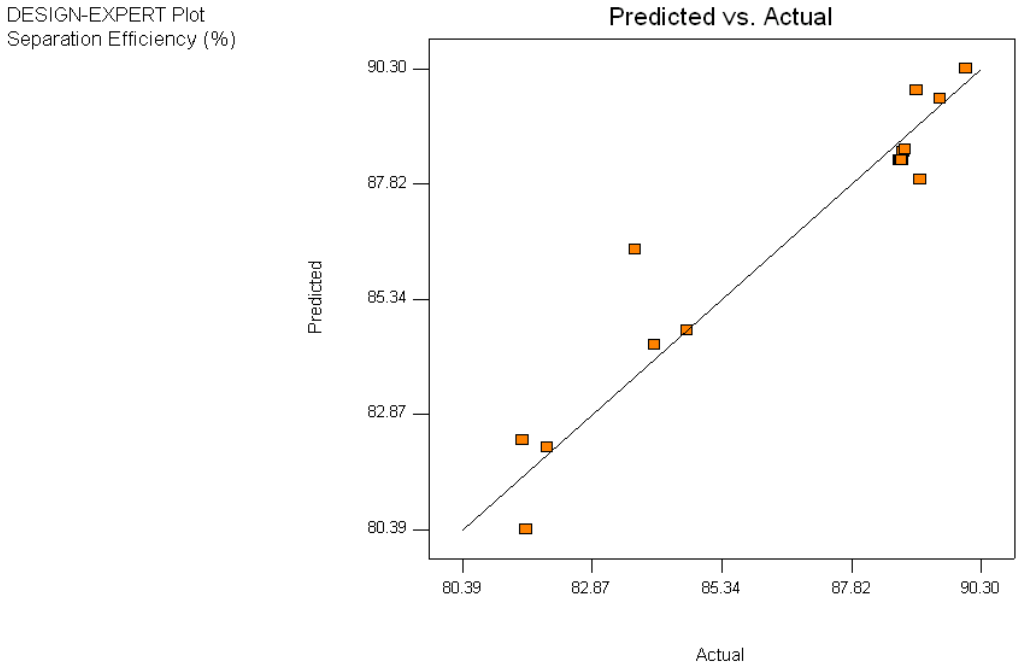

Figure 43. Relationship between Actual and Predicted Values of Separation Efficiency Model.

Figure 44 shows the effect of frother dosage and flow rate ratio on concentrate P_2O_5 grade when collector dosage was at 1.6 kg/ton. The response surface and contours suggest that the area of the highest concentrate P_2O_5 grade was attained at the high level of flow rate ratio and the middle to high level of frother dosage.

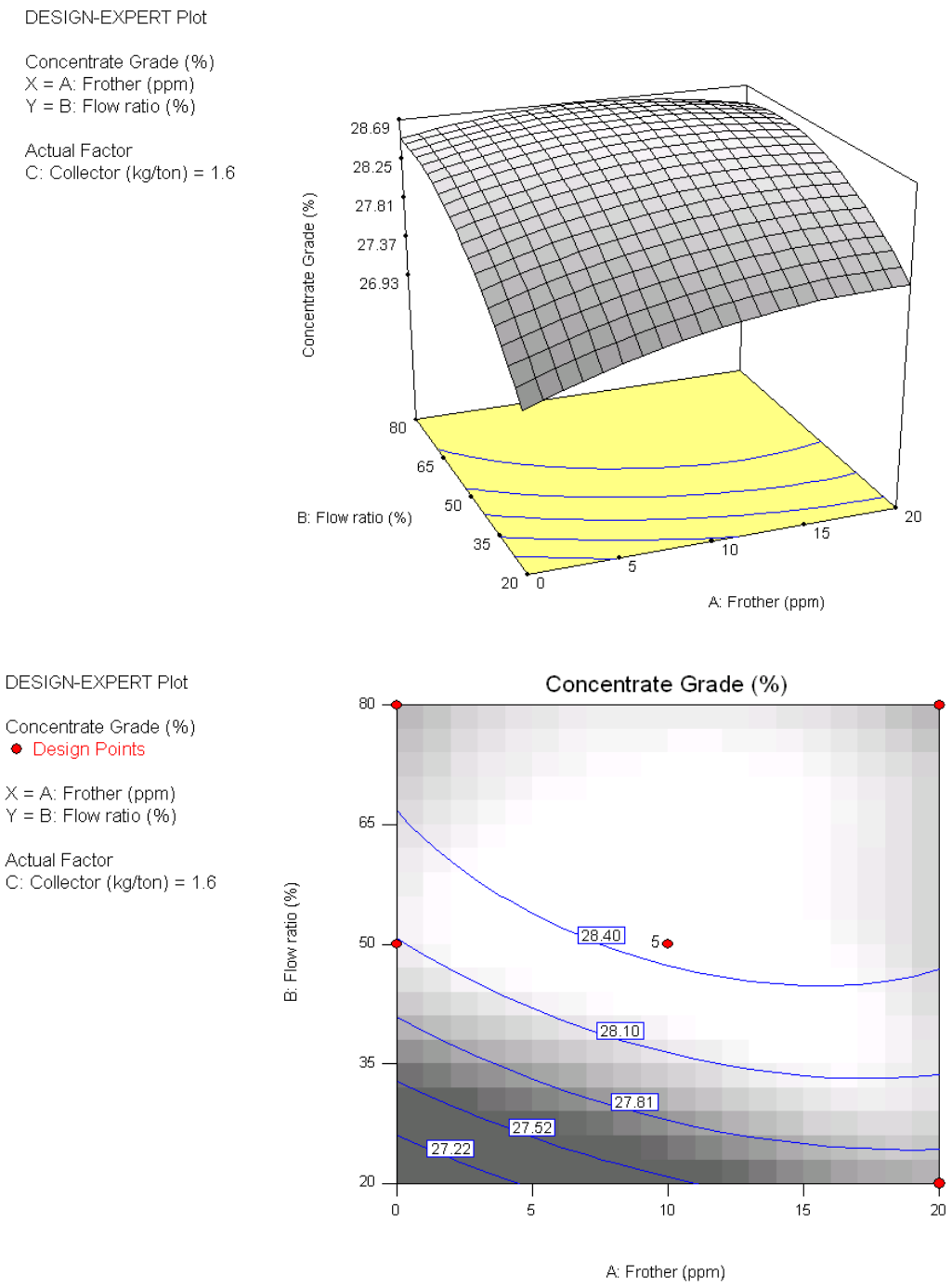

Figure 44. Effect of Frother Dosage and Flow Rate Ratio on Concentrate Grade.

Statistical analysis of the experimental data yielded Equation 5 for P_2O_5 concentrate grade in terms of coded factors:

Concentrate Grade (%) = +28.45

	+0.18	* A
	+0.60	* B
	+0.64	* C
	-0.19	* A^2
	-0.38	* B^2
	-0.40	* C^2
	-0.18	* A * B
	-0.046	* A * C
	-0.049	* B * C (5)

which is equivalent to Equation 6 in terms of actual factors:

Concentrate Grade (%) = +22.63348

	+0.094878	* Frother (ppm)
	+0.070946	* Flow ratio (%)
	+2.93255	* Collector (kg/ton)
	-1.89080E-003	* Frother $(ppm)^2$
	-4.18840E-004	* Flow ratio $(\%)^2$
	-0.61794	* Collector $(kg/ton)^2$
	-5.95983E-004	* Frother (ppm) * Flow ratio (%)
	-5.72125E-003	* Frother (ppm) * Collector (kg/ton)
	-2.03422E-003	* Flow ratio (%) * Collector (kg/ton) (6)

Under the conditions of 20 ppm frother dosage and 1.6 kg/ton collector dosage, a further study was conducted to assess the effect of the flow rate ratio (picobubbles) on the flotation performance of different size phosphate particles. Figure 45 shows the effect of the flow rate ratio (picobubbles) on product grade and flotation P_2O_5 recovery. It can be clearly seen from Figure 45 that flotation P_2O_5 recovery at the low flow ratio decreased from 96.7% to 93.9% to 85.7% and finally to 85.6% as phosphate particle size increased from 0.43 to 0.60 to 0.85 and finally to 1.18 mm, respectively. Figure 45 shows that the presence of picobubbles at the high flow ratio improved flotation recovery by 2.8% and 6.6% for phosphate particles of 0.6 mm and 0.8 mm, respectively. It can also be seen from Figure 45 that product grade was improved by increasing the flow rate ratio.

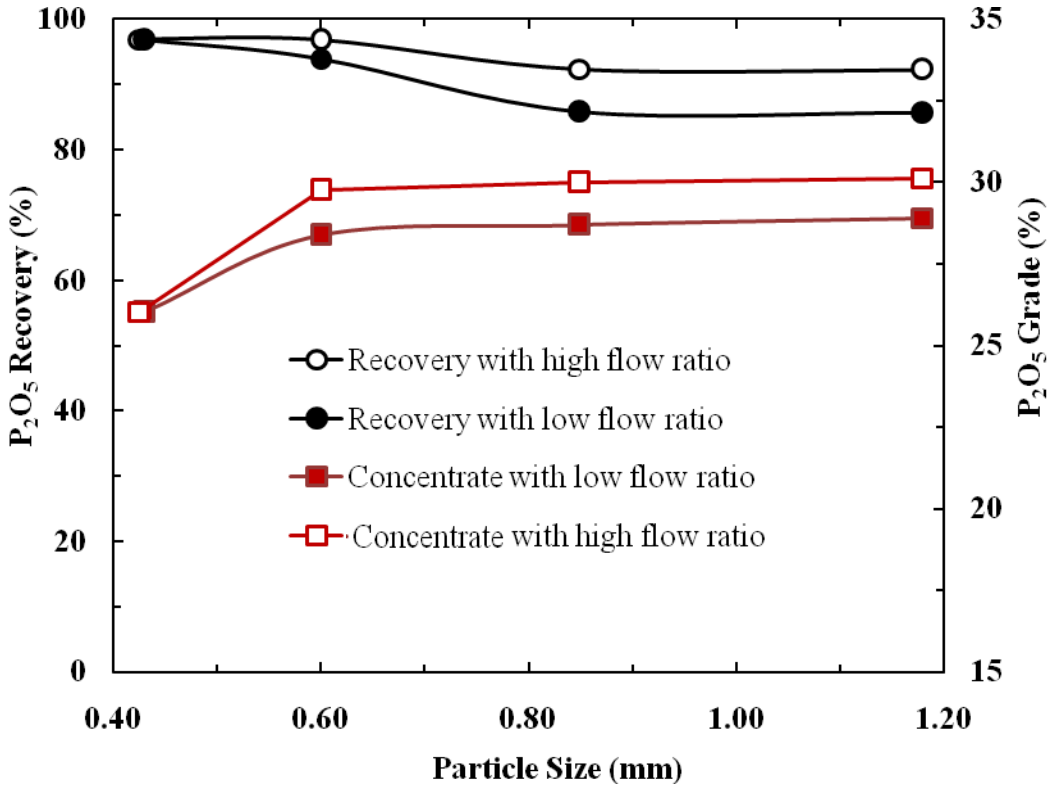

Figure 45. Effect of Picobubbles on Flotation P_2O_5 Recovery and Product Grade at Varying Phosphate Particle Size.

Figure 46 shows the effect of the flow rate ratio (picobubbles) on the separation efficiency of varying sizes of phosphate particles. It can be seen from Figure 46 that the separation efficiency at the low flow ratio decreased from 90.0% to 88.1%, then to 77.5% and finally 74.4% as phosphate particle size increased from 0.43 to 0.60 to 0.85 and finally to 1.18 mm, respectively. The presence of picobubbles at the high flow ratio improved flotation efficiency by 4.4% and 8.7% for phosphate particles of 0.6 mm and 0.8 mm, respectively.

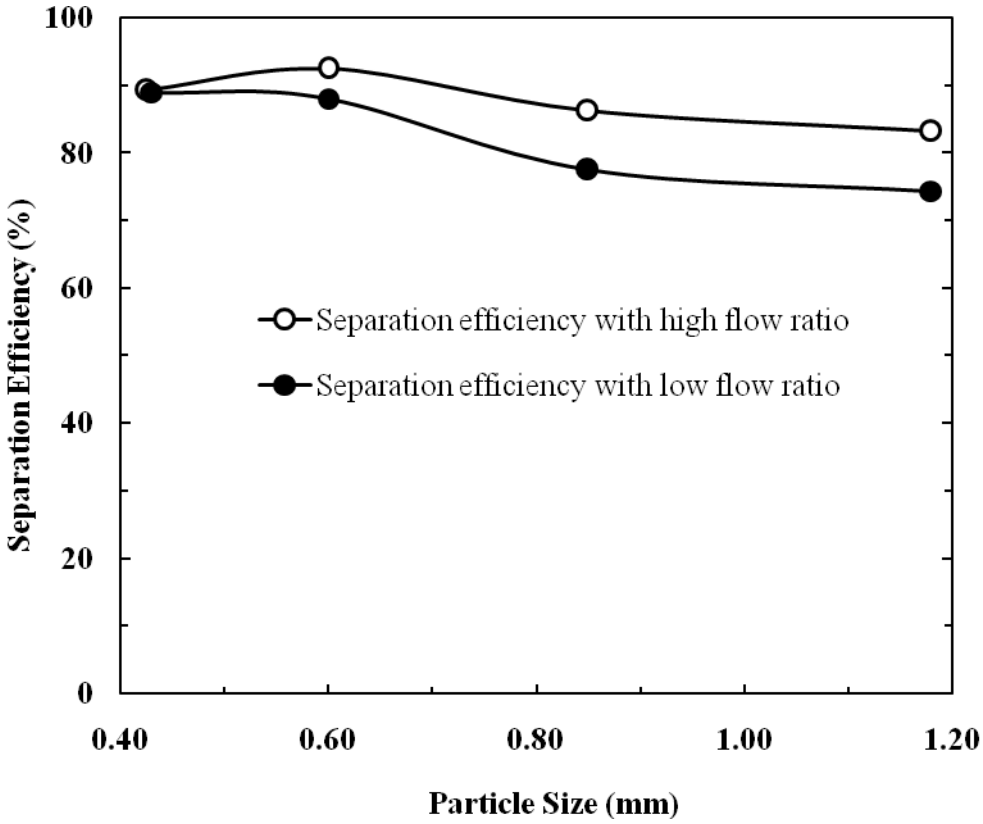

Figure 46. Effect of Flow Rate Ratio on Flotation Efficiency at Varying Phosphate Particle Size.

Long-duration tests of approximately two hours were carried out both in the presence of picobubbles (flow rate ratio: 50%), and in the absence of picobubbles (flow rate ratio: 0%). Figures 47 and 48 show the recovery and separation efficiency data of 35 tests with picobubbles, 20 tests without picobubbles and 9 tests of the mechanical flotation cell. It can be seen from the figures that the presence of picobubbles improved both flotation recovery and separation efficiency by approximately 5% on average.

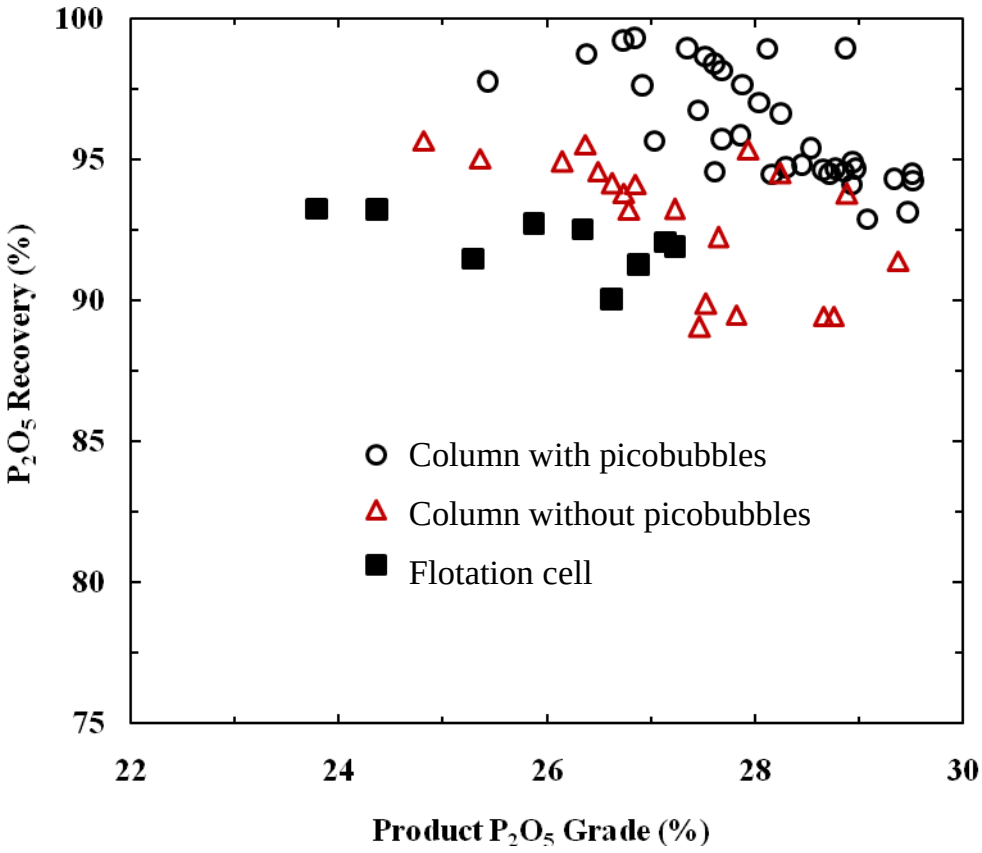

Figure 47. Flotation Recovery Data from Long-Duration Tests.

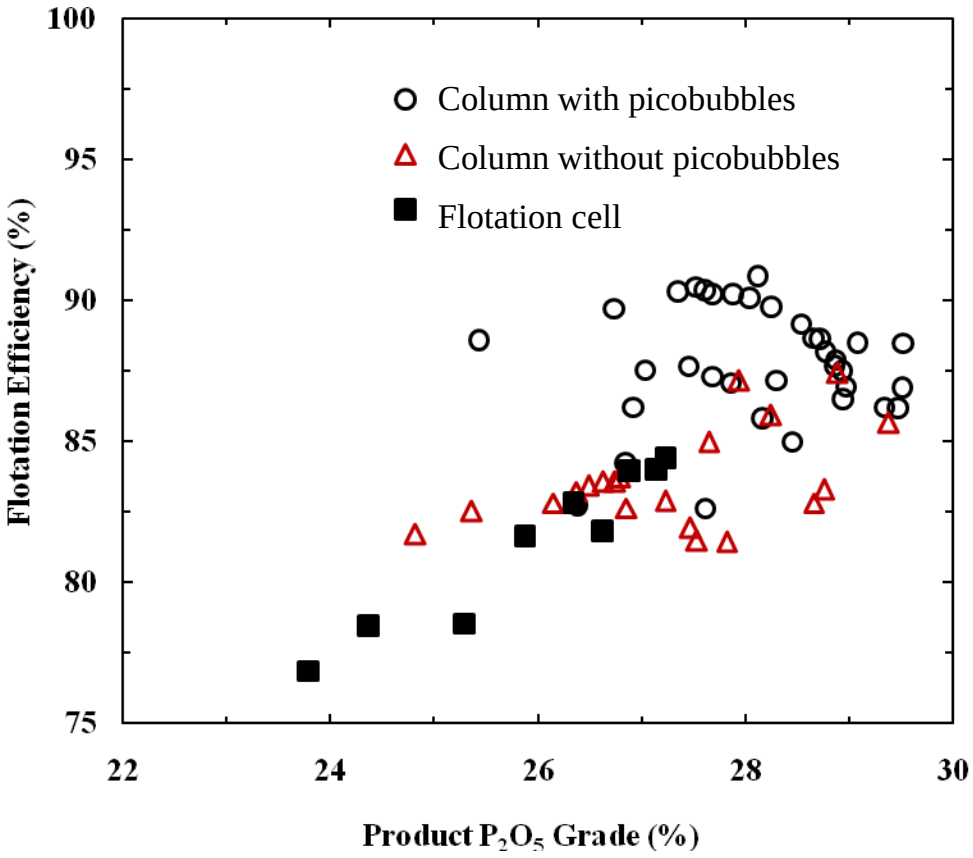

Figure 48. Flotation Efficiency Data from Long-Duration Tests.

INDUSTRIAL-SCALE PICOBUBBLE-ENHANCED FLOTATION

Picobubble-Enhanced Flotation of Unsized Phosphate Particles

Figure 49 shows the tailings of the unsized phosphate particle flotation without picobubbles (with no process water flow rate through the cavitation tube). It can be seen from the optical microscopic images of the flotation tailings that the phosphate particles lost were mainly coarse. Figure 50 shows the flotation tailings images obtained with picobubbles. In comparison, it can be clearly seen that the picobubbles improved the coarse phosphate particle flotation recovery. Figure 51 shows that there are no visible differences between flotation concentrates obtained with and without picobubbles.

(a) **(b)**

Figure 49. Flotation Tailing of Unsized Phosphate Particles without Picobubbles: (a) Photographic Image; (b) Optical Microscopic Image.

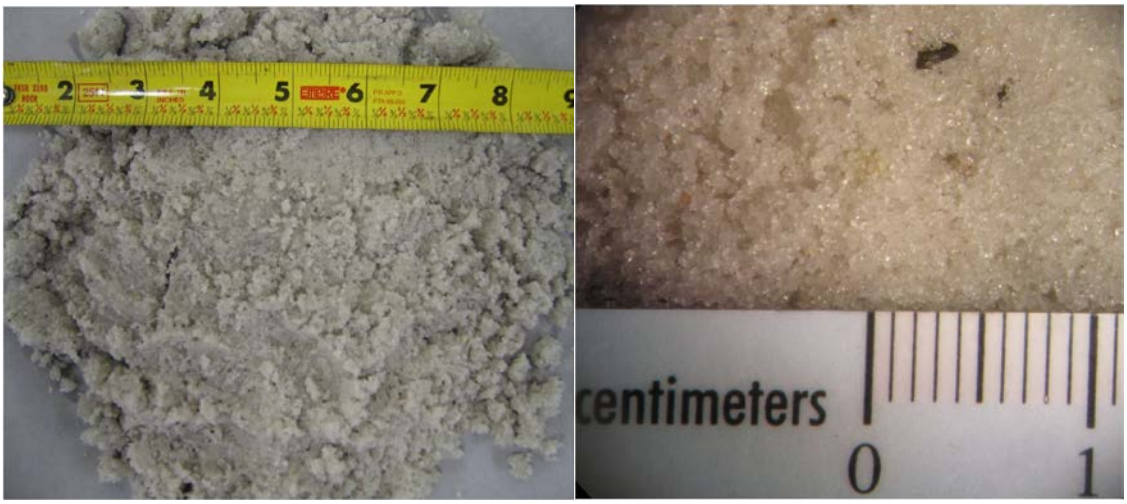

(a) **(b)**

Figure 50. Unsized Phosphate Flotation Tailing in the Presence of Picobubbles: (a) Photographic Image; (b) Optical Microscopic Image.

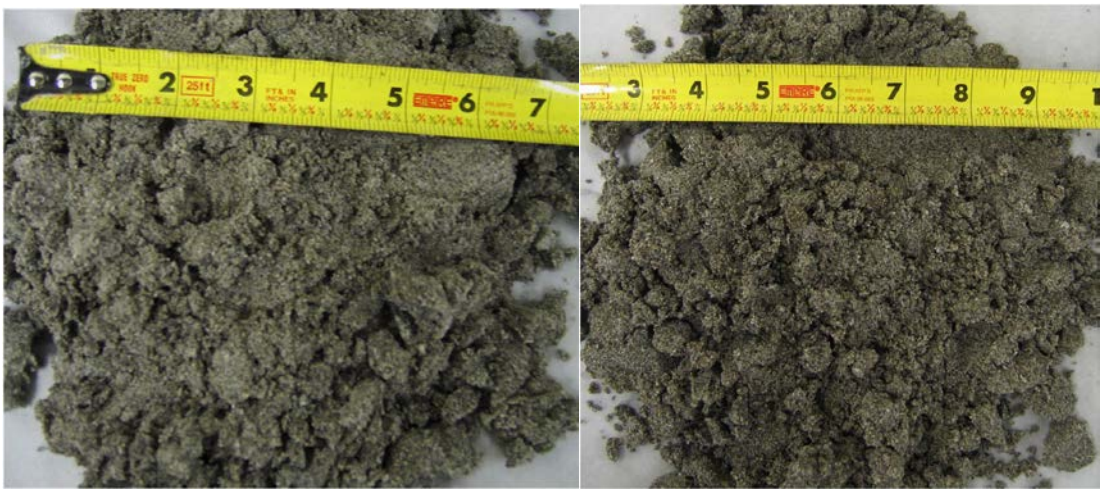

(a) **(b)**

Figure 51. Photographic Image of Unsized Phosphate Flotation Concentrate: (a) in the Absence of Picobubbles; (b) in the Presence of Picobubbles.

Response surface methodology was used to analyze the experimental data. Response surface, contours and cubic graphs were generated for P_2O_5 recovery, separation efficiency and concentrate grade as a function of air flow rate, frother flow rate and process water flow rate. Figures 52-57 depict the effect of the studied parameters on P_2O_5 recovery. Figures 58-63 reveal the effect of the studied parameters on separation efficiency.

The response surface and the contours of P_2O_5 recovery shown in Figure 52 depict the effect of the air flow rate and the frother flow rate on P_2O_5 recovery when the process water flow rate was at 3.4 m^3/min. The response surface and contours suggest that the area of the highest P_2O_5 recovery was attained at the middle level of the air flow rate and the high level of the frother flow rate. P_2O_5 recovery increased by about 0.7% as the frother flow rate increased from 0 to 0.05 liter/min.

Figure 53 shows the effect of the air flow rate and the process water flow rate on P_2O_5 recovery when the frother flow rate was 0.025 liter/min. The response surface and contours suggest that the area of the highest P_2O_5 recovery was attained at the middle level of the process water flow rate. The air flow rate had no significant effects on P_2O_5 recovery. P_2O_5 recovery increased by about 5.7% as the process water flow rate increased from 0 to 6.8 m^3/min. There were no picobubbles generated when the process water flow rate was zero. Therefore, Figure 53 indicates the presence of picobubbles had significant effects on P_2O_5 recovery.

Figure 54 depicts the effect of the frother flow rate and the process water flow rate on P_2O_5 recovery when the air flow rate was 85 liter/min. The response surface and contours suggest that the area of the highest P_2O_5 recovery was at the high level of the process water flow rate and the high level of the frother flow rate. P_2O_5 recovery increased by about 5.5% as the process water flow rate increased from 0 to 6.8 m^3/min. The presence of picobubbles generated by cavitation had more significant effects on P_2O_5 recovery.

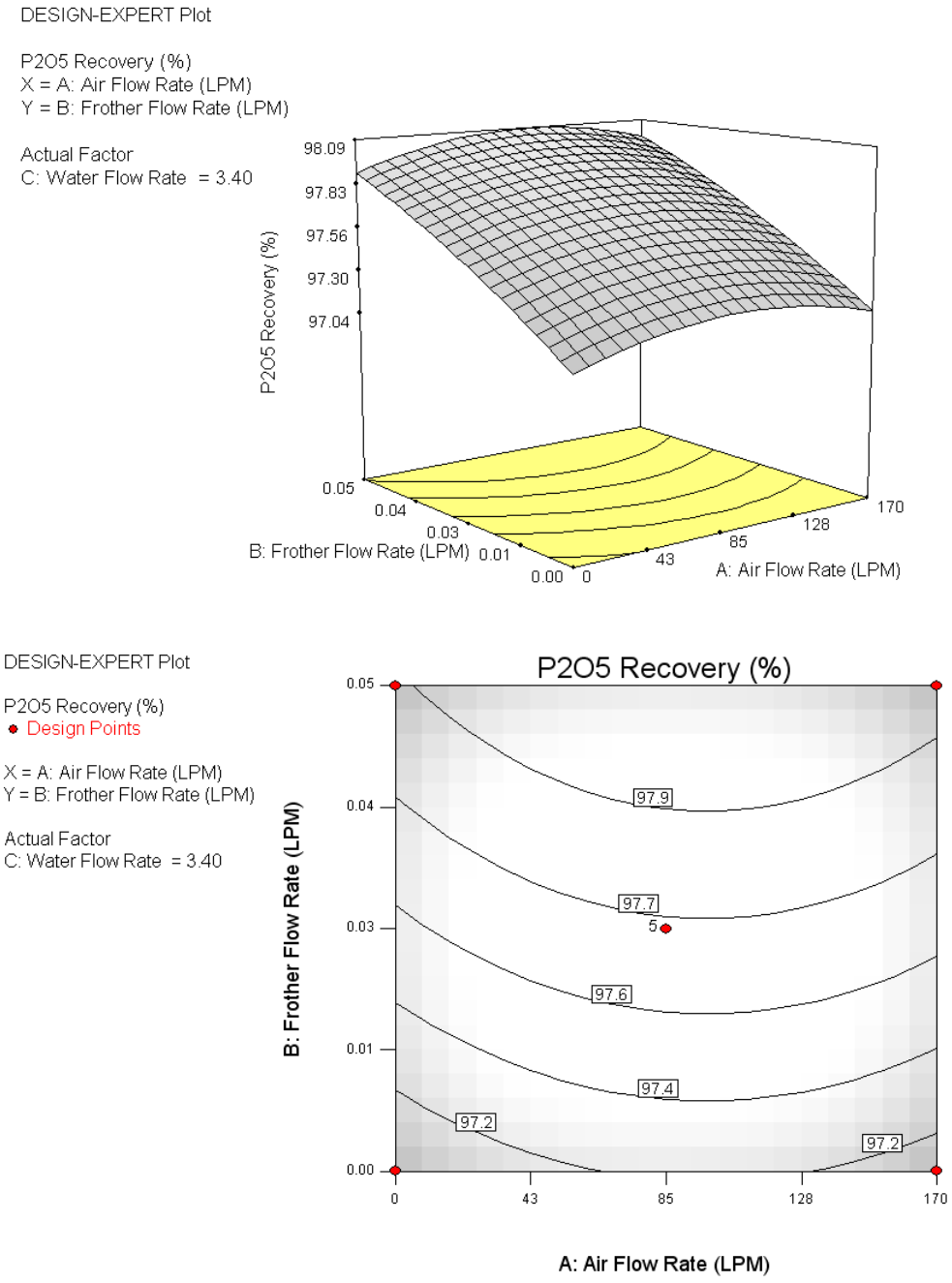

Figure 52. Effect of Air Flow Rate and Frother Flow Rate on P_2O_5 Recovery of Unsized Phosphate Particle Flotation.

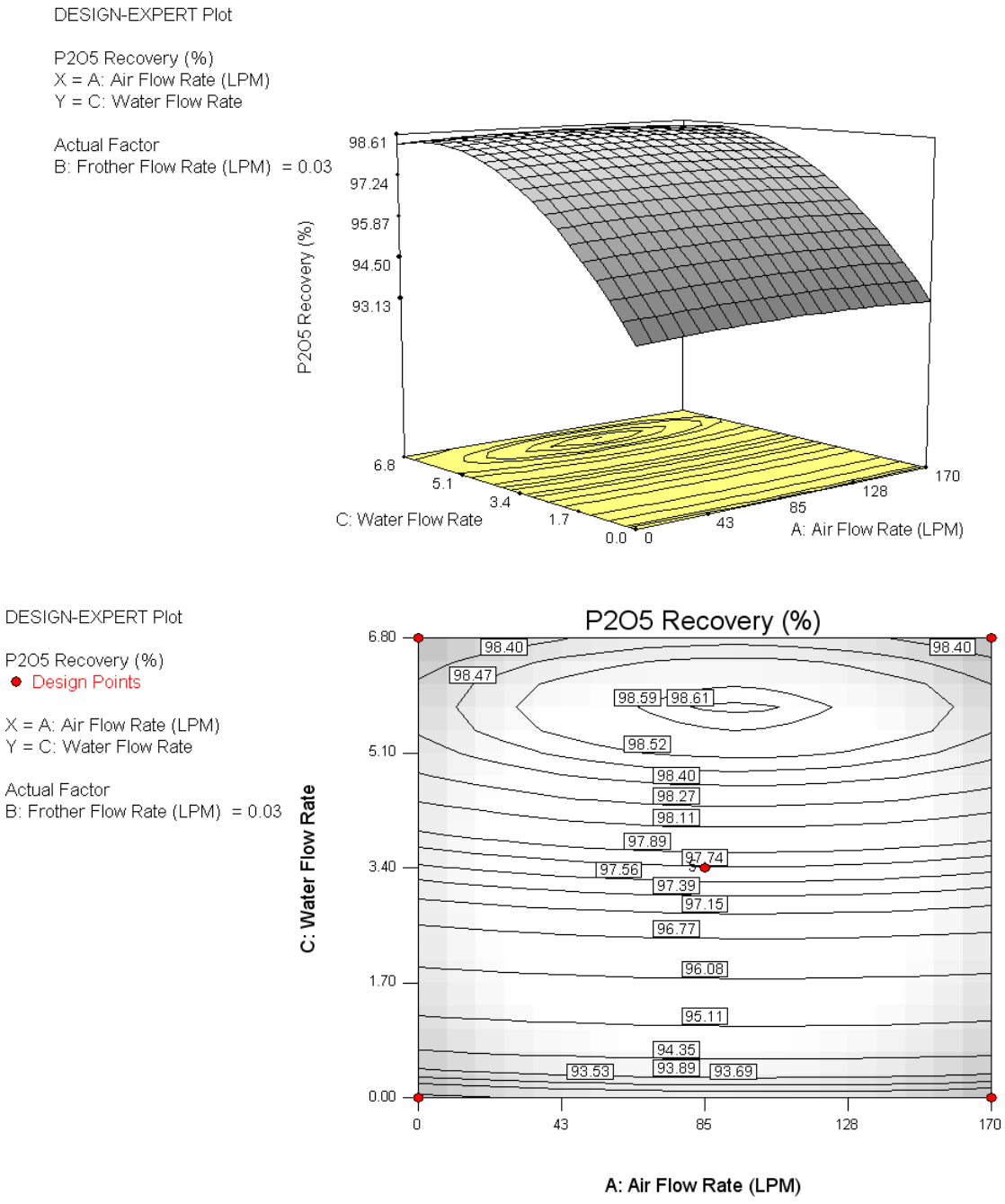

Figure 53. Effect of Air Flow Rate and Water Flow Rate on P_2O_5 Recovery of Unsized Phosphate Particle Flotation.

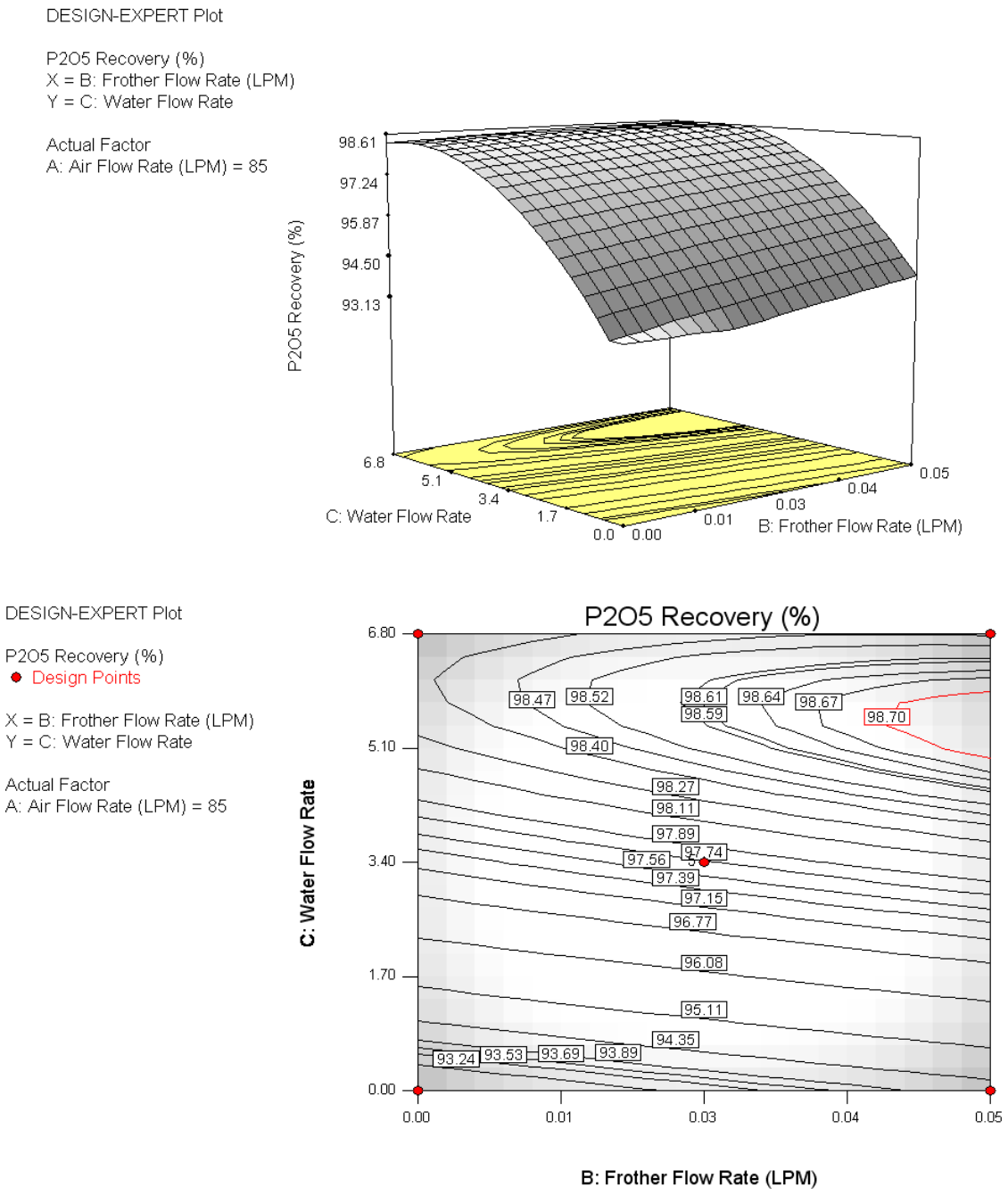

Figure 54. Effect of Frother Flow Rate and Process Water Flow Rate on P_2O_5 Recovery of Unsized Phosphate Particle Flotation.

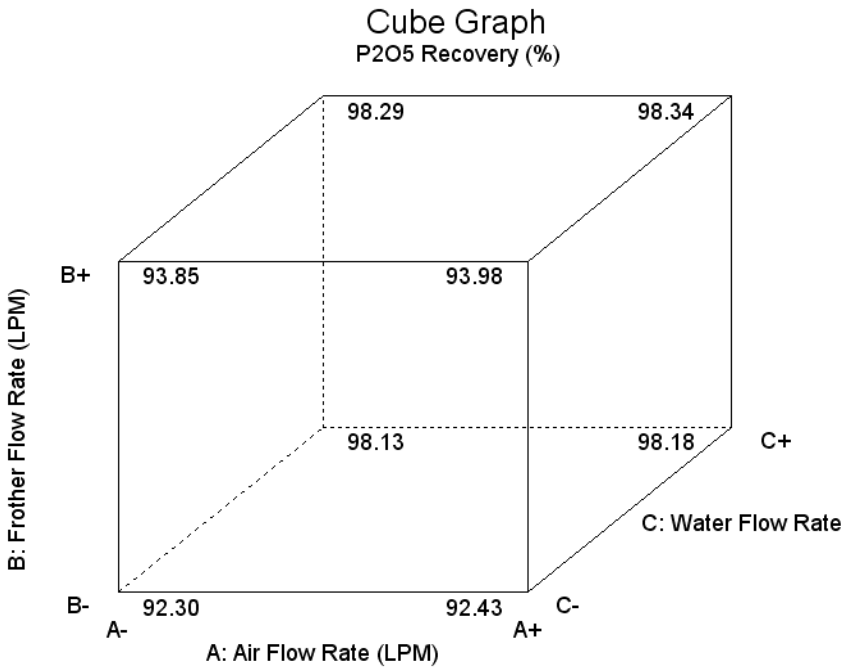

Figure 55. Effect of Air Flow Rate, Frother Flow Rate and Water Flow Rate on P_2O_5 Recovery of Unsized Phosphate Particle Flotation.

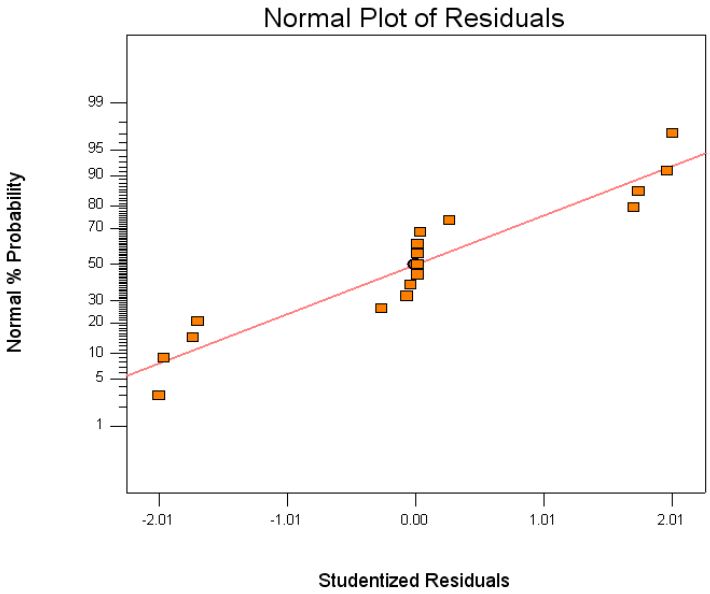

Figure 56. Normal Probability Plot of Residual for P_2O_5 Recovery of the Unsized Phosphate Particle Flotation.

Statistical analysis of the experimental data gave rise to Equation 6 for P_2O_5 recovery in terms of coded factors:

P_2O_5 Recovery (%) = 97.72 + 0.045*A + 0.43*B + 2.55*C – 0.15*A^2 – 0.059*B^2 –1.82*C^2 + 0.000*A*B – 0.020*A*C – 0.35*B*C (6)

which is equivalent to Equation 7:

P_2O_5 Recovery (%) =

+ 92.296		
+ 4.27059E-003	* Air Flow Rate (LPM)	
+ 35.82	* Frother Flow Rate (LPM)	
+ 1.93103	* Water Flow Rate	
- 2.06228E-005	* Air Flow Rate (LPM)^2	
- 94.40000	* Frother Flow Rate (LPM)^2	
- 0.15779	* Water Flow Rate^2	
- 1.32125E-014	* Air Flow Rate (LPM) * Frother Flow Rate (LPM)	
- 6.92042E-005	* Air Flow Rate (LPM) * Water Flow Rate	
- 4.11765	* Frother Flow Rate (LPM) * Water Flow Rate	(7)

Table 8. Analysis of Variance Table of P_2O_5 Recovery (%) for Industrial Flotation Tests.

Source	Sum of Squares	DF	Mean Square	F Value	Prob > F	
Model	68.27	9	7.59	437.46	< 0.0001	significant
A	*0.016*	*1*	*0.016*	*0.93*	*0.3660*	
B	*1.46*	*1*	*1.46*	*84.32*	*< 0.0001*	
C	*51.92*	*1*	*51.92*	*2994.12*	*< 0.0001*	
A²	*0.093*	*1*	*0.093*	*5.39*	*0.0533*	
B²	*0.015*	*1*	*0.015*	*0.85*	*0.3885*	
C²	*14.01*	*1*	*14.01*	*807.86*	*< 0.0001*	
AB	*0.000*	*1*	*0.000*	*0.000*	*1.0000*	
AC	*1.600E-003*	*1*	*1.600E-003*	*0.092*	*0.7701*	
BC	*0.49*	*1*	*0.49*	*28.26*	*0.0011*	
Residual	0.12	7	0.017			
Lack of Fit	*0.12*	*3*	*0.040*	*2021.67*	*< 0.0001*	*significant*
Pure Error	*8.000E-005*	*4*	*2.000E-005*			
Cor Total	68.39	16				

The model F-value of 437.46 implies the model is significant. There is only a 0.01% chance that a model F-value of this magnitude could occur due to noise. Values of Prob > F less than 0.0500 indicate model terms are significant. B, C, C^2, BC are significant model terms. Values greater than 0.1000 indicate the model terms are not significant. The Lack of Fit F-value of 2021.67 implies the lack of fit is significant. There is only a 0.01% chance that this Lack of Fit F-value could occur due to noise.

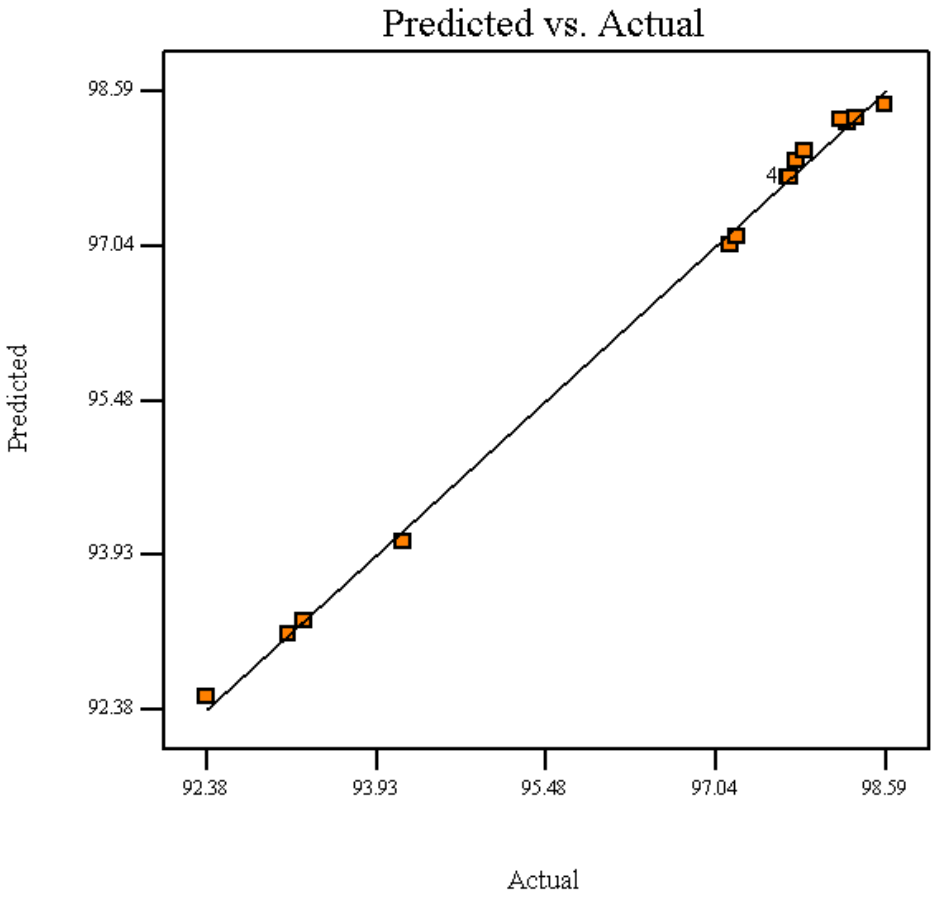

Figure 57. Relationship Between the Actual P_2O_5 Recovery Values and the Predicted P_2O_5 Recovery Values by the P_2O_5 Recovery Model.

Figure 58 depicts the effect of the air flow rate and the frother flow rate on separation efficiency (= P_2O_5 recovery + A.I. rejection –100%) when the process water flow rate was at 3.4 m^3/min. The response surface and contours suggest that the area of the highest separation efficiency was at the middle level of the air flow rate and the high level of the frother flow rate. The separation efficiency increased by about 0.7% as the frother flow rate increased from 0.00 to 0.05 liter/min.

Figure 59 shows the effect of the air flow rate and the process water flow rate on separation efficiency when the frother flow rate was 0.025 liter/min. The response surface and contours suggest that the area of the highest separation efficiency was attained at the middle level of the process water flow rate. The air flow rate had no significant effects on the separation efficiency. The separation efficiency increased by about 5.3% as the process water flow rate increased from 0 to 6.8 m^3/min. Figure 59 indicates the presence of picobubbles had significant effects on separation efficiency.

Figure 60 depicts the effect of the frother flow rate and the process water flow rate on separation efficiency when the air flow rate was at 85 liter/min. The response

surface and contours suggest that the area of the highest separation efficiency was attained at the high level of the process water flow rate and the high level of the frother flow rate. The separation efficiency increased by about 5.1% as the process water flow rate increased from 0 to 6.8 m^3/min. The presence of picobubbles generated by cavitation had more significant effects on separation efficiency.

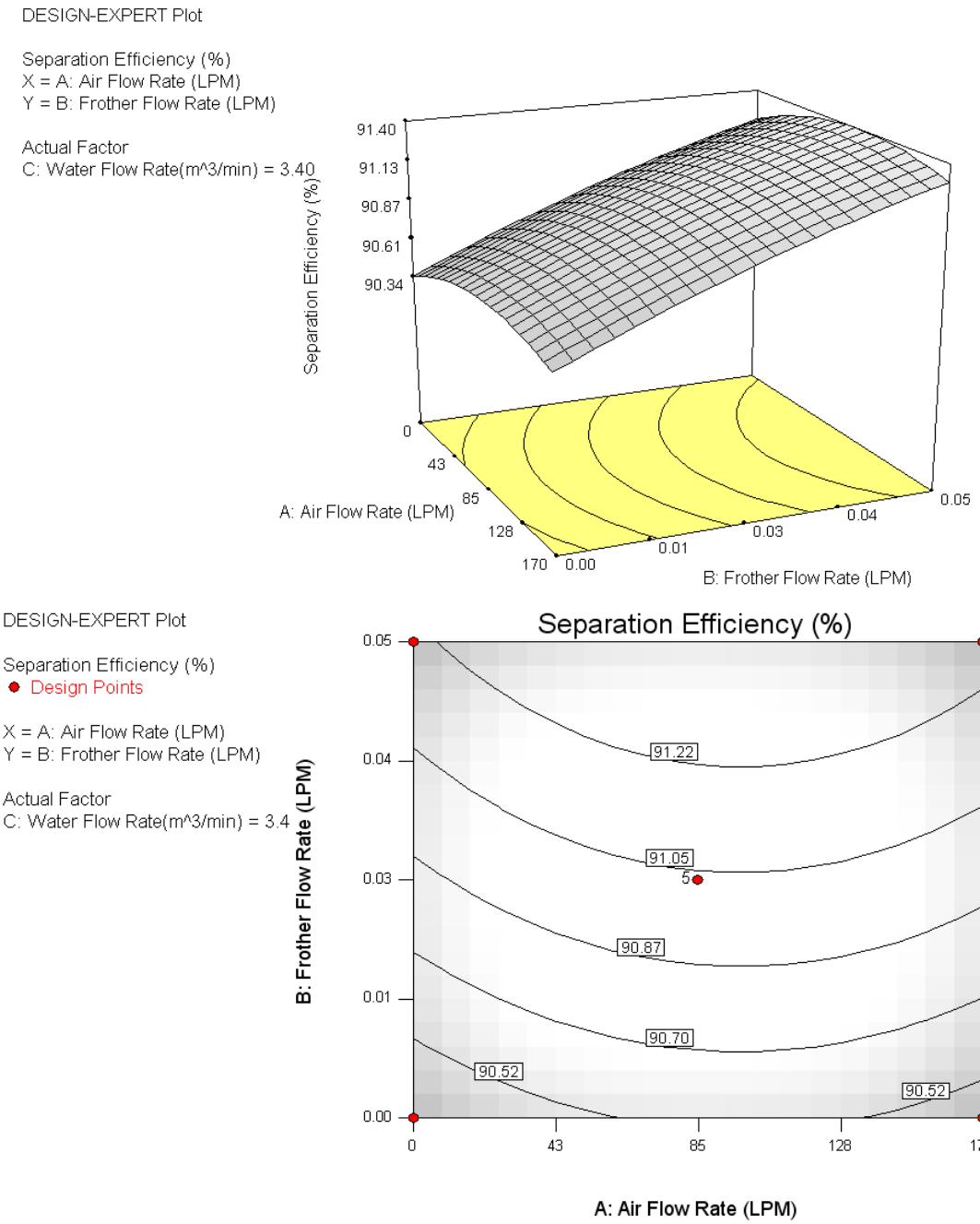

Figure 58. Effect of Air Flow Rate and Frother Flow Rate on Separation Efficiency of Unsized Phosphate Flotation.

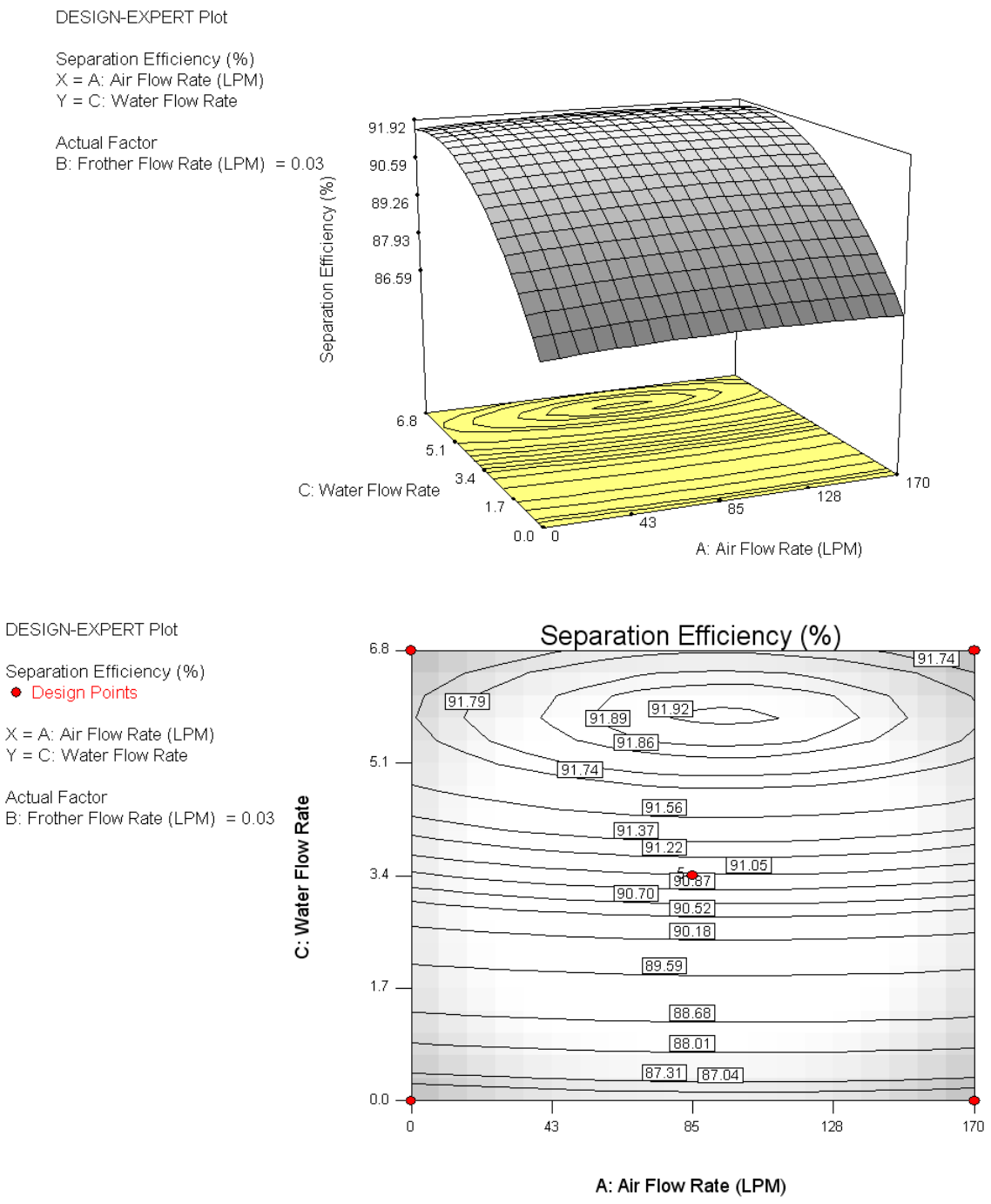

Figure 59. Effect of Air Flow Rate and Water Flow Rate on Separation Efficiency of Unsized Phosphate Flotation.

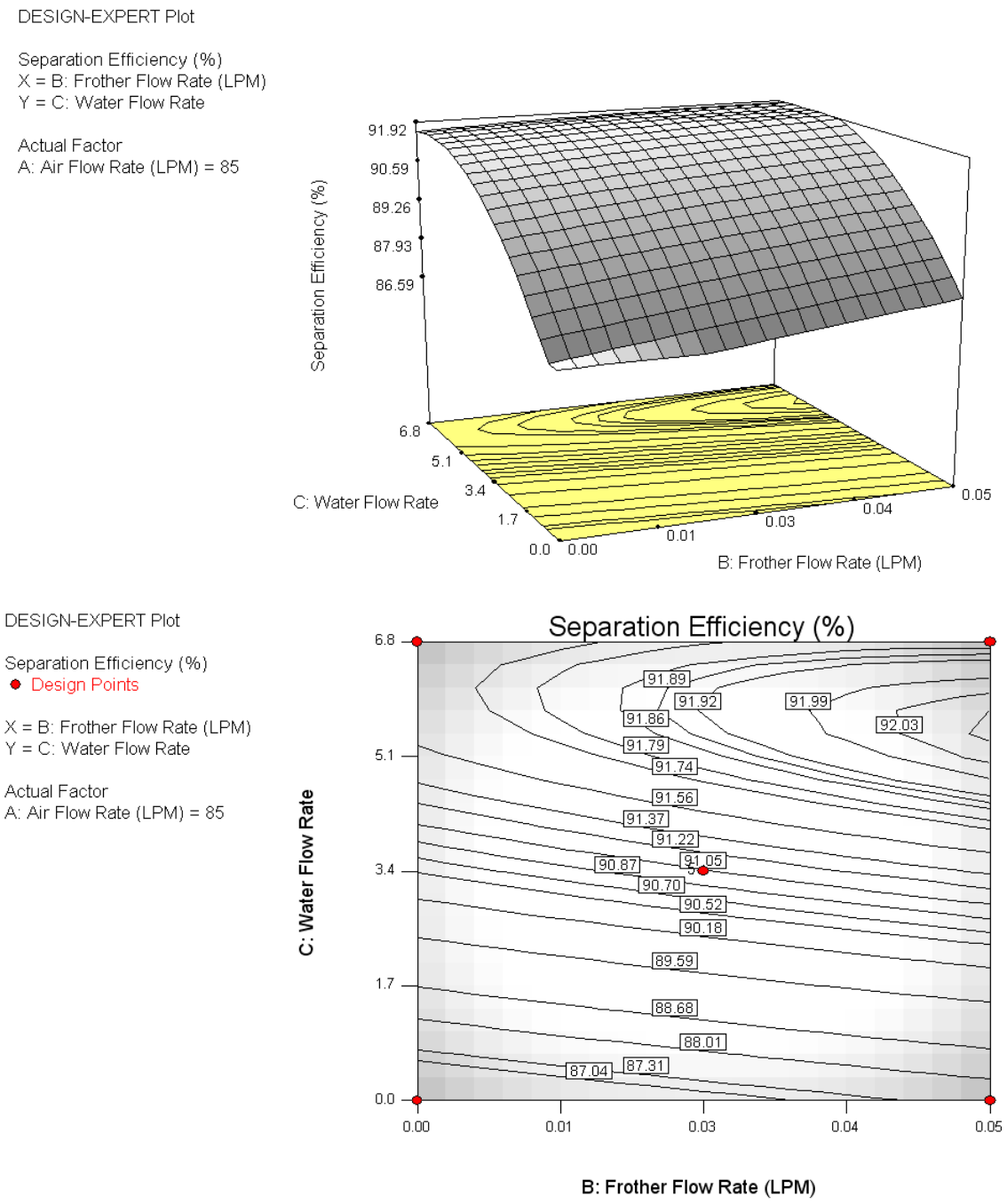

Figure 60. Effect of Frother Flow Rate and Water Flow Rate on Separation Efficiency of Unsized Phosphate Flotation.

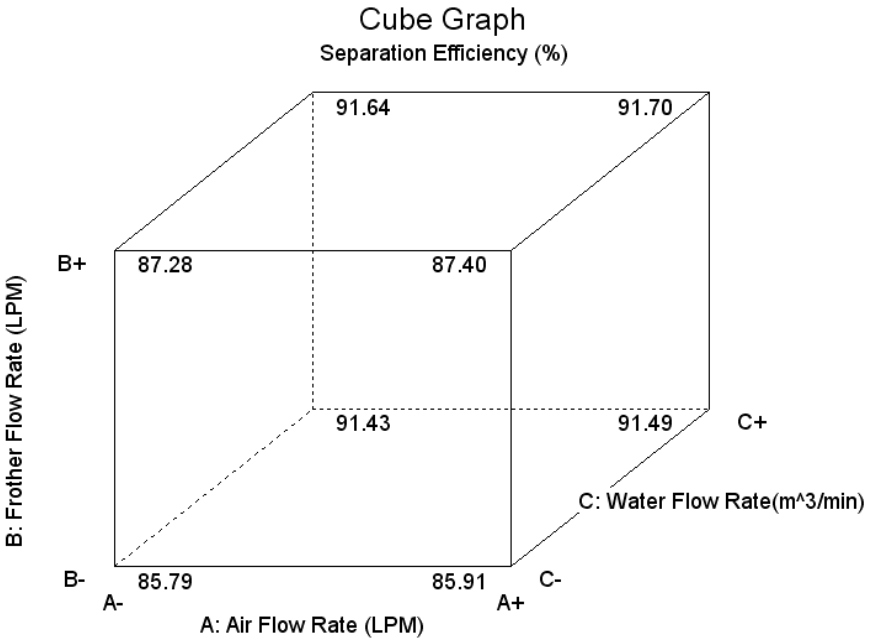

Figure 61. Effect of Air Flow Rate, Frother Flow Rate and Water Flow Rate on Separation Efficiency of Unsized Phosphate Flotation.

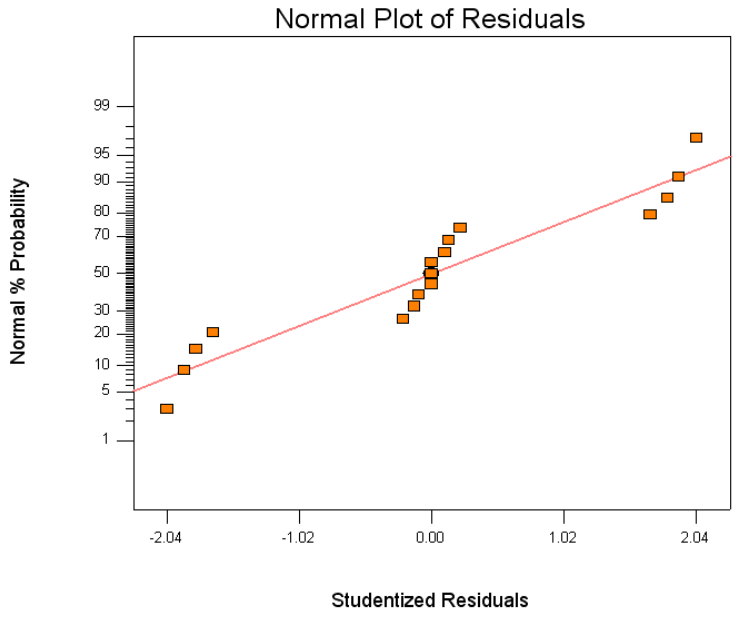

Figure 62. Normal Probability Plot of Residual for Separation Efficiency of Unsized Phosphate Particle Flotation.

Equation 8 for separation efficiency in terms of coded factors was obtained from statistical analysis of the experimental data:

Separation Efficiency (%) = 91.03 + 0.045*A + 0.43*B + 2.49*C – 0.16*A2 – 0.060*B2 – 1.73*C2 + 0.000*A*B – 0.015*A*C – 0.32*B*C (8)

Separation efficiency in terms of actual factors is described in Equation 9:

Separation Efficiency (%) =

+85.78750
+4.35294E-003 * Air Flow Rate (LPM)
+34.60000 * Frother Flow Rate (LPM)
+1.85074 * Water Flow Rate
- 2.14533E-005 * Air Flow Rate (LPM)^2
- 96.00000 * Frother Flow Rate (LPM)^2
- 0.15009 * Water Flow Rate^2
- 5.77643E-015 * Air Flow Rate (LPM) * Frother Flow Rate (LPM)
- 5.19031E-005 * Air Flow Rate (LPM) * Water Flow Rate
- 3.76471 * Frother Flow Rate (LPM) * Water Flow Rate (9)

Table 9. Analysis of Variance Table of Separation Efficiency for Industrial Flotation Cells.

Source	Sum of Squares	DF	Mean Square	F Value	Prob > F	
Model	64.42	9	7.16	561.39	< 0.0001	significant
A	*0.016*	*1*	*0.016*	*1.27*	*0.2968*	
B	*1.45*	*1*	*1.45*	*113.33*	*< 0.0001*	
C	*49.50*	*1*	*49.50*	*3882.45*	*< 0.0001*	
A²	*0.10*	*1*	*0.10*	*7.93*	*0.0259*	
B²	*0.015*	*1*	*0.015*	*1.19*	*0.3117*	
C²	*12.67*	*1*	*12.67*	*994.09*	*< 0.0001*	
AB	*0.000*	*1*	*0.000*	*0.000*	*1.0000*	
AC	*9.000E-004*	*1*	*9.000E-004*	*0.071*	*0.7981*	
BC	*0.41*	*1*	*0.41*	*32.13*	*0.0008*	
Residual	0.089	7	0.013			
Lack of Fit	*0.089*	*3*	*0.030*	*593.67*	*< 0.0001*	*significant*
Pure Error	*2.000E-004*	*4*	*5.000E-005*			
Cor Total	64.51	16				

The model F-value of 561.39 implies that the model is significant. There is only a 0.01% chance that this model F-value could occur due to noise. Since their values of Prob > F are less than 0.0500, B, C, A^2, C^2, and BC are significant model terms. Values greater than 0.1000 indicate the model terms are not significant. There is only a 0.01% chance that a Lack of Fit F-value this large could occur due to noise.

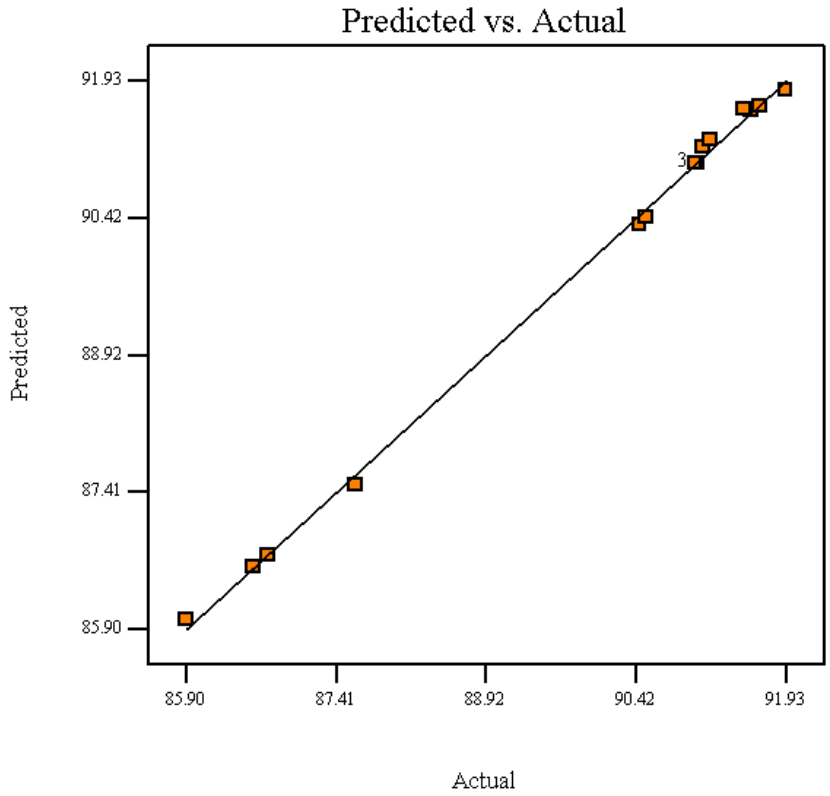

Figure 63. Relationship between Actual and Predicted Values of Separation Efficiency Model.

Figure 64 shows the effect of the frother flow rate and the process water flow rate on concentrate P_2O_5 grade when the air flow rate was at 85 liter/min. The response surface and contours suggest that the area of the highest concentrate P_2O_5 grade was attained at the high level of the process water flow rate and the high level of the frother flow rate. The concentrate P_2O_5 grade increased by about 0.2% as the process water flow rate increased from 0 to 6.8 m^3/min.

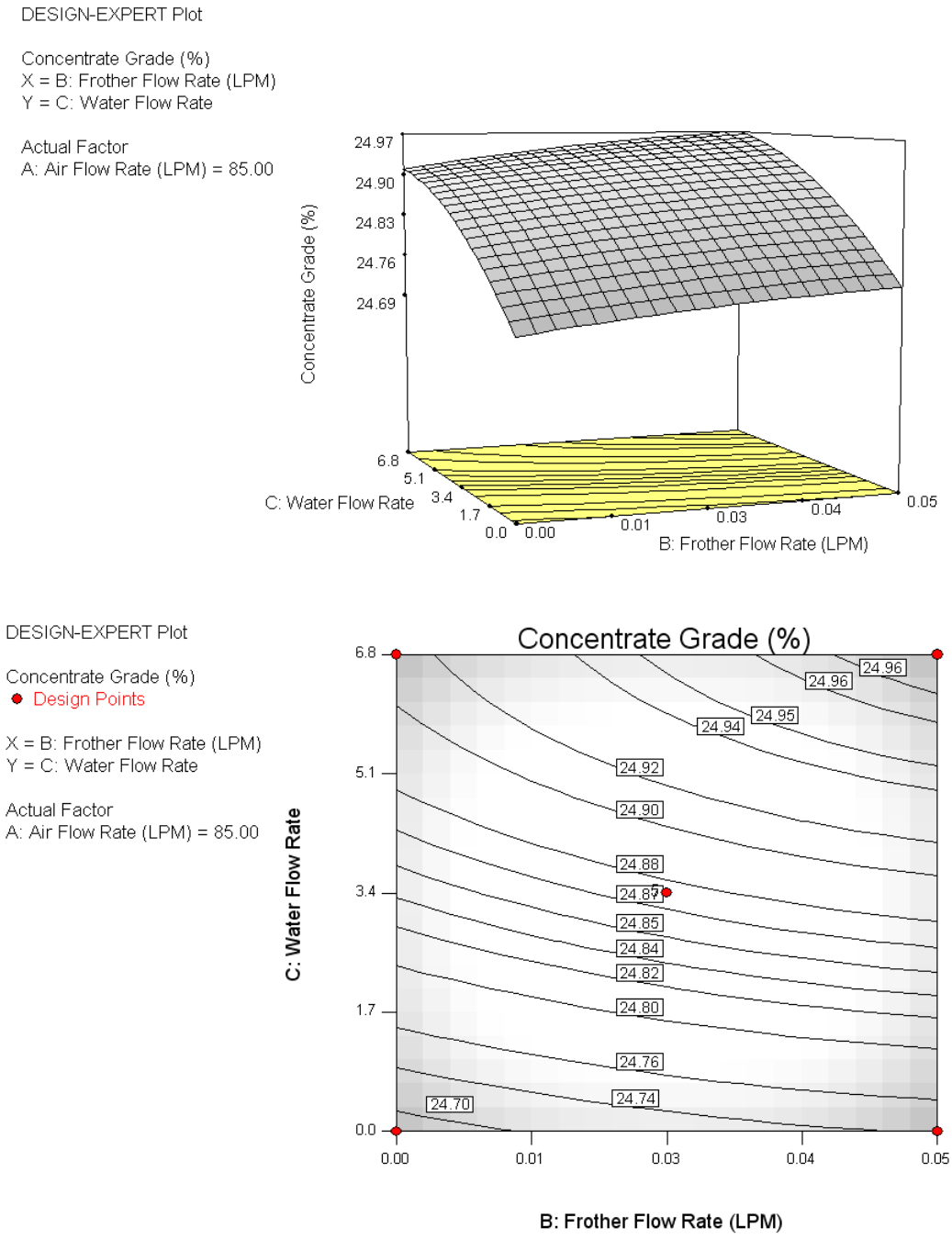

Figure 64. Effect of Frother Flow Rate and Water Flow Rate on Concentrate Grade of Unsized Phosphate Flotation.

Statistical analysis of the experimental data yields Equation 10 for P_2O_5 concentrate grade in terms of coded factors:

Concentrate Grade (%) =

+ 24.87

+ 3.750E-003 * A
+ 0.028 *B
+ 0.11 * C
− 0.025 *A^2
− 7.000E-003 * B^2
− 0.039 * C^2
− 2.500E-003*A * B
+2.500E-003* B * C (10)

which is equivalent to Equation 11:

Concentrate Grade (%) =
+ 24.65800
+ 6.50000E-004 * Air Flow Rate (LPM)
+ 1.66000 * Frother Flow Rate (LPM)
+ 0.055956 * Water Flow Rate
− 3.39100E-006 * Air Flow Rate (LPM)^2
− 11.20000 * Frother Flow Rate (LPM)^2
− 3.41696E-003 * Water Flow Rate^2
− 1.17647E-003 * Air Flow Rate (LPM) * Frother Flow Rate (LPM)
+ 0.029412 * Frother Flow Rate (LPM) * Water Flow Rate (11)

Table 10. Analysis of Variance Table of Concentrate Grade for Industrial Flotation Tests.

Source	Sum of Squares	DF	Mean Square	F Value	Prob > F	
Model	0.12	9	0.013	39.72	< 0.0001	significant
A	*1.125E-004*	*1*	*1.125E-004*	*0.34*	*0.5804*	
B	*6.050E-003*	*1*	*6.050E-003*	*18.06*	*0.0038*	
C	*0.10*	*1*	*0.10*	*308.99*	*< 0.0001*	
A^2	*2.527E-003*	*1*	*2.527E-003*	*7.54*	*0.0286*	
B^2	*2.063E-004*	*1*	*2.063E-004*	*0.62*	*0.4583*	
C^2	*6.569E-003*	*1*	*6.569E-003*	*19.61*	*0.0031*	
AB	*2.500E-005*	*1*	*2.500E-005*	*0.075*	*0.7926*	
AC	*0.000*	*1*	*0.000*	*0.000*	*1.0000*	
BC	*2.500E-005*	*1*	*2.500E-005*	*0.075*	*0.7926*	
Residual	2.345E-003	7	3.350E-004			
Lack of Fit	*1.825E-003*	*3*	*6.083E-004*	*4.68*	*0.0851*	*not significam*
Pure Error	*5.200E-004*	*4*	*1.300E-004*			
Cor Total	0.12	16				

The model F-value of 39.72 implies that the model is significant. There is only a 0.01% chance that this model F-value could occur due to noise. Since their values of Prob > F are less than 0.0500, model terms B, C, A^2, and C^2 are significant. The Lack of Fit F-value of 4.68 implies there is a 8.51% chance that the Lack of Fit F-value could occur due to noise.

In summary, the use of picobubbles increased P_2O_5 recovery by about 5.6% at varying frother flow rates and air flow rates; the presence of picobubbles increased the flotation separation efficiency (P_2O_5 recovery + A.I. rejection − 100%) by about 5.2% at varying frother flow rates and air flow rates; and concentrate P_2O_5 grade obtained in the presence of picobubbles was 0.2% higher than in the absence of picobubbles.

Picobubble-Enhanced Flotation of Coarse Phosphate Particles

A size-by-size study of flotation products was conducted to assess the effect of picobubbles on coarse phosphate flotation performance during the industrial picobubble-enhanced phosphate flotation tests. Particle size distribution, insol content and P_2O_5 grade analysis were carried out with flotation feed, concentrate and tailings samples collected from the unsized phosphate flotation with and without picobubbles. Figures 65-67 show the weight percentage and P_2O_5 grade of flotation feed, concentrate and tailings, respectively, as a function of particle size. It can be clearly seen from the curves that the weight content decreased with increasing phosphate particle size. However, the P_2O_5 grade of the flotation tailings increased more significantly than that of the flotation feed with increasing phosphate particle size, which means that the amount of P_2O_5 lost in the tailings increased with increasing phosphate particle size.

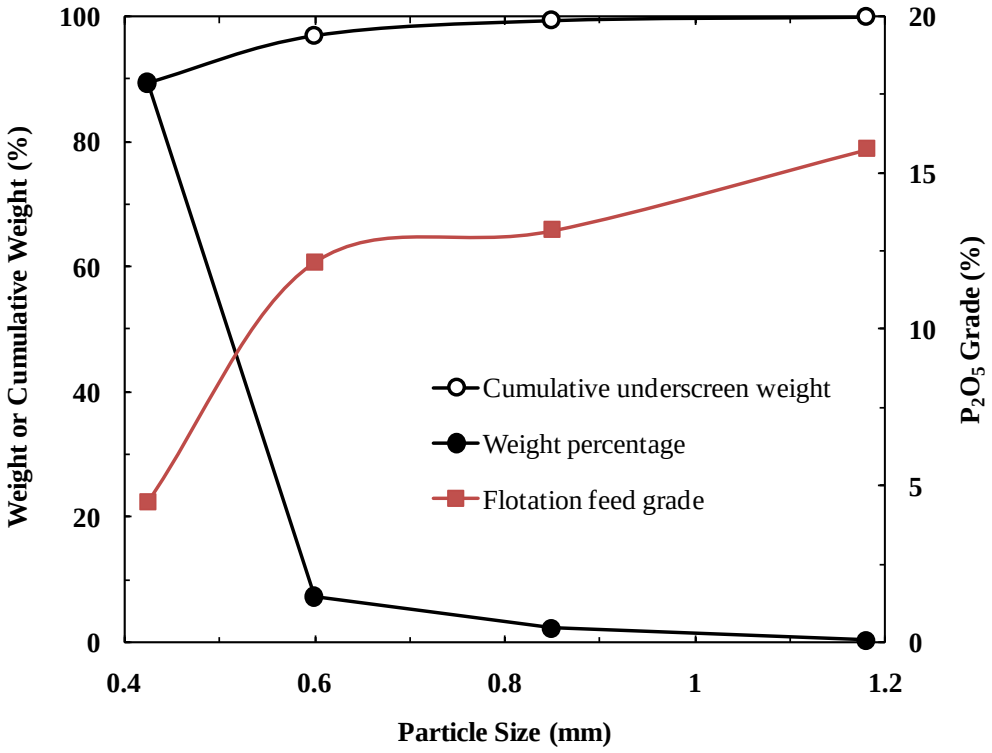

Figure 65. Weight Percentage and P_2O_5 Grade of Flotation Feed as a Function of Particle Size.

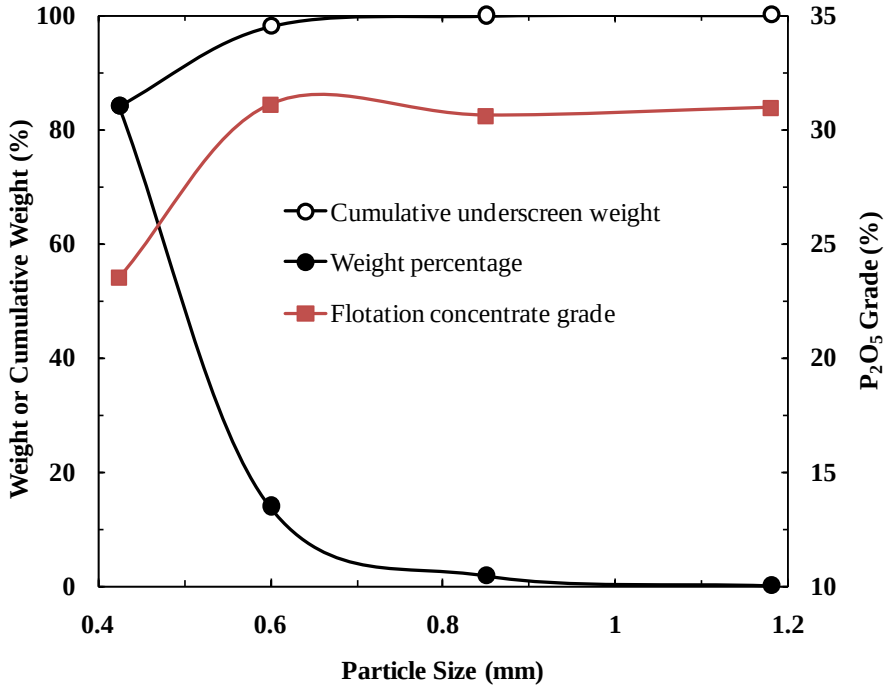

Figure 66. Weight Percentage and P_2O_5 Grade of Flotation Concentrate as a Function of Particle Size.

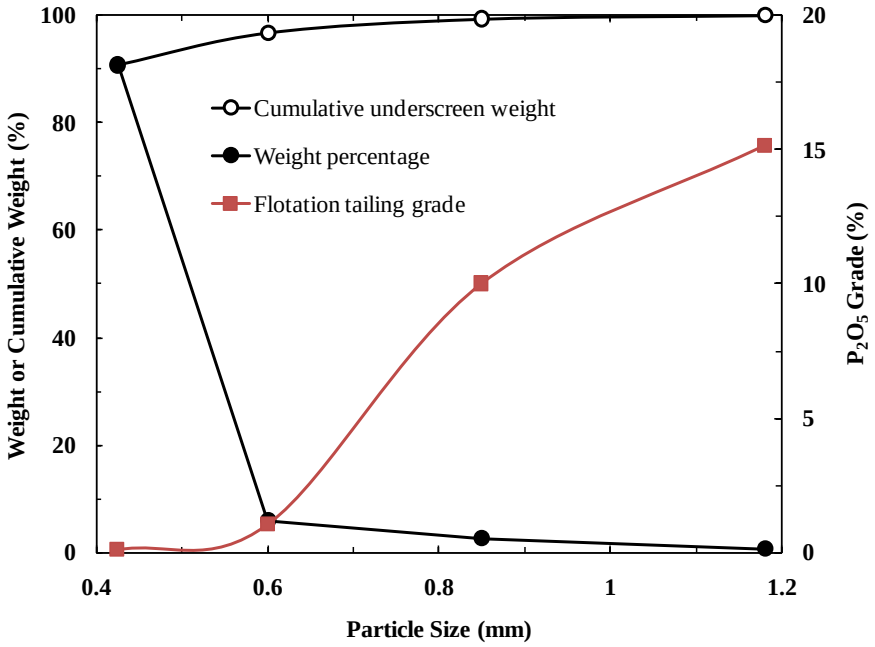

Figure 67. Weight Percentage and P_2O_5 Grade of Flotation Tailings as a Function of Particle Size.

Figures 68 and 69 show the effects of phosphate particle size on flotation P_2O_5 recovery, insol rejection, product grade and tailings grade without and with picobubbles, respectively. Figures 70 and 71 show the effects of picobubbles on particle size distribution and P_2O_5 grade of the tailings and concentrate, respectively, at varying phosphate particle sizes. Figure 72 shows the effects of picobubbles on flotation P_2O_5 recovery, product grade and tailings grade at varying phosphate particle sizes. Figures 68-72 reveal that the presence of picobubbles reduced the phosphate flotation tailings grade by 0.8%, 8.4% and 11.3% for 0.425-0.60 mm, 0.60-0.85 mm and 0.85-1.18 mm phosphate particles, respectively. There is not a large difference between the concentrate P_2O_5 grades obtained with and without picobubbles. It can be clearly seen from Figure 72 that the presence of picobubbles increased flotation recovery by 4.2%, 61.2% and 88.9% for 0.425-0.60 mm, 0.60-0.85 mm and 0.85-1.18 mm phosphate particles, respectively. The picobubbles had a greater impact on coarser phosphate flotation recovery.

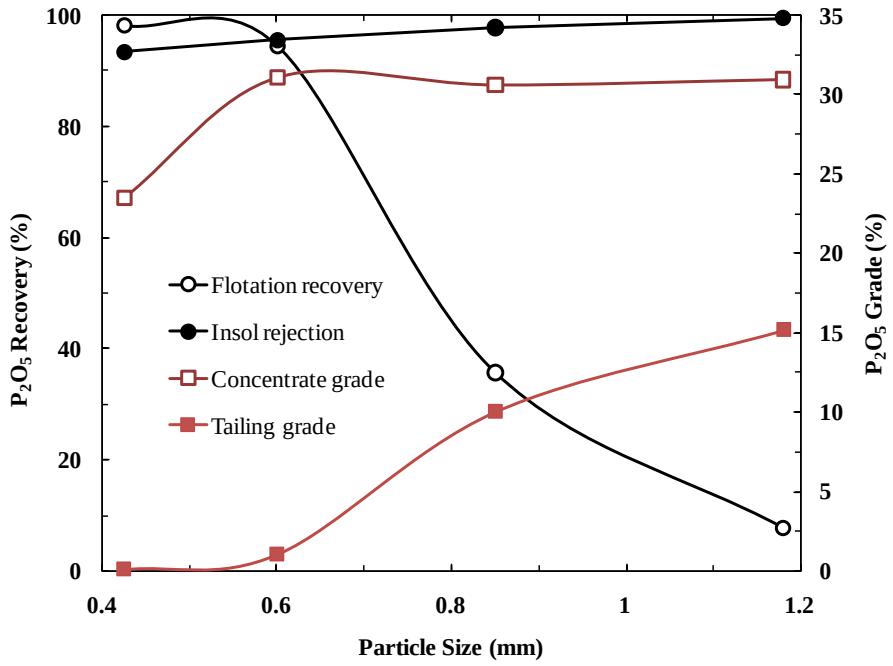

Figure 68. Effect of Phosphate Particle Size on Flotation P_2O_5 Recovery, Insol Rejection, Product Grade, and Tailing Grade without Picobubbles.

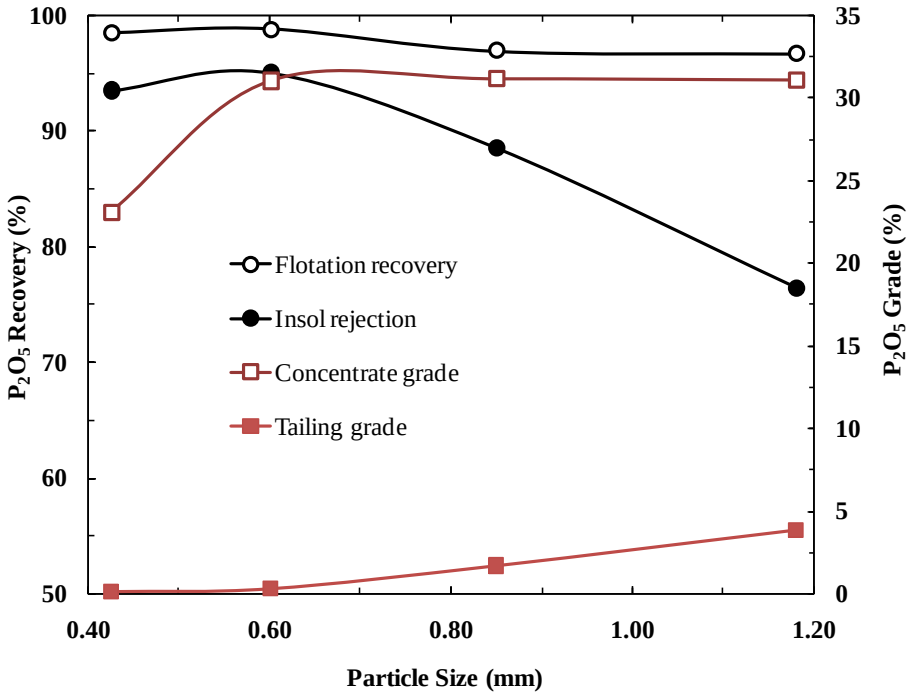

Figure 69. Effect of Phosphate Particle Size on Flotation P_2O_5 Recovery, Insol Rejection, Product Grade, and Tailing Grade with Picobubbles.

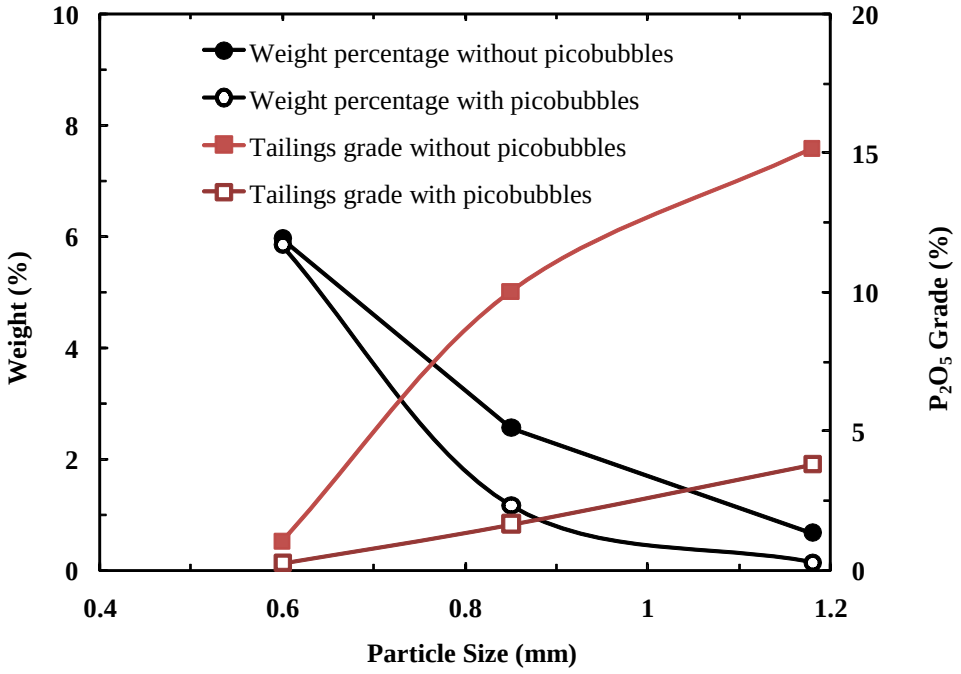

Figure 70. Effect of Picobubbles on Tailing Particle Size Distribution and Tailing P_2O_5 Grade at Varying Phosphate Particle Size.

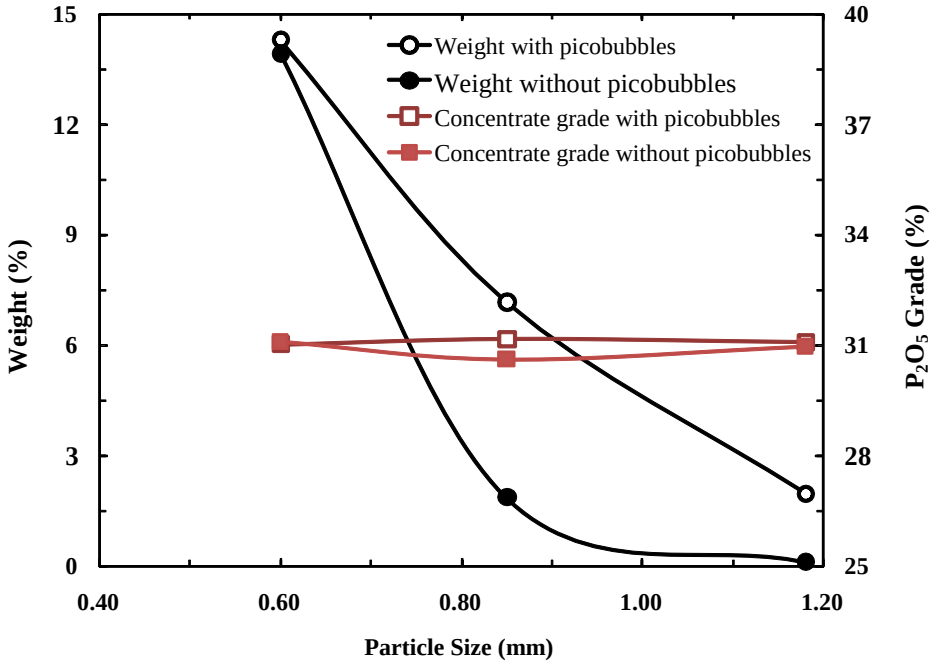

Figure 71. Effect of Picobubbles on Concentrate Particle Size Distribution and P_2O_5 Grade at Varying Phosphate Particle Size.

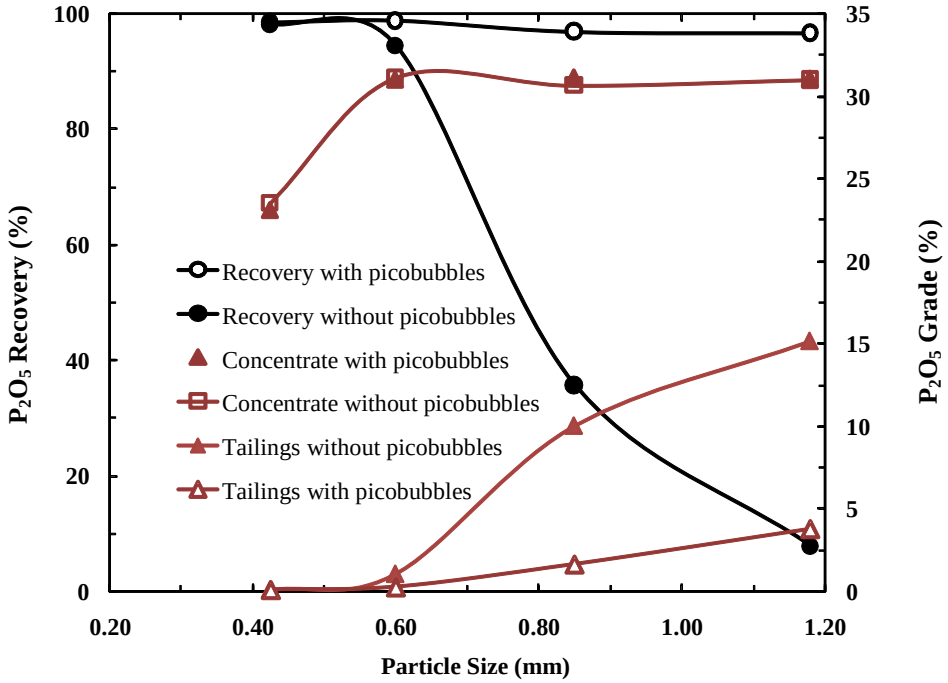

Figure 72. Effect of Picobubbles on Flotation P_2O_5 Recovery, Product Grade and Tailings Grade at Varying Phosphate Particle Size.

Economic Evaluation of Picobubble-Enhanced Phosphate Flotation

The P_2O_5 recovery model obtained in the previously discussed three-level three-factor industrial-scale tests, Equation 7, was used to predict the increased phosphate recovery and the increased income from adding the picobubbles into one bank of flotation cells. Figure 73 shows the increased income and costs per hour of adding picobubbles to one flotation bank as a function of process water flow rate through the cavitation tube. In this evaluation, the prices of phosphate, frother and electricity were assumed to be \$80/ton, \$700/ton and \$0.07/kW, respectively. It can be clearly seen from Figure 73 that the frother cost, electricity cost, and process water cost were major costs, which increased significantly with increasing process water flow rate. The figure reveals that the optimal process water flow rate was about 5 m^3/min under the test conditions.

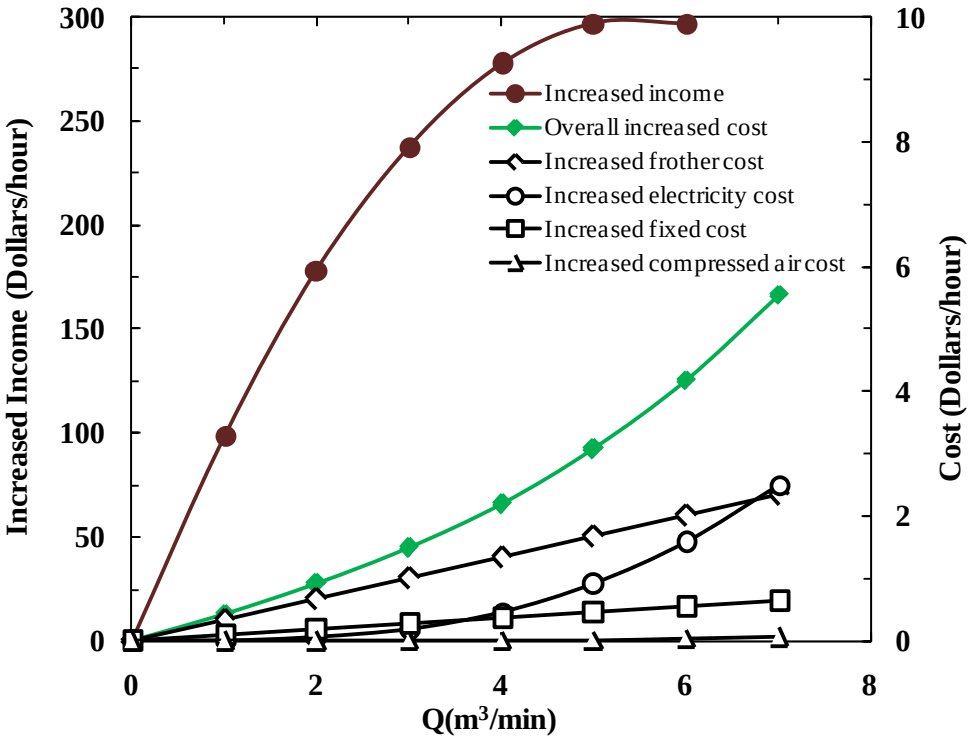

Figure 73. Evaluation of Increased Income and Cost Per Hour by Adding Picobubbles to One Bank of Flotation Cells.

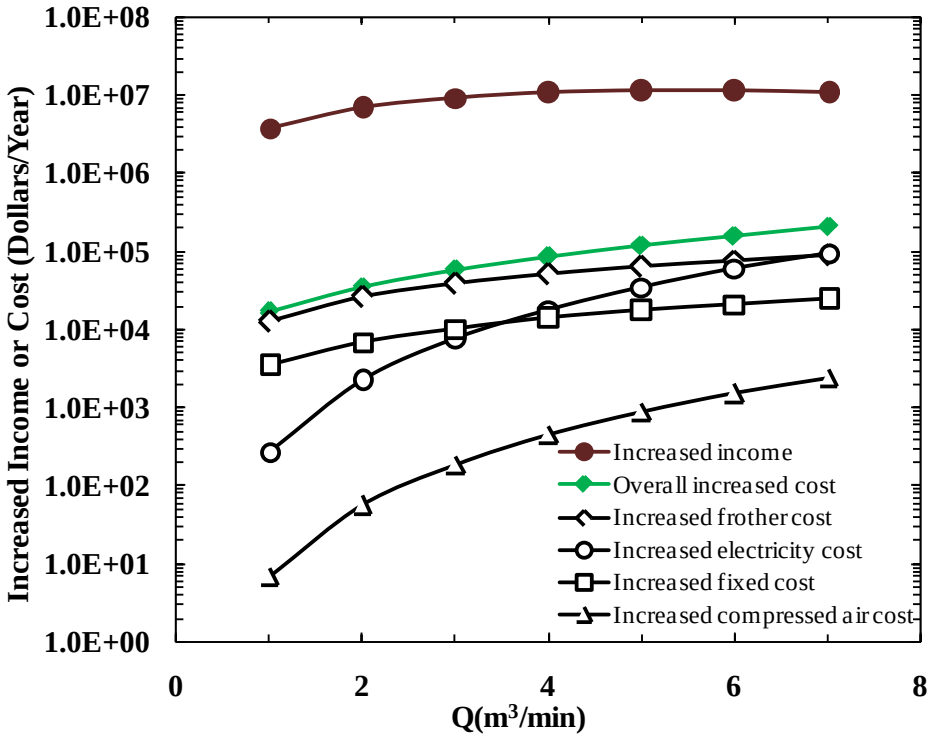

Figure 74. Evaluation of Increased Income and Cost Per Year by Adding Picobubbles to Eight Banks of Flotation Cells in Testing Plant.

Figure 74 shows the increased income and costs from adding the picobubbles into 8 banks of flotation cells per year as a function of process water flow rate through the cavitation tube. By comparing the increased income curve and the overall cost curve, we can see that income may be increased by about ten million dollars in one year by adding picobubbles to eight flotation banks of flotation cells in the testing plant.

SUMMARY AND CONCLUSIONS

The coarse phosphate sample for characterization and laboratory flotation tests from Mosaic Phosphates had 81.34% of the particles coarser than 0.3 mm; fewer than 2% of the particles were smaller than 0.15 mm and fewer than 1% of the particles were larger than 1.18 mm. The 0.425~1.18 mm portion accounted for 40.22%.

The XRD analyses of Mosaic Phosphates' black phosphate sample indicate that the major mineral composition was quartz (SiO_2) and apatite ($Ca_5F(PO_4)_3$). The content of other minerals such as dolomite ($CaMg(CO_3)_2$), wavellite ($(AlOH)_3(PO_4)_2 \cdot 5H_2O$), crandallite ($Ca_{0.7}Sr_{0.3}Al_3(PO_4)_2(OH)_5H_2O$), and K feldspar ($KAlSi_3O_8$) in the phosphate sample were very low. Analysis of the phosphate sample with an S4 Pioneer wavelength dispersive X-ray fluorescence spectrometer (WDXRF) showed that the major acid-insoluble constituent was SiO_2 (67.04%). The P_2O_5 content in the Mosaic Phosphates sample was 10.18%, and the content of another major acid-soluble constituent, CaO, was 16.74%.

The median size of Venturi-tube-generated bubbles was about 830 nm. There were two major peaks at bubble sizes of 900 nm and 70 μm on the population frequency curve of bubbles which represented bubbles generated by the Venturi tube and the static mixer, respectively.

Picobubble-enhanced laboratory column flotation studies showed that the picobubbles significantly improved flotation performances. A flotation yield of 35%, flotation recovery of 98% and separation efficiency of 94% were achieved at a lower collector dosage of 0.9 kg/t in the presence of picobubbles, producing a concentrate of 28.79% P_2O_5. In contrast, the maximum flotation yield of 33.8%, flotation recovery of 94% and separation efficiency of 89.8% were obtained at a collector dosage of 2.1 kg/t in the absence of picobubbles.

Size-by-size flotation tests indicated that the significance of the picobubbles' effect on phosphate flotation kinetics increased as particle size increased from 0.425-0.6 to 0.85-1.18 mm. The presence of picobubbles increased the phosphate flotation rate constant k for all size fractions of phosphate particles, and increased the P_2O_5 recovery of phosphate particles more significantly for the +0.85-1.18 mm particle size fraction than for the +0.85-1.18 mm and +0.60-0.85 mm fractions. The presence of picobubbles increased A.I. rejection, albeit less significantly for the +0.85-0.1.18 mm particle size fraction than the other particle size fractions since picobubbles increased flotation recovery much more significantly for the +0.85-0.1.18 mm fraction than the other particle size ranges. At a given P_2O_5 recovery, the presence of picobubbles increased the P_2O_5 grade by about 0.7-1.0%.

The pilot-scale picobubble-enhanced flotation tests indicated that the use of picobubbles increased P_2O_5 recovery and flotation separation efficiency by approximately 5 absolute percentage points on average. A size-by-size analysis of the

flotation products revealed that the presence of picobubbles at a high flow ratio improved flotation efficiency by 4.4% and 8.7% for phosphate particles of 0.6 mm and 0.8 mm, respectively.

The industrial picobubble-enhanced flotation tests with unsized phosphate feed indicated that the use of picobubbles increased P_2O_5 recovery, flotation separation efficiency, and concentrate grade by about 5.6, 5.2, and 0.2 absolute percentage points, respectively. A size-by-size analysis of flotation products revealed that the presence of picobubbles increased flotation recovery by 4.2, 61.2, and 88.9 absolute percentage points for the 0.425-0.60 mm, 0.60-0.85 mm and 0.85-1.18 mm phosphate particles, respectively. The presence of picobubbles had greater impact on coarser phosphate particles than finer particles. In the absence of picobubbles, P_2O_5 recovery decreased from 94.6% to 35.7% and 7.8% as the phosphate particle size increased from 0.60 mm to 0.85 mm and 1.18 mm, respectively. The commercial testing results were in good agreement with theoretical analyses and the lab flotation studies.

The economic analysis of the industrial flotation cells demonstrated that the application of picobubble-enhanced phosphate flotation was economically feasible. The major costs were those of the frother, electricity, and process water. It was shown that ten million dollars ($10 million) in net income can be raised in one year by adding picobubbles to eight flotation banks of flotation cells (14.2 m^3/cell) in the testing plant.

REFERENCES

AFPC (Association of Florida Phosphate Chemists). 1991. Methods used and adopted by the Association of Florida Phosphate Chemists. 7th ed. Bartow (FL): AFPC.

Attalla M, Chao C, Nicol SK. 2000. The role of cavitation in coal flotation. In: Proceedings of the Eighth Australian Coal Preparation Conference; 2000 Nov 12-16; Port Stephens, New South Wales, Australia. Paper nr H-3. p 237-50.

Bruker AXS. n.d. S4 PIONEER Wavelength dispersive X-ray fluorescence. Viewable online at: http://www.bruker-axs.com/s4_pioneer.html.

Davis BE, Hood GD. 1993. Improved recovery of coarse Florida phosphate. Mining Engineering 45(6): 596-9.

Drzymala J. 1994. Characterization of materials by Hallimond tube flotation. Part 2: maximum size of floating particles and contact angle. Int. J. Miner. Process. 42(3-4): 153-67.

Dzienisiewicz J, Pryor EJ. 1950. An investigation into the action of air in froth flotation. Trans. IMM., London 59: 455-91.

El-Shall H, Svoronos S, Abdel-Khalek NA. 2001a. Bubble generation, design, modeling and optimization of novel flotation columns for phosphate beneficiation. Bartow (FL): Florida Institute of Phosphate Research. FIPR Publication nr 02-111-175, Vol. I.

El-Shall H, Sharma R, Abdel-Khalek NA, Svoronos S, Gupta S. 2001b. Column flotation of Florida phosphate: an optimization study. Minerals and Metallurgical Processing 18(3): 142-6.

Fan M, Tao D. 2008a. A study on picobubble enhanced coarse phosphate froth flotation. Separation Science and Technology 43(1): 1-10.

Fan MM, Tao D. 2008b. Effect of picobubbles by hydrodynamic cavitation on coarse phosphate froth flotation. In: Zuo WD and others, editors. Proceedings of XXIV International Mineral Processing Congress; 2008 Sep 24-28; Beijing, China. Beijing: Science Press. Vol. 1, p 1308-13.

Fan M, Tao D. 2008c. The role of picobubbles on coarse phosphate flotation behavior. In: Zhang P and others, editors. Beneficiation of phosphates: technology advance and adoption. Littleton (CO): Society for Mining, Metallurgy & Exploration. p 27-34.

Feng D, Aldrich C. 1999. Effect of particle size on flotation performance of complex sulfide ores. Minerals Engineering 12(7): 721-31.

Gaudin AM, Groh JO, Henderson HB. 1931. Effect of particle size on flotation. American Institute of Mining and Metallurgical Engineering (AIME), Technical Publication nr 414. p 3-23.

Gurr TM. 2009. Industrial minerals 2008—phosphate rock. Mining Engineering 61(6): 63-5.

Johnson BD, Cooke RC. 1981. Generation of stabilized microbubbles in seawater. Science 213(4504): 209-11.

King RP. 1982. Flotation of fine particles. In: King RP, ed. Principles of flotation. Johannesburg: South African Institute of Mining and Metallurgy. Monograph series nr 3. p 215-25.

Klassen VI, Mokrousov VA. 1963. An introduction to the theory of flotation. London: Butterworth. p 493.

Maksimov II, Otrozhdennova LA, Borkin AD, Yemelyanov MF, Koltunova TY, Malinovskaya ND, Nechay LA. 1993. An investigation to increase the efficiency of coarse and fine particle flotation in ore processing of non-ferrous metals. In: Proceedings of XVIII International Mineral Processing Congress; 1993 May 23-28; Sydney, NSW, Australia. Parkville (Victoria, Australia): Australasian Institute of Mining and Metallurgy. p 685-7.

Morris TM. 1952. Measurement and evaluation of the rate of flotation as a function of particle size. Mining Engineering 4(8): 794-8.

Moudgil BM. 1992. Enhanced recovery of coarse particles during phosphate flotation. Bartow (FL): Florida Institute of Phosphate Research. Publication nr 02-067-099.

Oteyaka B, Soto H. 1995. Modelling of negative bias column for coarse particles flotation. Minerals Engineering 8(1/2): 91-100.

Ralston J, Dukhin SS. 1999. The interaction between particles and bubbles. Colloids and Surfaces, A: Physicochemical and Engineering Aspects 151(1-2): 3-14.

Rodrigues WJ, Leal Filho LS, Masini EA. 2001. Hydrodynamic dimensionless parameters and their influence on flotation performance of coarse particles. Mineral Engineering 14(9): 1047-54.

Shimoliizaka J, Matsuoka I. 1982. Applicability of air-dissolved flotation for separation. In: Maltby PDR, editor. Proceedings, XIV International Mineral Processing Congress; 1982 Oct 17-23; Toronto, Canada. Toronto: Canadian Institute of Mining and Metallurgy.

Tao D. 2004. Role of bubble size in flotation of coarse and fine particles—a review. Separation Science and Technology 39(4): 741-60. [a Tao 2003 is cited in text]

Tao D, Honaker R, Parekh BK, Fan M. 2006a. Development of picobubble flotation for enhanced recovery of coarse phosphate particles. Bartow (FL): Florida Institute of Phosphate Research. Publication nr 02-154-219.

Tao D, Fan M, Honaker RQ, Parekh BK. 2006b. Picobubble enhanced flotation of coarse phosphate particles. In: Proceedings, XXIII International Mineral Processing Congress; 2006 Sep 3-8; Istanbul , Turkey. Istanbul: YMGV.

Trahar WJ, Warren LJ. 1976. The floatability of very fine particles—a review. Inter. J. Miner. Process. 3(2): 103-31.

Yoon R-H. 2000. The role of hydrodynamic and surface forces in bubble-particle interaction. Inter. J. Miner. Proces. 58(1-4): 129-43.

Yoon R-H, Luttrell GG, Adel GT, Mankosa MJ. 1989. Recent advances in fine coal flotation. In: Chander S, ed. Advances in coal and mineral processing using flotation. Chapter 23. Littleton (CO): Society of Mining Engineers. p 211-8.

Yount DE. 1989. Growth of bubbles from nuclei. In: Brubakk AO, Hemmingsen BB, Sundnes G, eds. Supersaturation and bubble formation in fluids and organisms, an international symposium. Trondheim (Norway): The Royal Norwegian Society of Sciences and Letters, The Foundation. p 131-77.

Zhang P, Albarelli GR. 1995. Phosphatic clay bibliography. Bartow (FL): Florida Institute of Phosphate Research. Publication nr 02-097-114.

FOR ADDITIONAL READING

Cheng T-W, Holtham PN. 1995. The particle detachment process in flotation. Minerals Engineering 8(8): 883-91.

Dai Z, Dukhin S, Fornasiero D, Ralston J. 1998. The inertial hydrodynamic interaction of particles and rising bubbles with mobile surfaces. J. Colloid Interface Sci. 197(2): 275-92.

Deglon DA, Sawyerr F, O'Connor CT. 1999. A model to relate the flotation rate constant and the bubble surface area flux in mechanical flotation cells. Minerals Engineering 12(6): 599-608.

Finch JA, Dobby GS. 1990. Column flotation. Oxford: Pergamon Press. 180 p.

Finkelstein Y, Tamir A. 1985. Formation of gas bubbles in supersaturated solutions of gases in water. AIChE J. 31(9): 1409-19.

Flynn HG. 1964. Physics of acoustic cavitation in liquids. In: Mason WP, ed. Physical acoustics, principles and methods, Vol. 1B. New York: Academic Press. p 57-172.

Gaudin AM. 1957. Flotation. 2nd ed.. New York: McGraw-Hill.

Gerth WA, Hemmingsen EA. 1980. Heterogeneous nucleation of bubbles at solid surfaces in gas-supersaturated aqueous solutions. J. Colloid. Interface Sci. 74(1): 80-9.

Gorain BK, Franzidis JP, Manlapig EV. 1995. Studies on impeller type, impeller speed and air flow rate in an industrial scale flotation cell. Part 1. Effect on bubble size distribution. Minerals Engineering 8(6): 615-35.

Gorain BK, Franzidis JP, Manlapig EV. 1997. Studies on impeller type, impeller speed and air flow rate in an industrial scale flotation cell. Part 4. Effect of bubble surface area flux on flotation performance. Minerals Engineering 10(4): 367-79.

Hart G, Morgan S, Bramall N. 2002. Generation of picobubbles in flotation feed—a means to reduce collector use. In: Firth B, editor. Proceedings of the Ninth Australian Coal Preparation Conference; 2002 Oct 13-17; Yeppoon, Australia. p 136-48.

Heiskanen K. 2000. On the relationships between flotation rate and bubble surface area flux. Minerals Engineering 13(2): 141-9.

Holl JW. 1970. Nuclei and cavitation. J. Basic Engineering 92: 681-8.

Kirchberg H, Töpfer E. 1965. The mineralization of air bubbles in flotation. In: Arbiter NA, editor. Proceedings, VII Mineral Processing Congress; 1964 Sep 20-24; New York. New York: Gordon and Breach. p 157-68.

Luttrell GH, Yoon R-H. 1992. A hydrodynamic model for bubble-particle attachment. J. Colloid Interface Sci. 154(1): 129-37.

Mao L, Yoon R-H. 1997. Predicting flotation rates using a rate equation derived from first principles. Int. J. Miner. Process. 51(1-4): 171-81.

Ralston J, Fornasiero D, Hayes R. 1999a. Bubble-particle attachment and detachment in flotation. Int. J. Miner. Process. 56(1-4): 133-64.

Ralston J, Dukhin SS, Mishchuk NA. 1999b. Inertial hydrodynamic particle-bubble interaction in flotation. International Journal of Mineral Processing 56(1-4): 207-56.

Ryan WL, Hemmingsen EA. 1993. Bubble formation in water at smooth hydrophobic surfaces. J. Colloid. Interface Sci. 157: 312-7.

Schubert H, Bischofberger C. 1979. On the optimization of hydrodynamics in flotation processes. In: Proceedings of 13th International Mineral Processing Congress; 1979 Jun 4-9; Warsaw, Poland. Vol. 2, p 1261-87.

Soto HS, Barbery G. 1991. Flotation of coarse particles in a counter-current column cell. Minerals and Metallurgical Processing 8(1): 16-21.

Soto HS. 1992. Development of novel flotation elutriation method for coarse phosphate beneficiation. Bartow (FL): Florida Institute of Phosphate Research. Publication nr 02-070-098.

Sutherland KL. 1949. Physical chemistry of flotation: XI. Kinetics of the flotation process. J. Phys. Chem. 52: 394-425.

Tao D, Yu S, Zhou X, Honaker RQ, Parekh BK. 2008. Picobubble column flotation of fine coal. International Journal of Coal Preparation and Utilization 28(1): 1-14.

Van Der Spuy RCM, Ross VE. 1991. The recovery of coarse minerals by agglomeration and flotation. Minerals Engineering 4(7-11): 1153-66.

Weber ME, Paddock D. 1983. Interceptional and gravitational collision efficiencies for single collectors at intermediate Reynolds numbers. J. Colloid Interface Sci. 94(2): 328-35.

Weber ME. 1981. Collision efficiencies for small particles with a spherical collector at intermediate Reynolds numbers. Sep. Process. Technol. 2(1): 29-33.

Yoon R-H, Luttrell GH. 1989. The effect of bubble size on fine particle flotation. Miner. Process. Extr. Metall. Rev. 5(1): 101-22.

Yoon R-H, Mao L. 1996. Application of extended DLVO theory: IV. Derivation of flotation rate equation from first principles. J. Colloids Interface Sci. 181(2): 613-26.

Zhou ZA, Xu Z, Finch JA, Hu H, Rao SR. 1997. Role of hydrodynamic cavitation in fine particle flotation. Int. J. Miner. Process. 51(1-4): 139-49.